INFORMATION TO USERS

This manuscript has been reproduced from the microfilm master. UMI films the text directly from the original or copy submitted. Thus, some thesis and dissertation copies are in typewriter face, while others may be from any type of computer printer.

The quality of this reproduction is dependent upon the quality of the copy submitted. Broken or indistinct print, colored or poor quality illustrations and photographs, print bleedthrough, substandard margins, and improper alignment can adversely affect reproduction.

In the unlikely event that the author did not send UMI a complete manuscript and there are missing pages, these will be noted. Also, if unauthorized copyright material had to be removed, a note will indicate the deletion.

Oversize materials (e.g., maps, drawings, charts) are reproduced by sectioning the original, beginning at the upper left-hand corner and continuing from left to right in equal sections with small overlaps.

Photographs included in the original manuscript have been reproduced xerographically in this copy. Higher quality 6" x 9" black and white photographic prints are available for any photographs or illustrations appearing in this copy for an additional charge. Contact UMI directly to order.

ProQuest Information and Learning
300 North Zeeb Road, Ann Arbor, MI 48106-1346 USA
800-521-0600

ABSORBED POWER AS A MEASURE OF WHOLE BODY VEHICULAR VIBRATION EXPOSURE

Xiangyu Xie

A thesis

in

the Department

of

Mechanical Engineering

Presented in Partial Fulfillment of the Requirements
For the Degree of Master of Applied Science
Concordia University
Montreal, Quebec, Canada

June 2001

ABSTRACT

ABSORBED POWER AS A MEASURE OF WHOLE BODY VEHICULAR VIBRATION EXPOSURE

Xiangyu Xie

Occupational exposure to whole-body vehicular vibration and mechanical shocks can cause physical discomfort, adversely affect working efficiency and, in some circumstances, endanger health and safety. A variety of measures have been proposed and used to assess whole-body vibration exposure. The most commonly used standard for predicting health risk and discomfort from whole-body vibration exposure is the International Standard ISO 2631-1 (1997), which proposes using the frequency-weighted root-mean-square (rms) acceleration at the point of input of the vibration to the body as the primary measure of whole-body vibration exposure. Health guidance caution zones given in the ISO 2631-1 (1997) are also defined to provide health risk assessment. In accordance with this standard, the measurement of whole-body vibration exposure is carried out on the surface of the structure transmitting to the body and the vibration intensity is measured within the frequency range of 0.5 to 80 Hz in terms of frequency-weighted root-mean-square (rms) acceleration. A disadvantage with this measure is that it only describes the acceleration amplitude on the vibrating surface that transmits the vibration to the human body. As a result, it can be argued that it presents a poor description of the effects of vibrations actually felt by the human body.

In this thesis, absorbed power during exposure to vertical whole-body vibration is considered as a potential indicator of the physical stress affecting human health. The amount of vibration energy, either absorbed or exchanged between the source and body,

may be a good measure of the physical stress on the body since it takes into consideration the interaction between the vibrating structure and the body as well as the relative motion between the vibrating body parts. Moreover, energy is a scalar quantity that makes it easy to add up contributions from all directions and all body segments to a single value.

In order to study the energy content of the vibration transmitted to the whole body and to the different body segments, a four-degree-of–freedom linear biodynamic model used in earlier studies is chosen to represent the body. The local absorbed powers and the total power absorption under different excitations (*e.g.* sinusoidal excitation, random excitation, and transient excitation) are derived. On the basis of the model and of the guidance provided in ISO 2631-1 (1997) to relate vibration exposure with the risks of health effects, health guidance caution zones are established based on absorbed power. The results show that the absorbed power is strongly related to the frequency of the input vibration and that it peaks in the frequency range of 4 to 6 Hz corresponding to the primary body resonant frequency. Many types of vehicles produce whole-body vibration with frequencies that fall in the range where the absorbed power is the highest.

The eigenvalues and natural frequencies, damping ratios and damping ratio matrix, the vertical transmissibilities from seat to different body segments, and driving-point mechanical impedance for the 4-DOF biodynamic model are also computed. The frequency weighted rms acceleration responses, the fourth power vibration dose values (VDV), and power spectral density (PSD) of acceleration responses for different body segments are determined and discussed.

Conclusions are drawn on the merits of employing absorbed power in whole-body vibration as a measure of health risk.

ACKNOWLEDGEMENTS

I would like to express my sincere gratitude to my supervisors, Dr. Rama B. Bhat and Dr. Paul-Émile Boileau, for suggesting this thesis project topic and for their constant guidance and encouragement as well as financial support throughout the thesis work. Their valuable advice and contributions have helped in bringing the thesis to its present final form.

I am grateful to Harry, whose transient displacement input data has been employed in the study.

The completion of this thesis work would not have been possible without the understanding and support of my wife, Jing. I dedicate this thesis to her and to my loving daughter, Annie. I also dedicate this thesis to my parents.

TABLE OF CONTENTS

CHAPTER 2

MODELLING, NATURAL FREQUENCIES, AND DAMPING

CHAPTER 3

FREQENCY RESPONSE, TRANSMISSIBILITIES, AND RANDOM RESPONSES

CHAPTER 4

ABSORBED POWER, HEALTH RISK

CHAPTER 5

RESPONSE TO TRANSIENT EXCITATION

LIST OF FIGURES

LIST OF TABLES

LIST OF ABBREVIATIONS AND SYMBOLS

Abbreviations	Expansions
APMS	Apparent mass
DIS	Draft International Standard
DOF	Degree-of-freedom
DPMI	Driving-point mechanical impedance
DRI	Dynamic response index
EBS	Erect back supported
ENS	Erect back not supported
FFT	Fast Fourier Transform
IFFT	Inverse Fast Fourier Transform
HP	High-pass
ISO	International Standard Organization
LP	Low-pass
MDOF	Multiple-degree-of-freedom
MTVV	Maximum transient vibration value
PSD	Power spectral density
rms	Root-mean-square
SDOF	Single-degree-of-freedom
STHT	Seat-to-head transmissibility
VDV	Vibration dose value
WBV	Whole-body vibration

Symbols

a	Unweighted acceleration (m/s^2)
a_w	Frequency-weighted acceleration (m/s^2)
a_{rmq}	Root-mean-quad acceleration (m/s^2)
a_{rms}	Root-mean-square acceleration (m/s^2)
A	Amplitude of acceleration (m/s^2)
β_i	Eigenvalues of mass matrix M
C	Damping matrix
c_{cr}	Critical damping coefficient (*Ns/m*)
C_{cr}	Critical damping matrix
c_i	Damping coefficient (*Ns/m*)
E	Energy dissipated (*Nm*)
f	Frequency (*Hz*)
f_c	Crest factor
f_n	Natural frequency (*Hz*)
F	Force (*N*)
ϕ_i	Phase angle (*rad*)
g	Acceleration due to gravity (m/s^2)
$H(j\omega)$	Complex seat-to-head transmissibility
$H_i(j\omega)$	Complex transmissibility
$\lvert H_i(j\omega)\rvert$	Magnitude of complex transmissibility

$\boldsymbol{I}$	Identity matrix
j	Complex phaser
$\boldsymbol{K}$	Spring stiffness matrix
k_i	Stiffness coefficient (N/m)
λ_i	Eigenvalue
$\boldsymbol{M}$	Mass matrix
$M(j\omega)$	Apparent mass (kg)
m_i	Mass (kg)
P	Power (W)
P_{abs}	Absorbed power (W)
$p_{abs}(j\omega)$	Absorbed power density (W/Hz)
P_{el}	Elastic power (W)
P_{Tot}	Total absorbed power in the body (W)
P_{tr}	Transmitted power (W)
$P_{w,abs}$	Weighted absorbed power (W)
$p_{w,abs}(j\omega)$	Weighted absorbed power density (W/Hz)
$< P_{abs} >$	Averaged absorbed power per cycle (W)
s	Laplace transform variable
$S_i(j\omega)$	Acceleration PSD response, $\left(m/s^2\right)^2/Hz$
$S_0(j\omega)$	Acceleration PSD excitation, $\left(m/s^2\right)^2/Hz$
t	Time (s)

T	Exposure duration
v	Speed (*m/s*)
$V(x)$	Liapunov function
ω	Angular frequency (*rad/s*)
ω_n	Natural angular frequency (*rad/s*)
$W_k(j\omega)$	Frequency weighting factor in z-direction
x_i	Displacement (*m*)
X_i	Displacement amplitude (*m*)
$\boldsymbol{Z}$	Damping ratio matrix
$\boldsymbol{Z}_{dig}$	Diagonal matrix of eigenvalue of matrix $\boldsymbol{Z}$
$Z(j\omega)$	Complex DPMI (*Ns/m*)
ζ	Damping ratio
ζ_i^*	Modal damping ratios

CHAPTER 1

INTRODUCTION AND SURVEY OF LITERATURE

1.1 Effects of Vehicle Vibration

Vehicle drivers are exposed to whole-body vibrations (WBV) and mechanical shocks in their occupational life, especially drivers of off-road vehicles, such as road rollers, scrapers, bulldozers, excavators, forklift trucks, agricultural and forestry tractors, etc. The major adverse effects of vehicle vibration are reduced comfort and health, occurrence of motion sickness and interference with motor activities due to the perception of low-frequency vibration. Chronic health effects of WBV are low back pain, spinal disorders, abdominal pain, digestive and vision problem, *etc.* [1]. WBV is often complex, contains many frequencies, occurs in several directions and changes over time. Exposure to WBV causes a complex distribution of oscillatory motions and forces within the body. There can be large variations between subjects with respect to biological effects. WBV may cause sensations (*e.g.* discomfort or annoyance), influence human performance capability or present a health and safety risk (*e.g.* pathological damage or physiological change).

A number of scientific studies on WBV have been carried out and reported in literature, which have addressed the effects of vehicle vibration [2, 3, 4]. The main findings of these studies are as follows:

- ◊ The direction, frequency, magnitude and duration of motion are the main factors influencing human response to WBV. Thereby, the vibration type (*e.g.* sine, random, transient), magnitude (*e.g.* rms acceleration, peak acceleration),

frequency (*e.g.* range, spectra), direction (vertical, lateral, longitudinal, roll, pitch) and duration represent the factors that will likely influence the manner in which the body responds to vibration;

- ◊ Discomfort, fatigue and health risks generally increase with higher intensity or duration of vibration exposure;
- ◊ The range of frequencies most often associated with effects of WBV on health, comfort and activities is approximately from 0.5 to 80 Hz, and exposure to low frequency vibration in the 0.1 to 0.5 Hz frequency range possibly cause motion sickness;
- ◊ Effects of vehicle vibration constitute a complex phenomenon. Combinations of effects of vibration will occur simultaneously and one effect of vibration may modify the influence of another.

1.2 Vibration Exposure Assessment Methods

Evaluation of human exposure to whole-body vibration (WBV) and shock can be carried out by examining output quantities, such as frequency-weighted root-mean-square (rms) acceleration, fourth power vibration dose value (VDV), and maximum transient vibration value (MTVV).

1.2.1 Weighted root-mean-square acceleration

When evaluating vibration with respect to its possible effects on activities, the frequency weightings are required. The International Standard ISO 2631-1 (1997) [5]

defines three principal frequency weightings (W_k, W_d, and W_f) and three additional frequency weightings (W_c, W_e, and W_j). The subscripts c, d, e, f, j, k refer to the various frequency-weighting curves recommended for evaluation with respect to health, comfort, perception and motion sickness. The application of these weightings is restricted to vibration in the frequency range 1-80 Hz. The frequency weightings recommended for health assessment are the same as those for comfort.

The frequency-weighted rms acceleration is expressed in the time domain as:

$$a_{w,rms} = \left[\frac{1}{T} \int_0^T a_w^2(t) dt \right]^{1/2} \tag{1.1}$$

where $a_w(t)$ is the instantaneous frequency-weighted acceleration as a function of time; and T is the duration of the measurement.

In the frequency domain, the frequency-weighted rms acceleration may be determined by attaching weights to the narrow band or one-third octave band data and adding them appropriately. Accordingly,

$$a_{w,rms} = \left[\sum_{i=1}^{N} (W_i a_i)^2 \right]^{1/2} \tag{1.2}$$

where W_i is the weighting factor for i-th frequency band; a_i is the rms acceleration for i-th frequency band; and N is the total number of frequency bands considered.

The frequency-weighted rms acceleration also can be calculated from:

$$a_{w,rms} = \left[\int_{f_1}^{f_2} |W(f)|^2 S(f) df \right]^{1/2} \tag{1.3}$$

where $S(f)$ is the power spectral density of acceleration, and $W(f)$ is the frequency weighting for the human response to the vibration. f_1 and f_2 are the lower and upper limits of the frequency f.

The crest factor is defined as the ratio of the maximum instantaneous peak value of the frequency-weighted acceleration signal to its rms value. The peak value shall be determined over the duration of measurement, *i.e.* the time period T used for the integration of the weighted rms acceleration.

The crest factor may be used to investigate if the basic evaluation method relying on frequency-weighted rms acceleration is suitable for describing the severity of the vibration in relation to its effects on human beings. For vibration with crest factors below or equal to 9, the basic evaluation method using weighted rms acceleration is normally sufficient [5]. For vibration with crest factors above 9, the basic evaluation method, weighted rms acceleration is not sufficient. In the cases where the basic evaluation method may underestimate the effects of vibration (high crest factors, occasional shocks, transient vibration), one of the alternative measures of the running rms or the fourth power vibration dose value (VDV) may be determined.

1.2.2 Maximum transient vibration value (MTVV)

The running rms evaluation, taking into account occasional shocks and transient vibration by use of a short integration time constant is defined by:

$$a_w(t_0) = \left[\frac{1}{\tau} \int_{t_0-\tau}^{t_0} a_w^2(t)dt \right]^{1/2} \tag{1.4}$$

where $a_w(t)$ is the instantaneous weighted acceleration; τ is the integration time for averaging; t is the time (integration variable); and t_0 is time of observation (instantaneous time).

The vibration exposure under high magnitude shocks may be characterized by the maximum transient vibration value (MTVV), which is determined as:

$$\text{MTVV} = \max[a_w(t_0)] \tag{1.5}$$

1.2.3 Vibration dose value (VDV)

The VDV is more sensitive to peaks because it uses fourth power of acceleration unlike the basic evaluation method which uses the second power of the acceleration time history. It is defined as:

$$\text{VDV} = \left[\int_0^T a_w^4(t)dt \right]^{1/4} \tag{1.6}$$

where $a_w(t)$ is the instantaneous weighted acceleration; and T is the duration of measurement.

The additional evaluation methods, such as MTVV and VDV described above, will be important for the judgment of the effects of vibration on human beings when the crest factor above 9 or following ratios are exceeded:

$$\frac{MTVV}{a_w} \geq 1.5$$

$$\frac{VDV}{a_w T^{1/4}} \geq 1.75$$

1.3 Biodynamic Response Functions

The biodynamic response of the seated human body subjected to vibration has widely been assessed in terms of three different biodynamic response functions: driving-point mechanical impedance (DPMI), apparent mass (APMS) and seat-to-head transmissibility (STHT). While the first two functions have often been used interchangeably to describe "to the body" force-motion relationship as a frequency function at the human seat interface ("to the body" transfer function), the third function refers specifically to the transmission of motion through the body ("through the body" transfer function).

1.3.1 Driving-point mechanical impedance

The driving-point mechanical impedance, DPMI, is defined by the International Standard ISO/DIS 5982 (2000) [6] as: The complex ratio of applied periodic excitation

force at frequency f, $F(f)$, to the resulting vibration velocity at that frequency, $v(f)$, measured at the same point and in the same direction as the applied force. *i.e.*:

$$Z(f) = \frac{F(f)}{v(f)} \tag{1.7}$$

Impedance, $Z(f)$, is similar to the impedance or resistance in electrical systems and provides information on the external force necessary to produce a specific response in the system.

The DPMI has been used to characterize "to the body" biodynamic response. It is a complex quantity, that is, it possesses real and imaginary parts, from which may be calculated the magnitude and phase. In the case of non-harmonic vibration, driving-point mechanical impedance is determined from the force and velocity spectra.

Under random vibration, the DPMI may be derived from:

$$Z(f) = \frac{G_{FV}(f)}{G_{VV}(f)} \tag{1.8}$$

where $G_{FV}(f)$ represents the cross-spectral density of the input force and the output velocity, while $G_{VV}(f)$ represents the auto-spectral density of the response velocity.

1.3.2 Apparent mass

The apparent mass, APMS, is also defined by ISO/DIS 5982 (2000) as: The complex ratio of applied periodic excitation force at frequency f, $F(f)$, to the resulting

vibration acceleration at that frequency, $a(f)$, measured at the same point and in the same direction as the applied force. Hence, the APMS is formulated as:

$$M(f) = \frac{F(f)}{a(f)} = -j\frac{Z(f)}{2\pi f} \tag{1.9}$$

The APMS has also been used to characterize "to the body" biodynamic response. The relation between APMS and DPMI is entirely determined by the fixed relation between velocity and acceleration for which a 90° phase difference exists under periodic excitation. In the above expression, $j = \sqrt{-1}$ represents the complex phasor between DPMI and APMS. In the case of non-harmonic vibration, APMS is determined from the force and acceleration spectra.

The quantity apparent mass has the advantage that it can be obtained most directly from the signals provided by accelerometers and force transducers. Moreover, one of Newton's lows of motion gives apparent mass a simple intuitive meaning: a force applied to a body accelerates the body by an amount proportional to the force, the constant of proportionality being the mass of the body. When the human body is effectively rigid (e.g. at very low frequencies in the vertical axis) the apparent mass of the body is equal to its static mass and the force and acceleration are in phase. As the frequency increases, one or more resonances increase the apparent mass and there is an increasing phase difference between the force and acceleration. At higher frequencies the upper body segments are loosely coupled and the human body will no longer be rigid, the apparent mass falls and no longer equals the static mass of the human body. The force is dominated by the mass near the driving point.

1.3.3 Seat-to-head transmissibility

The seat-to-head transmissibility, STHT is a complex non-dimensional ratio of response motion of the head to the forced vibration motion at the seat-body interface. The ratio may be one of displacements, velocities or accelerations. It is expressed as:

$$H(j\omega) = \frac{X_h(j\omega)}{X_0(j\omega)} = \frac{\dot{X}_h(j\omega)}{\dot{X}_0(j\omega)} = \frac{\ddot{X}_h(j\omega)}{\ddot{X}_0(j\omega)} \tag{1.10}$$

where $H(j\omega)$ is the complex STHT function; $X_h(j\omega)$, $\dot{X}_h(j\omega)$, and $\ddot{X}_h(j\omega)$ are the displacement , velocity, and acceleration responses of the head due to the displacement, velocity, and acceleration excitations, $X_0(j\omega), \dot{X}_0(j\omega)$, and $\ddot{X}_0(j\omega)$ applied to the seat, respectively.

The STHT is a complex quantity, that is, it possesses real and imaginary parts, from which the non-dimensional modulus and the phase may be computed. Similar to the DPMI and the APMS, in the case of non-harmonic vibration, STHT is determined from the motion spectra.

The STHT represents "through the body" transfer function. Its modulus peaks at frequency corresponding to the resonant frequency of the body.

1.4 International Standard ISO 2631-1 (1997)

Presently, the most commonly used standard for evaluating human exposure to WBV and shock is the International Standard ISO 2631-1 (1997) developed by the International Standards Organization (ISO). This standard defines the frequency

weighting functions, which account for the variation of sensitivity with frequency. The frequency weighting procedure implies that human response to WBV is not only related to magnitude and duration but also to the frequency of the vibration. The purpose of the frequency weighting procedure is to compensate and to normalize for differences in human susceptibility and sensitivity at different frequencies. Figure 1.1 presents the frequency-weighting curve for principal weighting, W_k, which applies to vibrations in the vertical direction in order to assess health and comfort effects on seats. The standard also presents the main vibration exposure assessment methods based on frequency-weighted rms acceleration measured at the point of entry of the vibration in the body. This method must be complemented with additional assessment methods including a fourth power vibration dose value of acceleration (VDV), and /or a maximum transient vibration value (MTVV) to emphasize the added influence of transient vibration and high amplitude shock events. Evidently, the International Standard ISO 2631-1 (1997) provides guidance on comfort and health risk based on the frequency-weighted rms acceleration measured within the frequency range of 0.5 to 80 Hz at the seat-subject interface for a seated individual subjected to continuous broad-band vibration. On that basis, it must be supposed that the amount of vibration measured at the interface is a good indicator of the vibration transmitted to the body.

1.4.1 Effects on health

To determine the effects of exposure to vibration on health, the frequency weighted rms acceleration in the frequency range 0.5 to 80 Hz, from periodic, random or transient vibration that is transmitted through a seat pan to the seated body, has to be

calculated. ISO 2631-1 (1997) makes an additional definition of "Health Guidance Caution Zone" based on frequency-weighted rms acceleration measured along the dominant axis and indicated by the shaded area in Figure 1.2. For exposures below the zone, health effects are not clearly documented and/or objectively observed; inside the zone, caution with respect to potential health risks is indicated and above the zone health risks are likely. This recommendation is mainly based on exposure duration of 4 to 8 hours. The "Health Guidance Caution Zone" is based on the principle of energy conservation. Assuming that the response is related to energy, two different daily vibration exposures are equivalent when:

$$a_{w1} \cdot T_1^{1/2} = a_{w2} \cdot T_2^{1/2} \tag{1.11}$$

or

$$a_{w1} \cdot T_1^{1/4} = a_{w2} \cdot T_2^{1/4} \tag{1.12}$$

where a_{w1} and a_{w2} are the frequency-weighted rms acceleration values for the first and second exposures, respectively; T_1 and T_2 are the corresponding durations for the first and second exposures.

The estimated vibration dose values (VDV) corresponding to the lower and upper bounds of the zone given by Equation (1.12) and presented in Figure 1.2 are 8.5 and 17, respectively.

The health guidance caution zones for both Equations (1.11) and (1.12) are the same for durations from 4 h to 8 h for which occupational observations exist.

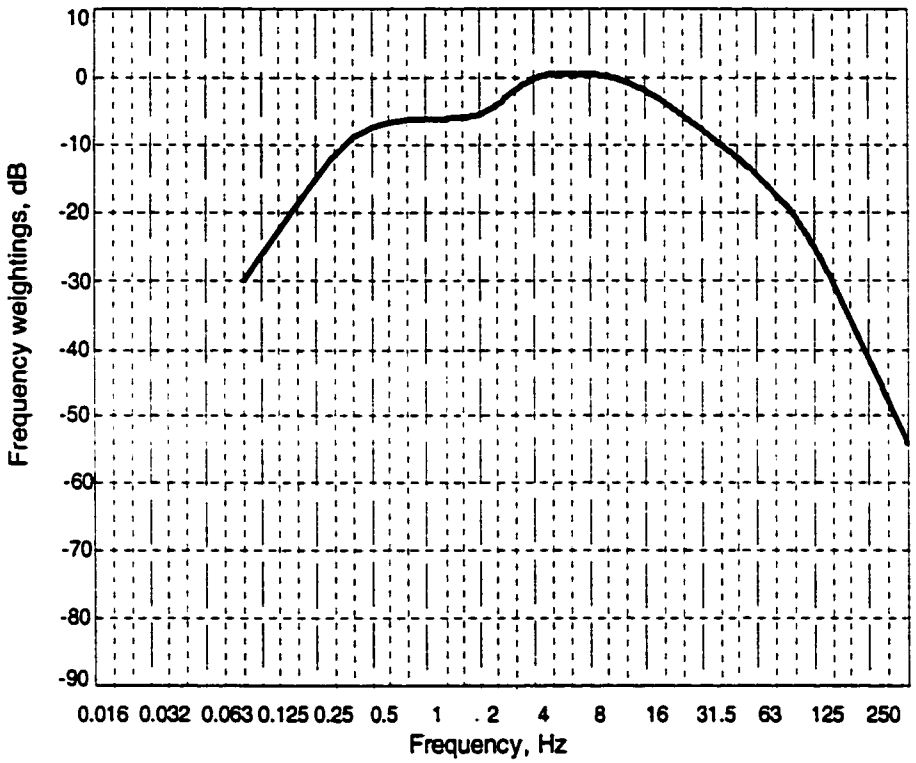

Figure 1.1 Frequency weighting curve for principal weighting, W_k, proposed in ISO 2631-1 (1997) [5]

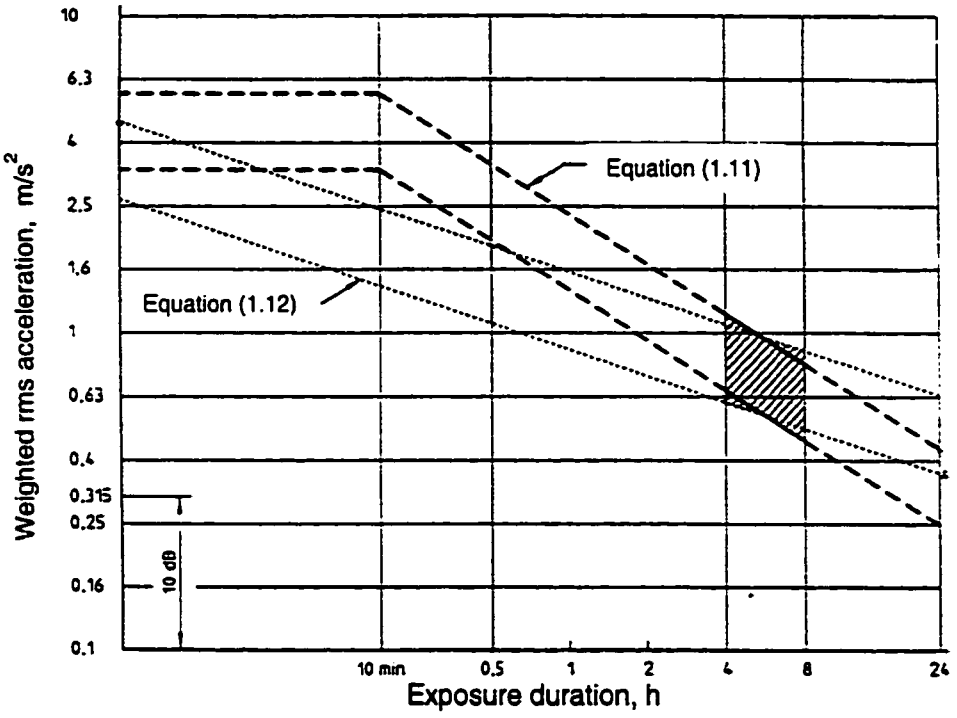

Figure 1.2 Health guidance caution zones defined in the ISO 2631-1 (1997) [5]

1.4.2 Effects on comfort

The effects of vibration on the comfort of a person exposed to periodic, random or transient vibration are also assessed in the frequency range 0.5 to 80 Hz. When assessing the effects on comfort, all the relevant vibration directions should be included and overall total value of vibration obtained:

$$a_{wT} = \left(k_x^2 a_{wx}^2 + k_y^2 a_{wy}^2 + k_z^2 a_{wz}^2\right)^{1/2} \tag{1.13}$$

where a_{wx}, a_{wy}, and a_{wz} are weighted rms accelerations with respect to the orthogonal axes x, y, z, respectively; k_x, k_y, and k_z are corresponding weighting coefficients.

The overall rms value of the frequency-weighting acceleration can be then compared with the following guidance:

$a_{wT} < 0.315$ m/s²	Not uncomfortable
$0.315 < a_{wT} < 0.63$ m/s²	A little uncomfortable
$0.5 < a_{wT} < 1$ m/s²	Fairly uncomfortable
$0.8 < a_{wT} < 1.6$ m/s²	Uncomfortable
$1.6 < a_{wT} < 2.5$ m/s²	Very uncomfortable
$a_{wT} > 2.5$ m/s²	Extremely uncomfortable

Before making this comparison, it is important to remember that reactions to various magnitudes of vibration depend on various factors such as comfort expectations,

annoyance and tolerance. Therefore, the above figures should be treated only as guidance.

1.4.3 Effects on perception and motion sickness

In ISO 2631-1 (1997) the determination of whether a vibration is perceptible is obtained from the peak value of the frequency-weighted acceleration. The weighted rms acceleration should be determined in the frequency range of 0.5 to 80 Hz on each axis and the highest value used in the assessment.

From the experimental data it was determined that 50% of alert, fit persons can detect a W_k weighted vibration with a peak magnitude of 0.015 m/s² and this figure is regarded as a perception threshold value.

To assess the motion sickness dose value, the weighted rms acceleration is determined for z-axis over frequency range 0.1 to 0.5 Hz. There are two alternative methods of calculating the motion sickness dose value:

◊ Measurements carried out over the full exposure period

$$\mathrm{MSDV_z} = \left\{ \int_0^T [a_w(t)]^2 \, dt \right\}^{1/2} \tag{1.14}$$

where $\mathrm{MSDV_z}$ represents motion sickness dose value; $a_w(t)$ is frequency weighted acceleration in z-direction, using the special frequency-weighting factor W_f in ISO 2631-1 (1997) ; and T is the total period of time in seconds.

◊ If the motion exposure is continuous and of relatively constant magnitude, then

$$\mathrm{MSDV}_z = a_w \mathrm{T}^{1/2} \tag{1.15}$$

1.5 Absorbed Power — An Indicator of Human Response to WBV

1.5.1 Basic concepts and terminology of absorbed power

Power is dissipated in a mechanical system as a result of an applied force. If a complex force $F(\omega)$ applied to a mechanical system produces a complex velocity $V(\omega)$, the resulting dissipated power is $\frac{1}{2}F(\omega)\cdot V(\omega)$. The vibratory absorbed power in the human body has variously been advocated as an indicator of fatigue from whole-body vibration or injury from hand-transmitted vibration [1].

The work, E, expended by a surface in moving a body during any period of time, T, is given by:

$$E = \int_0^T F(t)\cdot x(t)dt \tag{1.16}$$

where $F(t)$ is the force as a function of time; and $x(t)$ is the displacement as a function of time.

The power is defined as the rate of work done, and is the product of force and velocity.

When a sinusoidal force, $F_0 \sin(\omega t + \phi)$, acts through a displacement $X_0 \sin(\omega t)$, the power, P, is given by:

$$P = F(t) \cdot \frac{dx(t)}{dt}$$

$$= \frac{1}{2}\omega X_0 F_0 [\sin(2\omega t + \phi) + \sin\phi] \tag{1.17}$$

The first term of expression (1.17) is a sine wave of twice the oscillation frequency and indicates the fluctuating component of power. It is obvious that the average value of this fluctuating component, $\frac{1}{2}\omega X_0 F_0 \sin(2\omega t + \phi)$, over a complete cycle of motion is zero. The second term in the expression is a constant, $\frac{1}{2}\omega X_0 F_0 \sin\phi$, and depends on the phase, ϕ, between the force and displacement. Therefore, the time-averaged power over a complete cycle of motion may be written as:

$$< P >= \frac{1}{2}\omega X_0 F_0 \sin\phi \tag{1.18}$$

In the case of an ideal spring, the phase between force and displacement is zero, and hence, $\sin\phi = 0$. The work done by the force in deflecting the spring is followed by an equal amount of work done by the spring returning the force to the initial point. The total work done over a complete cycle is zero. All the energy in the system is in the form of kinetic energy as the system passes through the equilibrium position and all the energy is in the form of potential energy as the spring is fully compressed or extended. The total instantaneous energy stored in the spring is equal to the integration of the product of the force and the spring deflection.

In the case of an ideal damper, the phase between the force and displacement is 90^o, namely, $\sin\phi = 1$. Thus, there is both constant and a fluctuating component in the expression (1.17) for the power. When averaged over a complete cycle the fluctuating component, $\frac{1}{2}\omega X_0 F_0 \sin(2\omega t + \phi)$, is also zero. However, there is a constant term, $\frac{1}{2}\omega X_0 F_0$, which represents the absorbed power in the damper.

$$< P_{abs} >= \frac{1}{2}\omega X_0 F_0 \tag{1.19}$$

In the case of a force acting on a pure mass, the force and displacement are out of phase at 180^o, and hence, $\sin\phi = 0$. There is work done by the force in accelerating and decelerating the mass, however, the energy is converted back and forth between kinetic and potential energies and no energy is dissipated.

For a complex dynamic system containing masses, springs and dampers the above relations may be used to calculate the absorbed power. It is observed from Equation (1.17) that the absorbed power is proportional to the sine of the phase between the force and displacement.

The expressions of absorbed power can be modified to express the movement in terms of velocity or acceleration by multiplying by ω or ω^2. They also can be modified to replace the force by a measure of impedance in terms of the following relationship:

$$F(\omega) = Z(\omega) \cdot V(\omega) \tag{1.20}$$

where $Z(\omega)$ represents the driving-point mechanical impedance.

1.5.2 Studies on absorbed power in human vibration

The concept of absorbed power was first discussed in the mid-1960s by a number of researchers. The studies of Pradko *et al.* (1965a [7], 1965b [8], 1966 [9]), Lee and Pradko (1968) [10] are largely responsible for the interest in absorbed power as an indicator of human response to WBV. They achieved results that subjective experience of vibration is related to the amount of vibration energy absorbed by the human body and the absorbed power may be used as an indicator of subjective response. Pradko and Lee suggested that the time dependency of fatigue or discomfort might be determined from the absorbed power. A decade later, Janeway (1975a [11], 1975b [12]) strongly advocated these observations and pointed out that the concept of energy absorption should be added in the standard ISO 2631, at least for the occupational comfort criteria. Since then, very little has appeared in published literature in this area. However, in regard to hand-arm vibration, the concept of absorbed power (energy) has been discussed more widely. For instance, Lidstrom (1977) [13] presented that the prevalence of vibration-induced injuries within different occupational groups is related to the amount of absorbed energy.

In recent years, Lundstrom, Holmlund, and Lindberg (1998) [14] have carried out the investigation of WBV energy absorption during different experimental conditions. The relation between absorbed power and frequency, exposure level, direction, upper-body position, body weight and gender were focused in the study. The experimental procedure for all test runs followed a predestined protocol. After weighting in a standing

position the subjects sat on the seat plate with feet positioned on an adjustable footrest. The footrest was adjusted so that the lower legs were vertical and the upper legs horizontal. The static weight on the force plate and the footrest were then determined. On each occasion the subject was exposed to one of the four acceleration levels, 0.5, 0.7, 1.0 or 1.4 m/s^2 rms in both erect and relaxed upper-body posture. The posture was visually checked by the experimenter during each test run and if necessary corrected during measurement pauses. The measurement period for each frequency was 15 second followed by a 5 second pause. The frequency was increased from 2 to 100 Hz in steps of 1/3 octaves, except in the range 2.5 to 20 Hz where the steps were 1/6 octaves. The collected data were processed and analyzed with LabView™. For each test frequency the collected acceleration signal $a(t)$ was integrated to get the velocity $v(t)$. The total force $F_{Means}(t)$ registered by the force cells also consist of a contribution generated by the mass of the seat plate (m_{plate}). This contribution is always in phase with acceleration signal and was cancelled by vectorial substraction. The force $F(t)$ transmitted to the sitting subject was determined as $F(t) = F_{Means}(t) - m_{plate} \cdot a(t)$. Therefore, the time-average absorbed power $< P_{abs} >$ was determined according to $< P_{abs} >=< F(t) \cdot v(t) >$. Their experimental results showed that: i) the absorbed power was strongly related to the frequency of the vibration, with peaks in the range of 4-6 Hz; ii) the amount of absorbed power increases with the frequency up to a peak in the range of 4 to 6 Hz during exposure at a constant acceleration level; iii) absorbed power at each frequency was proportional to the square of the acceleration; and iv) maximal absorption tended to increase and slide towards lower frequencies when the body position was changed from erect to relaxed.

They concluded that absorbed power might be a better quantity for risk assessment than those specified in ISO 2631 (1997) since it also takes the dynamic force applied to the human body into account.

Mansfield, Holmlund and Lundstrom (2000) [15] reported a laboratory study comparing subjective judgments of vibration and shock severity with the absorbed power and with all combinations of standard frequency weighting and analysis methods. In their experiment, 24 human subjects (11 males and 13 females) were exposed to 15 vertical vibration stimuli (5 stimulus types) comprising of random vibration, repeated shocks and combinations of random vibration and shocks at 0.5, 1.0, and 1.5 m/s^2 rms unweighted acceleration. Each stimulus lasted 20 seconds. Subjects rated the discomfort from the vibration on a numerical scale after each exposure. Stimulus 1 consisted of random vibration in the frequency range of 2 to 20 Hz. Stimulus 2 consisted of 20 repeated mechanical shocks at equally spaced 1-s intervals (*i.e.*, non-predictable). Stimulus 3 consisted of 20 repeated shocks that were not equally spaced (*i.e.*, non-predictable). Stimuli 4 and 5 were combinations of stimuli 1 and 2 and of 1 and 3, respectively, with half the energy coming from the shocks, scaled to give the appropriate acceleration magnitude. The shocks were defined as sync pulses that were high-pass and low-pass filtered at 2 and 20 Hz using elliptic filters. The stimuli used to generate the vibration were equalized for the response of the amplifier and shaker to produce a flat spectrum at the seat. Consequently, each stimulus had nominally identical power spectra for each of the three vibration magnitudes. For each of the frequency-weighted signals, three analyses (rms acceleration, VDV, and total absorbed power) were carried out to enable comparisons of all combinations of frequency weighting and analysis methods. The rms

acceleration and VDV are defined in ISO 2631-1 (1997). Acceleration and force were combined to give a measure of absorbed power. The total absorbed power $P_{abs}(total)$ is defined as [16]:

$$P_{abs}(\text{total}) = \int_{2}^{20} |G_{Fv}(f)| \cdot \cos\phi(f) df \tag{1.21}$$

where $|G_{Fv}(f)|$ is the modulus and $\phi(f)$ is the phase of the cross-spectral density between the force, F, and the velocity, v, at the frequency f.

For assessment of all stimuli types together, absorbed power gave higher correlation with subjective discomfort than acceleration-based methods. Some of their conclusions are: i) absorbed power correlates well to subjective discomfort; ii) absorbed power was significantly better than rms or MTVV methods at predicating discomfort; and iii) ISO 2631-1 requires clarification and amendment.

Evidently, the standard ISO 2631-1 only gives the guidelines of the acceleration magnitude on the vibrating surface; however, in many studies especially on hand-arm vibrations, the absorbed power is related to fatigue and injury. As a result, it is logical to follow a similar approach to describe the extent of vibration actually being transmitted to and absorbed by the human body. Energy (power) dissipation is a scalar quantity that makes it easy to add up contributions from all three directions to a single value. Therefore, the absorbed power in the body will be a better indicator of fatigue and occupational health hazard. Such an approach can be extended to the driver comfort studies also.

1.6 Review of Biodynamic Models

Vehicular vibration introduces vibratory input to the vehicle operator. Such a vibratory excitation will result in whole body vibration in the operator, since human body behaves like a vibrating physical system with distributed properties of mass, elasticity and damping. Previous studies on absorbed power in whole body vibration have been carried out using single-degree of freedom models. In order to study both whole body absorbed power and local absorbed powers within body parts, it is essential to model the body as either a single-degree-freedom (SDOF) system or a multi-degree-freedom (MDOF) system, respectively, depending on the study objectives. A number of biodynamic models, ranging from linear simple SDOF models to nonlinear complex MDOF models have been reported to account for the biodynamic response characteristics of the seated human body.

The biodynamic response characteristics of seated human body subject to vibration has widely been described in terms of driving-point mechanical impedance, apparent mass, and seat-to-head transmissibility. Majority of the models proposed in the literature are lumped-parameter models, where the parameters are mostly identified from measured biodynamic response data. The model parameters are mostly identified from either measured driving-point mechanical impedance or vibration transmissibility characteristics (e.g. magnitude and phase transmissibility of seat to head) of the human subjects.

The parameters of most models are derived from driving-point mechanical impedance or apparent mass, such as single-degree of freedom dynamic response index (DRI) model (1962) [17] shown in Figure 1.3, improved DRI model proposed by Payne

(1978) [18] shown in Figure 1.4, SDOF model proposed by Fairly and Griffin (1989) [19] shown in Figure 1.5, 2-DOF model proposed by Suggs et al (1969) [20, 21] shown in Figure 1.6, 2-DOF model proposed by Allen (1978) [22] shown in Figure 1.7, 3-DOF non-linear model proposed by Demic (1987) [23] shown in Figure 1.8, 4-DOF model proposed by Payne and Band (1971) [24] shown in Figure 1.9.

The parameters of only a few models are derived from both driving-point mechanical impedance or apparent mass and seat-to-head transmissibility. Two of them are 3-DOF model proposed in the International Standard ISO/DIS 5982 (2000), and 4-DOF model proposed by Boileau (1995) [25].

A 3-DOF biodynamic model shown in Figure 1.10 is proposed in the Draft International Standard ISO/DIS 5982 (2000) to characterize the standardized driving-point mechanical impedance and apparent mass as well as seat-to-head transmissibility. In this model, the masses, springs and dampers do not correspond to physiological structures within the body. The input force is considered to be applied to mass m_0 for which the resulting displacement is represented by x_0. The model parameters were derived to obtain closest agreement with the weighted mean (target) values defined for driving-point mechanical impedance/apparent mass and seat-to-head transmissibility. They would most likely apply to a subject with total body mass of 75 kg, while assuming that 73% of the mass is resting on the seat. Values are supplemented for total body masses of 55 kg and 90 kg simply by modifying the parameter value for mass m_3. For the purpose of computing seat-to-head transmissibility, mass m_2 may tentatively be taken to represent the head. The model results in relatively good agreement with the standardized mechanical impedance magnitude, though large discrepancies occur with the impedance

phase. Considerable differences in the transmissibility magnitude near the natural frequency of 5 Hz are observed. The model response reveals large errors in the transmissibility phase over most of the frequency range considered.

Boileau (1995) proposed a 4-DOF linear biodynamic model, shown in Figure 1.11, based upon measured and synthesized values of driving point mechanical impedance and seat-to-head vibration transmissibility characteristics. Off-road vehicle drivers frequently assume an erect back not supported (ENS) posture, due to excessive vehicle vibration and the desire to maintain adequate grip on the steering wheel. The baseline model is thus established for the ENS posture alone. The particularities of this model are that the model satisfies two biodynamic response functions (*i.e.* driving-point mechanical impedance and seat-to-head transmissibility) and model components correspond to body segments. From the driving-point mechanical impedance function, the resonant frequency of the model is 5.5 Hz, compared to 4.875 Hz derived from the target values. The peak model response, 2833 Ns/m, however, is quite close to the corresponding target value, 2867 Ns/m, an error of approximately 1.2%. Driving-point mechanical impedance phase response of the model correlates well with the target data at frequencies up to 6 Hz, while the phase error increases at higher frequencies. For the seat-to-head transmissibility, while the model response exhibits a resonant peak of 1.77 at 4.8 Hz, the corresponding target value is 1.45 at 5 Hz. The resonant frequencies correlate reasonably well, the model, however, tends to overestimate the transmissibility magnitude by 30% at frequencies below 7 Hz. A relatively good agreement is observed for the phase response at frequencies below 6 Hz.

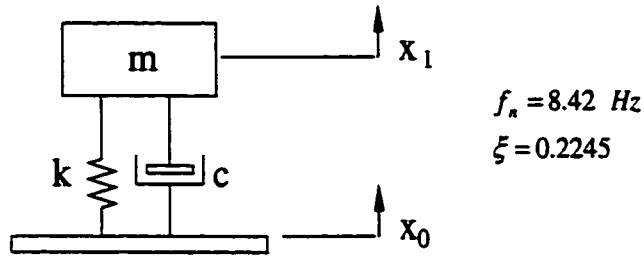

Figure 1.3 DRI model [17]

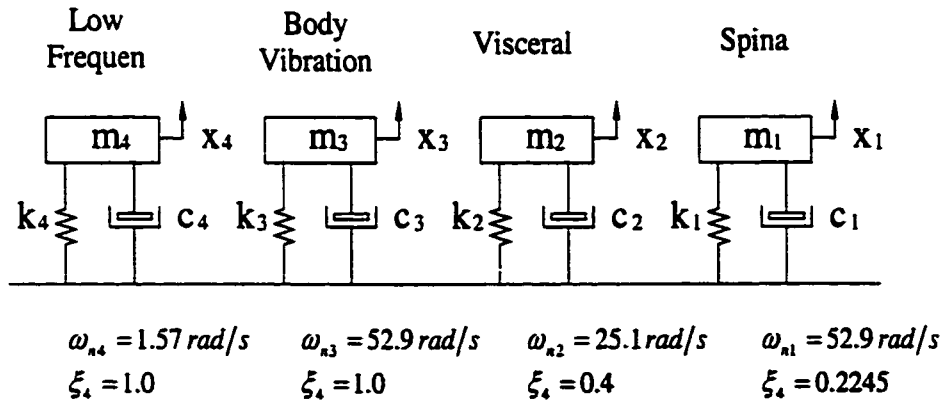

Figure 1.4 Improved DRI model proposed by Payne (1978) [18]

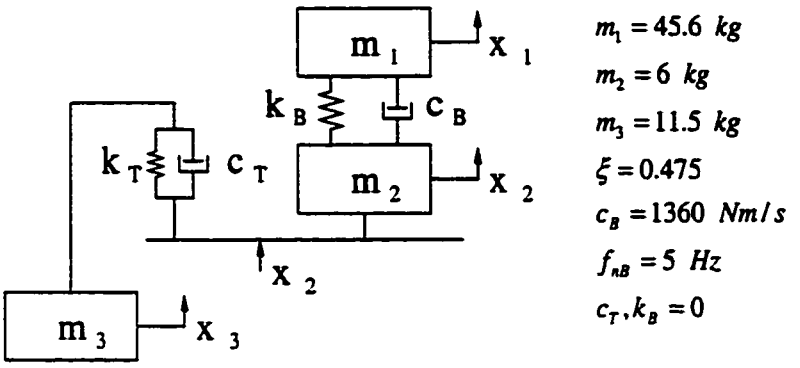

Figure 1.5 SDOF model proposed by Fairly and Griffin (1989) [19]

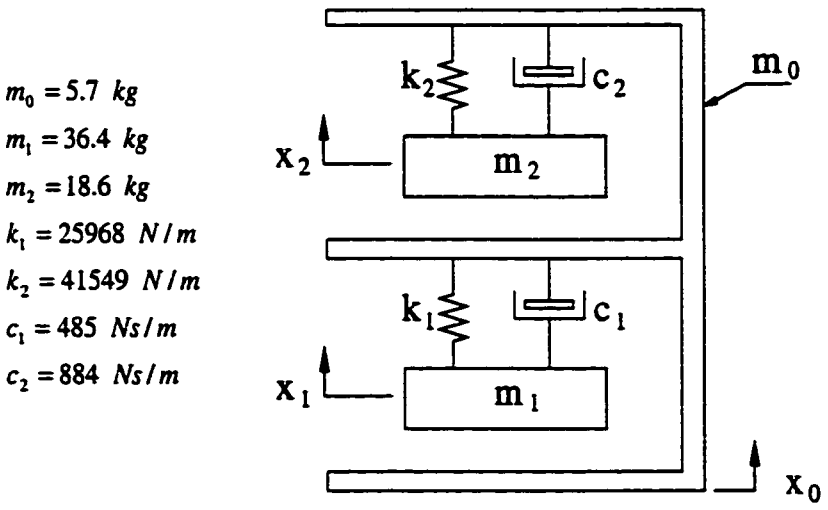

Figure 1.6 2-DOF model proposed by Suggs *et al.* (1969) [20, 21]

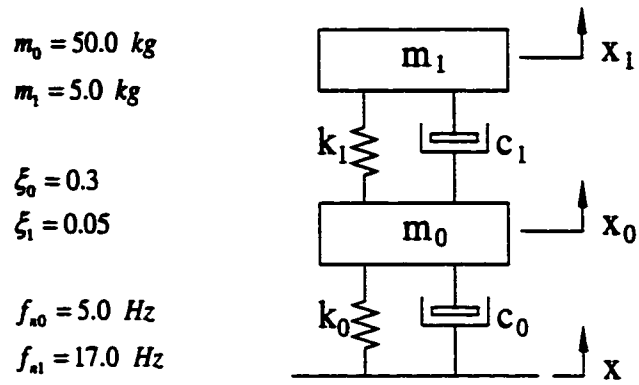

Figure 1.7 2-DOF model proposed by Allen (1978) [22]

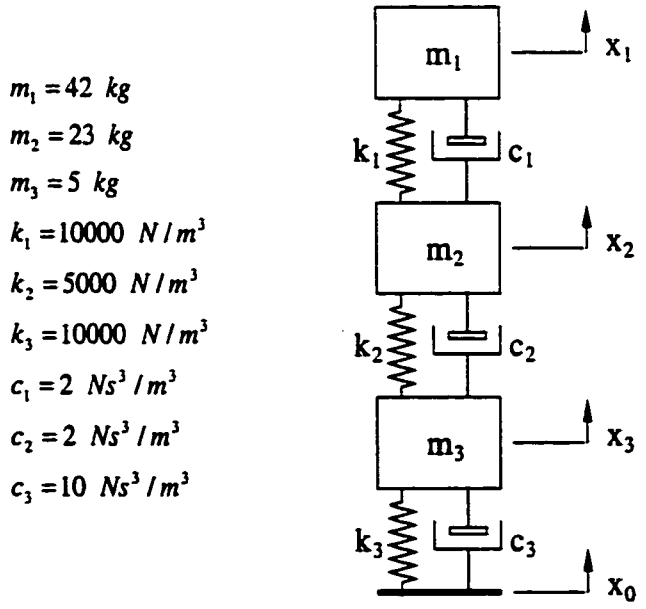

Figure 1.8 3-DOF non-linear model proposed by Demic (1987) [23]

$m_1 = 29.0\ kg$	$k_1 = variable$	$\zeta_1 = 0.25$
$m_2 = 6.8\ kg$	$k_2 = 2838\ N/m$	$\zeta_2 = 0.50$
$m_3 = 21.8\ kg$	$k_3 = variable\ kg$	$\zeta_3 = 0.10$
$m_4 = 5.45\ kg$	$k_4 = 204820\ N/m$	$\zeta_4 = 0.15$

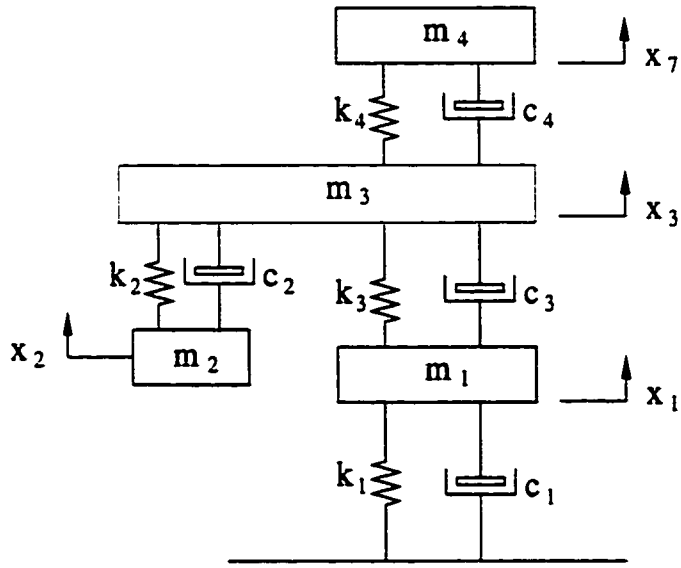

Figure 1.9 4-DOF model proposed by Payne and Band (1971) [24]

$m_0 = 2\ kg$

$m_1 = 6\ kg$

$m_2 = 2\ kg$

$m_3 = 45\ kg$

$k_1 = 9.99 \times 10^3\ N/m$

$k_2 = 3.44 \times 10^4\ N/m$

$k_3 = 3.62 \times 10^4\ N/m$

$c_1 = 387\ Ns/m$

$c_2 = 234\ Ns/m$

$c_3 = 1.39 \times 10^3\ N/m$

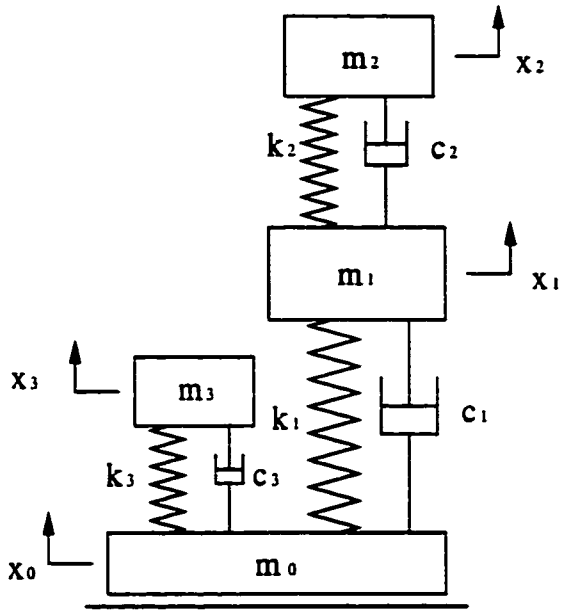

Figure 1.10 3-DOF model proposed in ISO/DIS 5982 (2000) [6]

$m_1 = 5.31\ kg$

$m_2 = 28.49\ kg$

$m_3 = 8.62\ kg$

$m_4 = 12.78\ kg$

$\sum_{i=1}^{4} m_i = 55.2\ kg$

$k_1 = 310\ kN/m$

$k_2 = 183\ kN/m$

$k_3 = 162.8\ kN/m$

$k_4 = 90\ kN/m$

$c_1 = 400\ Ns/m$

$c_2 = 4750\ Ns/m$

$c_3 = 4585\ Ns/m$

$c_4 = 2064\ Ns/m$

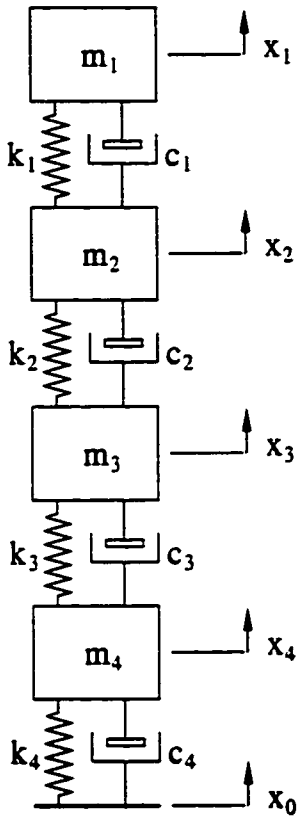

Figure 1.11 4-DOF linear model proposed by Boileau (1995) [25]

In the present study, the 4-DOF biodynamic model of Boileau (1995) is selected to study the local and whole body absorbed powers, since the results for the local biodynamic behavior of different segments of the body and the vibration characteristics of the whole body are available for comparison. This biodynamic model will be especially described in the section 3.2 in Chapter 2.

1.7 Objectives of the Thesis

The main objective of this study is to establish a relationship between total vibration absorbed power and frequency-weighted rms acceleration in an attempt to define a health guidance caution zone on the basis of absorbed power. This is realized through the analysis of a 4-DOF lumped parameter model representing the portion of the body resting on the seat for a seated individual. It is proposed to derive and study the total absorbed power in the body and local absorbed powers in different body segments under different excitations, such as harmonic excitation, random excitation and transient excitation. Another important objective is to compare and analyze the relationships between absorbed power and frequency-weighted acceleration under different excitations. Furthermore, it is proposed to study the steady-state response and biodynamic response functions of the model, including eigenvalues, natural frequencies, damping ratio matrix, acceleration transmissibilities from the seat to different parts of the body, apparent mass and driving-point mechanical impedance.

1.8 Organization of the Thesis

This thesis is organized into six chapters. The literature is briefly surveyed in Chapter 1 highlighting the research contributions on the various subjects to the general area of the topic of this thesis by earlier researchers.

In Chapter 2, the 4-DOF linear biodynamic model proposed by Boileau (1995) is selected to study the total absorbed power in the body and local absorbed powers in different body segments. The eigenvaues and natural frequencies of the biodynamic system are calculated. The biodynamic model is found to belong to a mixed system, in which some modes oscillate and some do not, by calculating the damping ratio matrix of the model. The stability of the model is identified by solving the eigenvalue problem of the biodynamic system.

In Chapter 3, the frequency response function, transmissibility characteristics of magnitudes and phases for seat to different parts of the body are derived. The response analysis of the biodynamic system is carried out under sinusoidal and random excitations. The natural frequencies obtained in Chapter 2 will be identified by the figure of transmissibility characteristics in this Chapter. The driving-point mechanical impedance, apparent mass and the real and imaginary parts of the frequency response functions for seat to each segment in the body are discussed.

In Chapter 4, the absorbed power as the recommended indicator for health risk is discussed in detail. The local absorbed powers in different parts of the body and total absorbed power the body are derived under various excitations, such as constant acceleration input, sinusoidal displacement excitation, and random excitation. The correlation between total absorbed power in the body and frequency-weighted rms

acceleration is established. Consequently, similar to the guideline represented in ISO 2631-1 (1997), the health guidance based on absorbed power is established and it also shows the exposure duration of 4 to 8 hours as indicated by the shaded area.

In Chapter 5, the vibration responses on transient acceleration excitation are discussed. By means of SIMULINK software package, the acceleration and absorbed power responses of different parts of the body under a transient acceleration input are derived. Moreover, the fourth power method, vibration dose value (VDV), and root-mean-square (rms) acceleration are calculated. The relationships between the weighted total absorbed power in the body and weighted rms acceleration and VDV are determined. The correlations between total absorbed power and frequency-weighted rms acceleration under random excitation and transient input are compared.

The discussion and conclusions as well as recommendation for future works are finally presented in Chapter 6.

CHAPTER 2

MODELLING, NATURAL FREQUENCIES, AND DAMPING

2.1 Introduction

Since the human body behaves like a vibrating physical system, an appropriate mathematical model can be developed using its mass, elastic and damping properties. Most current models are MDOF models, which represent the human body by combining masses, springs, and dampers, corresponding to the different body parts.

The natural frequencies of a vibrating system are the most important parameters needed to study the steady-state and dynamic behavior of the system. The concept of the eigenvalue of a matrix is closely related to the concept of natural frequency of vibration in a vibrating system. An undamped n-DOF system has n number of natural frequencies. A damped n-DOF system also will have n number of natural frequencies which are complex and some of them, however, may have overdamped modes.

The classification of critical damping, overdamping, and underdamping, for the system can be carried out by examining the damping ratios or damping ratio matrix of the system.

2.2 Biodynamic Modeling

There are two broad categories of biodynamic models: continuous-parameter models and lumped-parameter models. Continuous-parameter systems are presented by partial differential equations. Their inertia, spring, and damping effects are distributed continuously (or piecewise continuously) over the system. In lumped-parameter models,

various characteristics in the system are lumped into representative elements. In an analytical model, these individual characteristics can be approximated by a separate mass element, a spring element, and a damper element, which are interconnected in parallel or series configuration. In terms of the component energy, the basic system elements can be divided into two groups: energy-storage elements (i.e. masses and springs) and energy-dissipation elements (*i.e.* dampers).

When human body is subjected to vibration, different parts of the body move relative to each other. Thus, the body behaves like a vibrating physical system with distributed energy-storage elements (masses, springs) and energy-dissipation elements (dampers). In order to study the biodynamic behavior of different segments in the body, it is possible to model the body system by a MDOF lumped-parameter biodynamic system. A common approach used in formulating biodynamic models consists in basing the model on DPMI or APMS and/or STHT data measured from the same subject group under predefined test conditions representing typical vibration work conditions of off-road vehicle drivers. The model is mathematically derived by curve-fitting the data sets presented applying either the DPMI /APMS, or/and the STHT functions, while consideration of the biodynamical data is avoided due to associated uncertainties and complexities. The degrees of freedom and the structure of the model are based on the general trends observed from the measured biodynamic data, and available models, instead of knowledge of anatomy and anthropometrics.

Off-road vehicle drivers are subjected to random vibration. When driving, the feet are generally supported either on a vibrating cab floor or pedals, and the hands are in contact with either a steering wheel or handles. For a seated driver, the weight

distribution on the seat may vary with the sitting posture adopted, such as erect or slouched positions, with or without backrest support. However, off-road vehicle drivers commonly sit with an erect back and unsupported posture, due to excessive vehicle vibration and the desire to maintain adequate grip on the controls. Based on these considerations, Boileau (1995) proposed a 4-DOF lumped-parameter biodynamic linear model as shown in Figure 2.1. The model comprises four masses, coupled by linear elastic and damping elements. The four masses represent the following four body segments for a seated individual: the head and neck (m_1); the chest and upper torso (m_2); the lower torso (m_3); and the thighs and pelvis in contact with the seat (m_4). The mass due to lower legs and feet is not included in this representation, assuming that their contribution to the biodynamic response of the seated body is negligible. Similarly, the hand and arm mass supported on the steering wheel is considered negligible. The stiffness and damping properties of the various body segments are represented by the constants k_i and c_i, respectively, where i = 1 to 4. The parameters of the model are estimated using the target values of both DPMI and STHT magnitude and phase at frequencies below 10 Hz. Model parameters are also defined on the basis of constraints imposed to relate to biomechanical data on mass, stiffness, and damping properties of body segments. The target values for DPMI are identified from laboratory measurements performed with seated subjects maintaining various postures under different types of random and sinusoidal excitations with 1.0 to 2.0 m/s^2 rms acceleration. The target values of STHT characteristics are established from the synthesis of published data reported under similar test conditions. The derived model provides closer agreement with the DPMI target values, and the main body resonant frequency predicted from both

biodynamic functions is found to correspond within close bounds to that expected for the human body. The parameters of this model are given as follows:

$m_1 = 5.31$ kg $\quad k_1 = 310$ kN/m $\quad c_1 = 400$ Ns/m

$m_2 = 28.49$ kg $\quad k_2 = 183$ kN/m $\quad c_2 = 4750$ Ns/m

$m_3 = 8.62$ kg $\quad k_3 = 162.8$ kN/m $\quad c_3 = 4585$ Ns/m

$m_4 = 12.78$ kg $\quad k_4 = 90$ kN/m $\quad c_4 = 2064$ Ns/m

$\sum_{i=1}^{4} m_i = 55.2$ kg

In this thesis, the 4-DOF biodynamic model is selected as the study model. The reasons for choosing this model are:

It is a seated MDOF model. The model components correspond to the body segments, so that the local vibration response characteristics of different body parts can be studied.

It is a linear model since within the excitation amplitude range considered in deriving the model (i.e. 1.0 to 2.0 m/s^2), the biodynamic response of the body was found to be independent of vibration amplitude [25].

The model parameters of this model satisfy two biodynamic functions (i.e. "to the body" biodynamic function: driving-point mechanical impedance, and "through the body" biodynamic function: seat-to-head transmissibility), while the model parameters for most of the biodynamic models satisfy only one function.

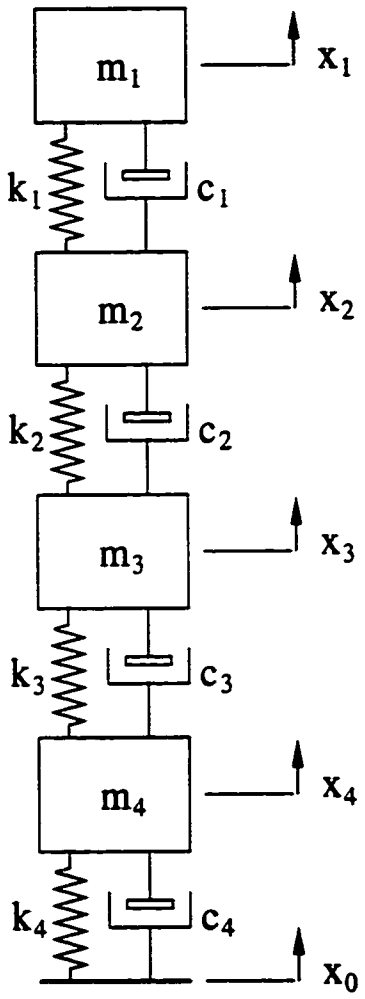

Figure 2.1 4-DOF linear biodynamic model proposed by Boileau (1995)

2.3 Eigenvalues and Natural Frequencies

The natural frequencies are the main factors influencing human response to WBV. The concept of the eigenvalue of a matrix is closely related to the concept of natural frequency of the vibration in dynamic structures, just as the roots of the characteristic equation and natural frequency of a SDOF system are related. For a MDOF system, therefore, the natual frequencies can be determined by solving the eigenvalue problem of the system.

2.3.1 Equations of motion of the system

By using Newton's law, the equations of motion for the model shown in Figure 2.1 can be derived as follows:

$$\begin{cases} m_1\ddot{x}_1 - c_1(\dot{x}_2 - \dot{x}_1) - k_1(x_2 - x_1) = 0 \\ m_2\ddot{x}_2 + c_1(\dot{x}_2 - \dot{x}_1) - c_2(\dot{x}_3 - \dot{x}_2) + k_1(x_2 - x_1) - k_2(x_3 - x_2) = 0 \\ m_3\ddot{x}_3 + c_2(\dot{x}_3 - \dot{x}_2) - c_3(\dot{x}_4 - \dot{x}_3) + k_2(x_3 - x_2) - k_3(x_4 - x_3) = 0 \\ m_4\ddot{x}_4 + c_3(\dot{x}_4 - \dot{x}_3) - c_4(\dot{x}_0 - \dot{x}_4) + k_3(x_4 - x_3) - k_4(x_0 - x_4) = 0 \end{cases} \tag{2.1}$$

where x_0 represents the displacement excitation, and x_1, x_2, x_3 and x_4 represent the displacement responses of the body segments m_1, m_2, m_3 and m_4, respectively.

2.3.2 Eigenvalue problem

Equation (2.1) may be written in matrix form as:

$$\begin{bmatrix} m_1 & 0 & 0 & 0 \\ 0 & m_2 & 0 & 0 \\ 0 & 0 & m_3 & 0 \\ 0 & 0 & 0 & m_4 \end{bmatrix} \begin{Bmatrix} \ddot{x}_1 \\ \ddot{x}_2 \\ \ddot{x}_3 \\ \ddot{x}_4 \end{Bmatrix} + \begin{bmatrix} c_1 & -c_1 & 0 & 0 \\ -c_1 & c_1+c_2 & -c_2 & 0 \\ 0 & -c_2 & c_2+c_3 & -c_3 \\ 0 & 0 & -c_3 & c_3+c_4 \end{bmatrix} \begin{Bmatrix} \dot{x}_1 \\ \dot{x}_2 \\ \dot{x}_3 \\ \dot{x}_4 \end{Bmatrix} +$$

$$\begin{bmatrix} k_1 & -k_1 & 0 & 0 \\ -k_1 & k_1+k_2 & -k_2 & 0 \\ 0 & -k_2 & k_2+k_3 & -k_3 \\ 0 & 0 & -k_3 & k_3+k_4 \end{bmatrix} \begin{Bmatrix} x_1 \\ x_2 \\ x_3 \\ x_4 \end{Bmatrix} = \begin{Bmatrix} 0 \\ 0 \\ 0 \\ k_4 x_0 + c_4 \dot{x}_0 \end{Bmatrix} \qquad (2.2)$$

Solving the homogeneous form of Equation (2.2), the eigenvalues are obtained as:

$\lambda_1 = -7.6 - 40.4i$ (Hz) $\qquad \lambda_2 = -7.6 + 40.4i$ (Hz)

$\lambda_3 = -213.7$ (Hz) $\qquad \lambda_4 = -49.6$ (Hz)

$\lambda_5 = -7.2$ (Hz) $\qquad \lambda_6 = -6.0$ (Hz)

$\lambda_7 = -2.0 - 4.7i$ (Hz) $\qquad \lambda_8 = -2.0 + 4.7i$ (Hz)

Only four of the complex natural frequencies (eigenvalues) have imaginary parts indicating that the system can perform free oscillations at only two frequencies, at 4.7 Hz, and at 40.4 Hz. The other four complex natural frequencies do not possess imaginary parts and hence do not have oscillations. The real parts of these four natural frequencies have negative values only, and thus the resulting motion decays down monotonically. These four modes are overdamped and more discussions on this behavior will follow in the next section.

2.4 Determination of Damping Ratios

The definitions of critical damping, overdamping, and underdamping in SDOF systems can be extended to MDOF systems. In order to determine the damping ratios (or damping matrix) of MDOF systems, the expression for the damping ratio for SDOF model is first derived.

2.4.1 Damping ratio for SDOF system

For a SDOF system, the equation of motion is obtained as:

$$m\ddot{x} + c\dot{x} + kx = 0 \tag{2.3}$$

Rewriting the equation after dividing through by m,

$$\ddot{x} + \frac{c}{m}\dot{x} + \frac{k}{m}x = 0 \tag{2.4}$$

Assuming $x = Ae^{\lambda t}$, and substituting into Equation (2.4), yields:

$$\lambda^2 + \frac{c}{m}\lambda + \frac{k}{m} = 0 \tag{2.5}$$

Introducing $c_s = \frac{c}{m}$, $k_s = \frac{k}{m}$, the Equation (2.5) becomes:

$$\lambda^2 + c_s\lambda + k_s = 0 \tag{2.6}$$

Equation (2.6) is the characteristic equation of Equation (2.3). The two solutions for eigenvalues λ are given as:

$$\lambda_{1,2} = -\frac{c_s}{2} \pm \frac{1}{2}\sqrt{c_s^{\,2} - 4k_s} \tag{2.7}$$

For Equation (2.7), as $c_s^{\,2} - 4k_s = 0$, the critical value of c_s is obtained as:

$$c_{cr} = 2k_s^{\,1/2} \tag{2.8}$$

The damping ratio is defined as:

$$\zeta = \frac{c_s}{c_{cr}} = \frac{c_s}{2\sqrt{k_s}} \tag{2.9}$$

2.4.2 Damping ratio matrix for MDOF system

For a MDOF system, the equations of motion may be written in a matrix form as:

$$\boldsymbol{M}\{\ddot{x}\} + \boldsymbol{C}\{\dot{x}\} + \boldsymbol{K}\{x\} = \boldsymbol{0} \tag{2.10}$$

Since the matrix $\boldsymbol{M}$ is positive definite, it has a positive definite square root. That is, there exists a unique positive definite matrix $\boldsymbol{M}^{1/2}$ such that $\boldsymbol{M}^{1/2}\,\boldsymbol{M}^{1/2} = \boldsymbol{M}$. The eigenvalues of $\boldsymbol{M}^{1/2}$ are $\beta_i^{1/2}$, where β_i are the eigenvalues of $\boldsymbol{M}$.

Thus, Equation (2.10) is rewritten as:

$$\{\ddot{x}\}+ M^{-1/2}C M^{-1/2}\{\dot{x}\}+ M^{-1/2}K M^{-1/2}\{x\}=0 \tag{2.11}$$

The difference between $M^{-1/2}C M^{-1/2}$, $M^{-1/2}K M^{-1/2}$and $M^{-1}C$, $M^{-1}K$ is that the matrices $M^{-1/2}C M^{-1/2}$, $M^{-1/2}K M^{-1/2}$are symmetric and positive definite, whereas $M^{-1}C$, $M^{-1}K$ are not necessarily symmetric.

Following the treatment of the SDOF system, introduce

$$C_s = M^{-1/2}C M^{-1/2} \tag{2.12}$$

$$K_s = M^{-1/2}K M^{-1/2} \tag{2.13}$$

In a form imitating the SDOF case, a critical damping matrix is defined to be:

$$C_{cr} = 2 K_s^{1/2} \tag{2.14}$$

The damping ratio matrix for a MDOF model is defined by:

$$Z = C_{cr}^{-1/2} C_s C_{cr}^{-1/2} \tag{2.15}$$

Furthermore, define the matrix Z_{diag} to be the diagonal matrix of eigenvalues of the matrix Z, *i.e.*(Inman (1990) [26]):

$$\boldsymbol{Z}_{diag} = \text{diag}[\lambda_i(\boldsymbol{Z})] = \text{diag}[\zeta_i^*] \tag{2.16}$$

where the ζ_i^* are modal damping ratios in that if $0 < \zeta_i^* < 1$, the system is underdamped, if $\zeta_i^* > 1$, the system is overdamped, if $\zeta_i^* = 1$, the system is critically damped, and if ζ_i^* are indefinite, the system is said to exhibit mixed damping.

For Equation (2.10), it may be seen that if $\boldsymbol{CM}^{-1}\boldsymbol{K} = \boldsymbol{KM}^{-1}\boldsymbol{C}$ (normal model case), then $\boldsymbol{Z} = \boldsymbol{Z}_{diag}$.

Then the following classifications (Inman and Andry (1980) [27]) can be derived.

- If $\boldsymbol{C}_s = \boldsymbol{C}_{cr}$ (or $[\boldsymbol{I} - \boldsymbol{Z}] = \boldsymbol{0}$, where $\boldsymbol{I}$ is the identical matrix), then the system is said to be a critically damped system, each mode of vibration is critically damped, and each eigenvalue of the system is a repeated negative real number. The response of such systems will not oscillate, and all the eigenvectors are real.
- If the matrix $\boldsymbol{C}_s - \boldsymbol{C}_{cr}$ is positive definite (or $[\boldsymbol{I} - \boldsymbol{Z}] < \boldsymbol{0}$), then the system is said to be an overdamped system, each "mode" of the structure is overdamped, and each eigenvalue is a negative real number. The response of such systems will not oscillate, and all the eigenvectors are real.
- If the matrix $\boldsymbol{C}_s - \boldsymbol{C}_{cr}$ is negative definite (or $[\boldsymbol{I} - \boldsymbol{Z}] > \boldsymbol{0}$), then the system is said to be an underdamped system, each mode of vibration is underdamped, and each eigenvalue is a complex conjugate pair with negative real part. The response of such systems oscillates with decaying amplitude and the eigenvectors are, in general, complex (unless $\boldsymbol{CM}^{-1}\boldsymbol{K} = \boldsymbol{KM}^{-1}\boldsymbol{C}$).

◊ A fourth possibility exists for the matrix case. That is, the matrix $C_s - C_{cr}$ (or $[I - Z]$) could be indefinite. In this case the system is said to exhibit mixed damping, and at least one mode oscillates and at least one mode does not oscillate.

2.4.3 Calculation of damping ratio matrix

Substituting the parameters of the system under study into Equations (2.12) to (2.14), the critical damping matrix is obtained as:

$$C_{cr} = \begin{bmatrix} 455.3476 & -160.4888 & -18.9432 & -8.0428 \\ -160.4888 & 185.0142 & -93.0351 & -23.9753 \\ -18.9432 & -93.0351 & 375.7953 & -101.1314 \\ -8.0428 & -23.9753 & -101.1314 & 261.2596 \end{bmatrix}$$

The damping ratio matrix is determined as follows, by using Equation (2.15).

$$Z = \begin{bmatrix} 0.1762 & 0.0831 & -0.0550 & -0.0451 \\ 0.0831 & 0.7461 & -0.6123 & -0.2000 \\ -0.0550 & -0.6123 & 2.5304 & -0.7597 \\ -0.0451 & -0.2000 & -0.7597 & 1.6719 \end{bmatrix}$$

The matrix $[I - Z]$ (where I is the identity matrix) is obtained as:

$$[I - Z] = \begin{bmatrix} 0.8238 & -0.0831 & 0.0550 & 0.0451 \\ -0.0831 & 0.2539 & 0.6123 & 0.2000 \\ 0.0550 & 0.6123 & -1.5304 & 0.7597 \\ 0.0451 & 0.2000 & 0.7597 & -0.6719 \end{bmatrix}$$

The matrix $[I - Z]$ is indefinite. Therefore, the system is said to exhibit mixed damping, based on above classifications.

Furthermore, considering

$$Z_{diag} = \text{diag}[\lambda_i(Z)] = \text{diag}[\zeta_i^*]$$

$$= \begin{bmatrix} 0.1637 & 0 & 0 & 0 \\ 0 & 1.5017 & 0 & 0 \\ 0 & 0 & 3.0571 & 0 \\ 0 & 0 & 0 & 0.4021 \end{bmatrix}$$

In the matrix of Z_{diag}, $0 < \zeta_1^* (= 0.1637) < 1$ and $0 < \zeta_3^* (= 0.4021) < 1$, and hence they are underdamped; however, $\zeta_2^* (= 1.5017) > 1$ and $\zeta_4^* (= 3.0571) > 1$, and they are overdamped. As a result, the model of human body considered here is a mixed damping system, and it is also established that the model has only two undamped natural frequencies and the other two are overdamped.

The system can be shown to be a mixed damping system using following approximate method.

The undamped modal frequencies are approximately expressed as:

$$\omega_i^* \approx \sqrt{\frac{k_i}{m_i}},$$

The modal damping ratios are approximately calculated by:

$$\varsigma_i^* = \frac{c_i}{c_{cri}} \approx \frac{c_i}{2\sqrt{k_i m_i}}$$

For damper 1,

$$\varsigma_1^* = \frac{c_1}{c_{cr1}} \approx \frac{c_1}{2\sqrt{k_1 m_1}} = \frac{400}{2\sqrt{310{,}000 * 5.31}} = 0.156 < 1$$

Underdamped

For damper 2,

$$\varsigma_2^* = \frac{c_2}{c_{cr2}} \approx \frac{c_2}{2\sqrt{k_2 m_2}} = \frac{4750}{2\sqrt{183{,}000 * 28.49}} = 1.040 > 1$$

Overdamped

For damper 3,

$$\varsigma_3^* = \frac{c_3}{c_{cr3}} \approx \frac{c_3}{2\sqrt{k_3 m_3}} = \frac{4585}{2\sqrt{162800 * 8.62}} = 1.935 > 1$$

Overdamped

For damper 4,

$$\varsigma_4^* = \frac{c_4}{c_{cr4}} \approx \frac{c_4}{2\sqrt{k_4 m_4}} = \frac{2064}{2\sqrt{90{,}000 * 12.78}} = 0.962 < 1$$

Underdamped

Consequently, the biodynamic system is a mixed damping model.

In fact, from an examination of the damping matrix or damping ratios of biodynamic models, it can be seen that they are generally mixed damping systems.

2.5 Stability of the Model

There are many theories that apply to the stability of MDOF systems. The most common method of analyzing the stability of such systems is to show the existence of a Liapunov function for the system. A Liapunov function, denoted by V(**x**), is a real scalar function of the vector **x**(t), which has continuous first partial derivatives and satisfies the following conditions:

1. $V(\mathbf{x}) > 0$ for all values of $\mathbf{x}(t) \neq 0$;
2. $\dot{V}(\mathbf{x}) \leq 0$ for all values of $\mathbf{x}(t) \neq 0$.

where $\dot{V}(\mathbf{x})$ denotes the time derivative of the function $V(\mathbf{x})$. For the 4-DOF model, $\mathbf{x}(t)=[x_1(t), x_2(t), x_3(t), x_4(t)]^T$.

Based on the definition of a Liapunov function, several extremely useful stability theorems can be stated. The first result states that if there exists a Liapunov function for a given system, then that system is stable. If, in addition, the function $\dot{V}(\mathbf{x})$ is strictly less than zero, the system is asymptotically stable. It should be noted that if a Liapunov function cannot be found, nothing can be concluded about the stability of the system, as the Liapunov theorems are only sufficient conditions for stability.

The stability of a system can also be characterized by the eigenvalues of the system, which is similar to the existence of a Liapunov function. In fact, it can be easily shown that a given linear system is stable if and only if it has no eigenvalue with positive real part. Moreover, the system will be asymptotically stable if and only if all of its

eigenvalues have negative real parts (no zero parts allowed). The eigenvalue approach to stability has the attraction of being both necessary and sufficient.

Consequently, the 4-DOF biodynamic model is asymptotically stable since the real parts of all of eight eigenvalues are negative.

2.6 Summary

A 4-DOF linear human driver model proposed by Boileau (1995) is selected for studying the biodynamic response characteristics of the whole-body and different segments in the body.

The selected 4-DOF model is a mixed damping system in which two modes oscillate and two modes are overdamped. In consequence, the model has only two natural frequencies at 4.7 Hz and 40.4 Hz, rather than four.

The 4-DOF system is asymptotically stable since the real parts of all of eight eigenvalues are negative.

The next chapter will discuss the frequency response, transmissibilities and the random response of the 4-DOF human body model.

CHAPTER 3

FREQUENCY RESPONSE, TRANSMISSIBILITIES, AND RANDOM RESPONSE

3.1 Introduction

The behavior of a dynamic system subjected to a certain excitation may be studied in terms of system-response analysis. System response may be studied either in the time domain, where the independent variable of system response is time, or in the frequency domain, where the independent variable of system response is frequency. Time-domain analysis and frequency domain analysis are equivalent but do not convey the same information for complex signals. Variables in the two domains are connected through Fourier (integral) transform or Laplace transform. The Frequency response function (FRF) and transmissibility frequency characteristics may be determined from the differential equation of motion of the model in terms of the transforms.

The biodynamic response behavior of the seated human body subjected to vibration has widely been characterized in terms of DPMI/APMS and STHT. While the first two biodynamic functions relate the force and motion at the point of entrance of vibration to the body ("to the body" transfer functions), the last function refers specifically to the transmission of motion through the body ("through the body" transfer function).

The vibration transmissibility through the body is usually examined between the seat surface (considered to be the input) and the head (considered to be the output). The interest in the head is mostly justified for consideration linked to ease of measuring vibration at the head in comparison to other internal organs or systems of the body.

However, there have been no past attempts to relate vertical seat-to-head transmissibility data to measures of discomfort, activity disturbance or health effects. Furthermore, the disadvantage of STHT is that it cannot characterize the response behaviors of different parts of the body.

Measurements to different body locations on the surface of the body have occasionally been reported: to the hip (Guignard, 1959) [28], shoulder (Rowlands, 1977) [29], thorax (Donati and Bonthoux, 1983) [30], and cervical vertebrae (Cooper, 1986) [31]. The FRFs or vibration transmissibility frequency transfer function from the seat to the different parts of the body have not been widely measured for obvious reasons associated with the difficulties in performing such measurements. The FRFs and the transmissibilities from seat to different body segments are computed on the basis of the 4-DOF biodynamic model described in chapter 2. The frequency weighting, DPMI of the model, and random responses are also discussed and calculated in this chapter.

3.2 Frequency Responses and Vibration Transmissibilities

Applying Laplace transformation, Equation (2.1) can be written as:

$$\begin{cases} (m_1 s^2 + c_1 s + k_1)X_1(s) - (c_1 s + k_1)X_2(s) = 0 \\ -(c_1 s + k_1)X_1(s) + (m_2 s^2 + c_1 s + c_2 s + k_1 + k_2)X_2(s) - (c_2 s + k_2)X_3(s) = 0 \\ -(c_2 s + k_2)X_2(s) + (m_3 s^2 + c_2 s + c_3 s + k_2 + k_3)X_3(s) - (c_3 s + k_3)X_4(s) = 0 \\ -(c_3 s + k_3)X_3(s) + (m_4 s^2 + c_3 s + c_4 s + k_3 + k_4)X_4(s) = (c_4 s + k_4)X_0(s) \end{cases} \quad (3.1)$$

These equations are written in matrix form as:

$$\begin{bmatrix} m_1s^2+c_1s+k_1 & -(c_1s+k_1) & 0 & 0 \\ -(c_1s+k_1) & m_2s^2+c_1s+c_2s+k_1+k_2 & -(c_2s+k_2) & 0 \\ 0 & -(c_2s+k_2) & m_3s^2+c_2s+c_3s+k_2+k_3 & -(c_3s+k_3) \\ 0 & 0 & -(c_3s+k_3) & m_4s^2+c_3s+c_4s+k_3+k_4 \end{bmatrix} \begin{Bmatrix} X_1(s) \\ X_2(s) \\ X_3(s) \\ X_4(s) \end{Bmatrix}$$

$$= \begin{Bmatrix} 0 \\ 0 \\ 0 \\ c_4s+k_4 \end{Bmatrix} X_0(s) \qquad (3.2)$$

Letting $s = j\omega$, the complex frequency response expressions are determined as:

$$\begin{Bmatrix} H_1(j\omega) \\ H_2(j\omega) \\ H_3(j\omega) \\ H_4(j\omega) \end{Bmatrix} = \begin{Bmatrix} X_1(j\omega)/X_0(j\omega) \\ X_2(j\omega)/X_0(j\omega) \\ X_3(j\omega)/X_0(j\omega) \\ X_4(j\omega)/X_0(j\omega) \end{Bmatrix} = [A]^{-1} \begin{Bmatrix} 0 \\ 0 \\ 0 \\ jc_4\omega+k_4 \end{Bmatrix} \qquad (3.3)$$

where

$$[A] =$$

$$\begin{bmatrix} -m_1\omega^2+jc_1\omega+k_1 & -(jc_1\omega+k_1) & 0 & 0 \\ -(jc_1\omega+k_1) & -m_2\omega^2+j\omega(c_1+c_2)+k_1+k_2 & -(jc_2\omega+k_2) & 0 \\ 0 & -(jc_2\omega+k_2) & -m_3\omega^2+j\omega(c_2+c_3)+k_2+k_3 & -(jc_3\omega+k_3) \\ 0 & 0 & -(jc_3\omega+k_3) & -m_4\omega^2+j\omega(c_3+c_4)+k_3+k_4 \end{bmatrix}$$

The magnitudes of the frequency response functions are given by:

$$\begin{Bmatrix} |H_1(j\omega)| \\ |H_2(j\omega)| \\ |H_3(j\omega)| \\ |H_4(j\omega)| \end{Bmatrix} = abs\left([A]^{-1} \begin{Bmatrix} 0 \\ 0 \\ 0 \\ jc_4\omega + k_4 \end{Bmatrix} \right) \tag{3.4}$$

The phases of the frequency response functions can be determined using following expressions:

$$\phi_i(j\omega) = \tan^{-1}\left(\frac{\text{Imag}(H_i(j\omega))}{\text{Real}(H_i(j\omega))} \right) \tag{3.5}$$

where $\text{Imag}(H_i(j\omega))$ and $\text{Real}(H_i(j\omega))$ represent the imaginary and real parts of the complex transfer function $H_i(j\omega)$.

From Equation (3.4), the transmissibility magnitude and phase responses can be determined at each frequency ω provided that the mass, stiffness and damping characteristics of the body segments are known.

For the model represented in Figure 2.1, the transmissibility characteristics within frequency regions of 0.4 to 20 Hz and 0.4 to 80 Hz are illustrated in Figure 3.1 and Figure 3.2, respectively. Figure 3.3 shows the real and imaginary parts of the corresponding frequency response functions (FRF) to each of the body segments represented in the model.

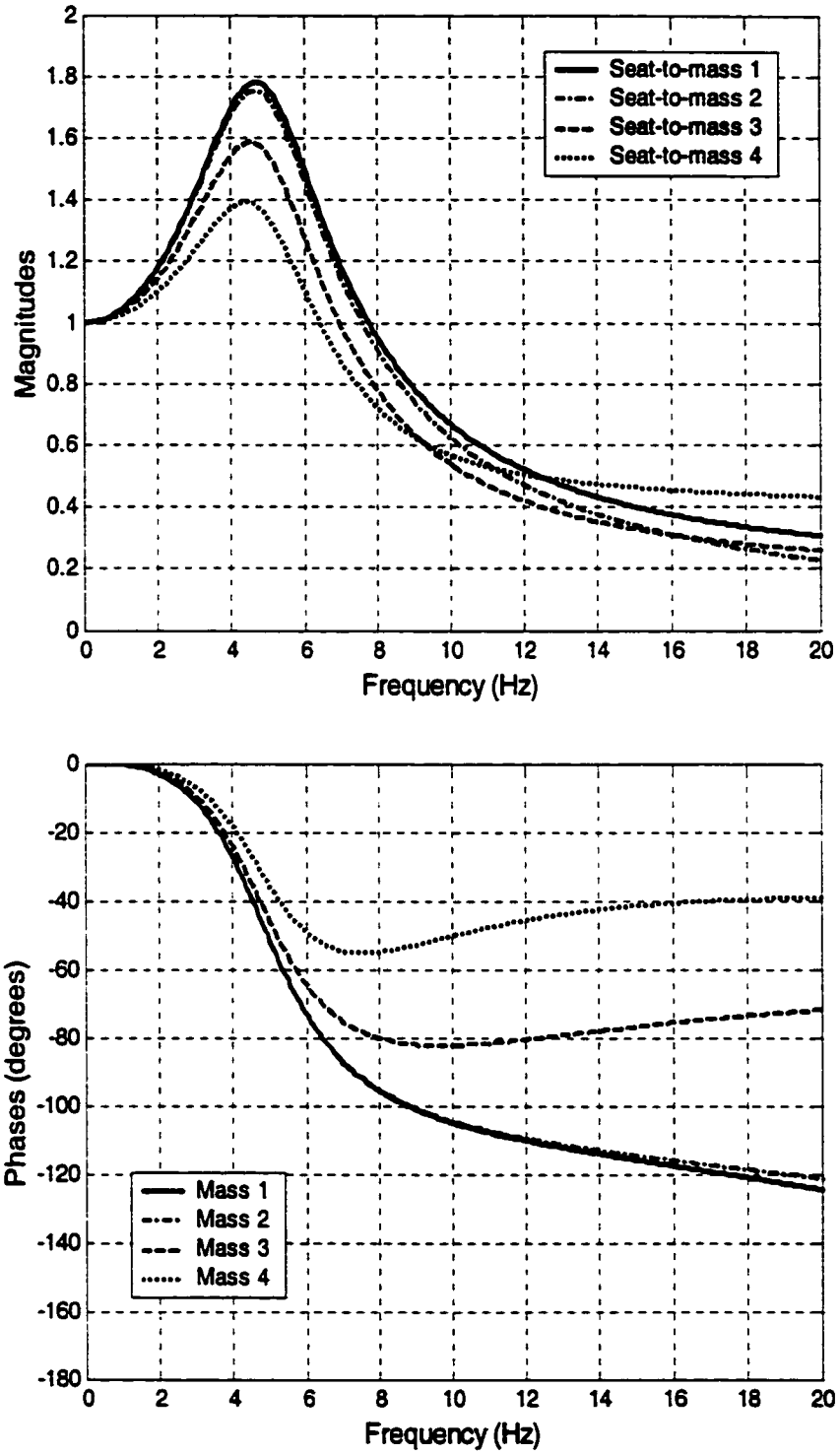

Figure 3.1 Transmissibility frequency characteristics (seat to body segments 1 to 4) within frequency range of 0.4 to 20 Hz

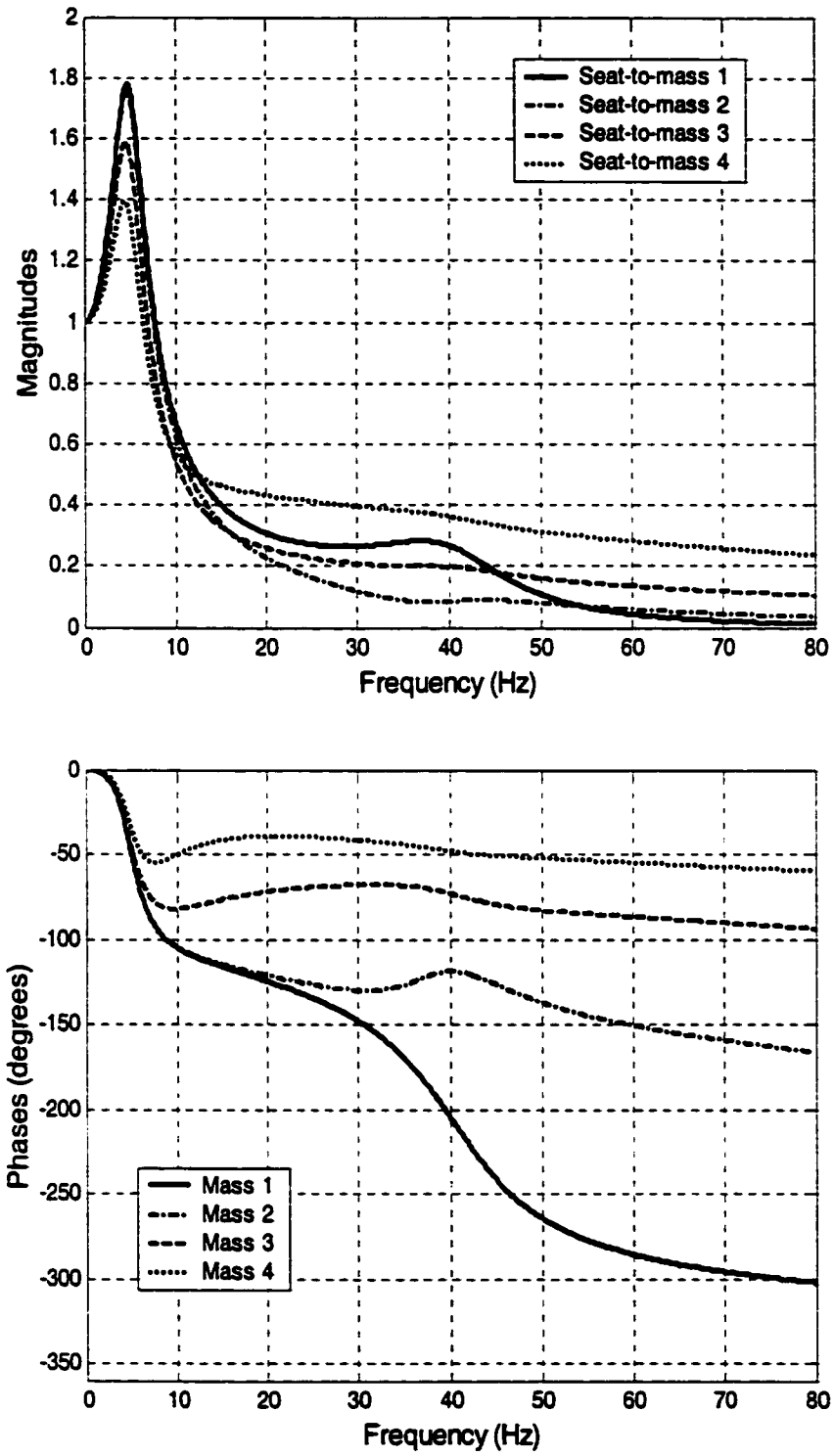

Figure 3.2 Transmissibility frequency characteristics (seat to body segments 1 to 4) within frequency range of 0.4 to 80 Hz

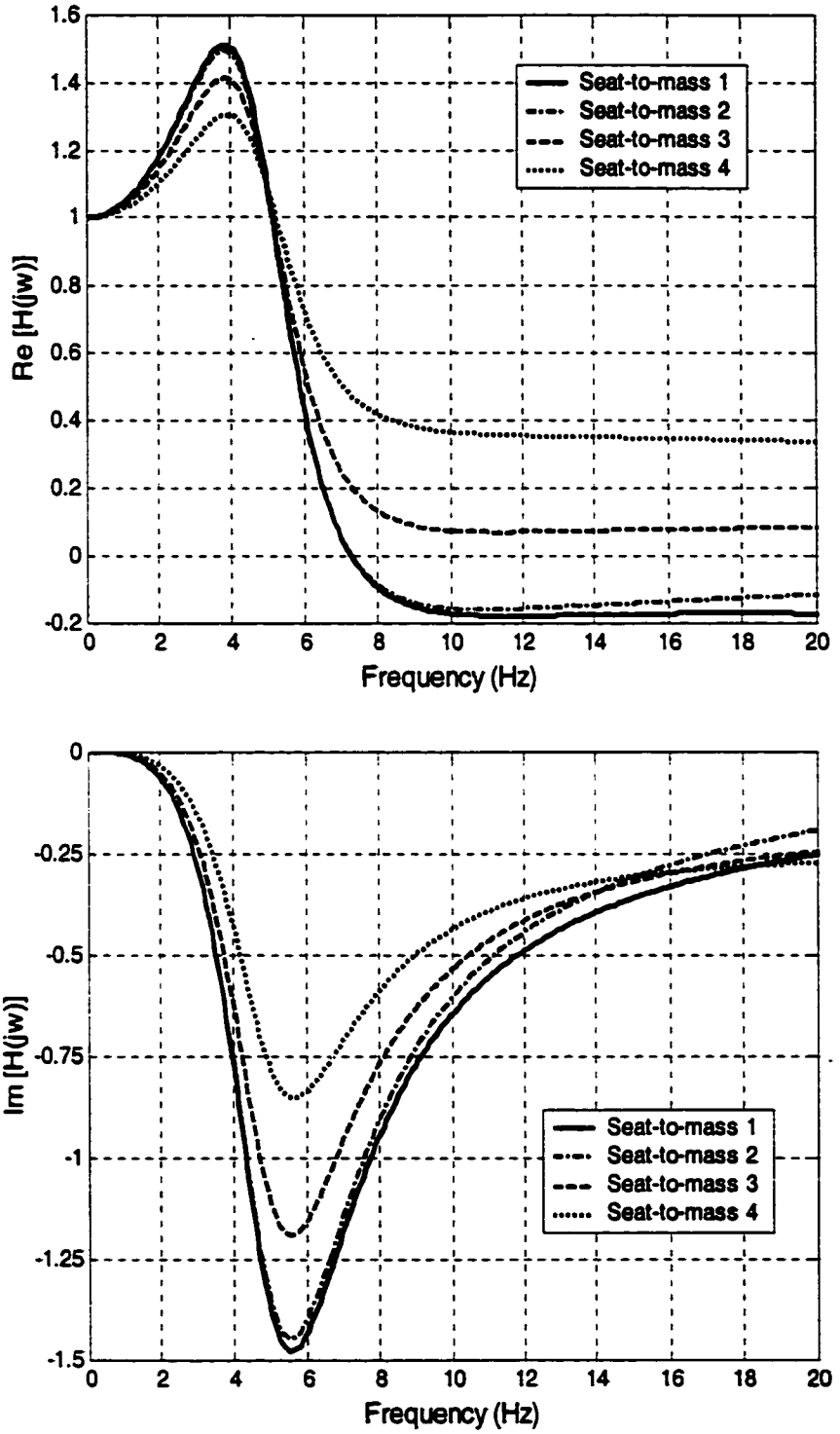

Figure 3.3 Real and imaginary parts of frequency response functions

(transmissibilities from seat to body segments 1 to 4)

From Figure 3.1, all of the curves of transmissiblities from seat to different segments in the body have peaks occurring at the first natural frequency close to 4.7 Hz. While the transmissibility from seat to the mass 1 (head) exhibits a resonant peak of 1.77 at the first natural frequency, the corresponding transmissibilities from seat to mass 2, 3, and 4 exhibit resonant peaks of 1.74, 1.59, and 1.40, respectively. The curves of transmissibilities from seat to different segments in the body have a relatively similar shape since all the masses (segments) are part of the same dynamical system. In consequence, all the segments in the body show a similar resonant peak but the peak magnitude may differ. Figure 3.1 also shows that the phases of transmissibilities from seat to different body segments have less difference at frequencies below 6 Hz, while they have large difference at frequencies above 10 Hz.

Figure 3.2 shows that the curves of the transmissibility characteristics from seat to mass 1 and seat to mass 4 have two peaks near the natural frequencies 4.7 Hz and 40.4 Hz (but the peak of the second one is very small). It also shows that both the curves of the transmissibilities from seat to mass 2 and seat to mass 3 have only one peak occurring at the first resonant frequency 4.7 Hz. These behaviors are in agreement with the calculations of eigenvalues and damping ratios in Chapter 2, which concludes that the 4-DOF biodynamic model is a mixed damping system, and it has only two natural frequencies due to the overdamped modes of mass 2 and mass 3.

Figure 3.3 illustrates that the peaks of the real parts of FRF occur close to a frequency of 3.8 Hz. The peak values of the real parts of the FRFs from seat-to-mass 1, seat-to-mass 2, seat-to-mass 3, and seat-to-mass 4 are 1.51, 1.50, 1.41, and 1.30, respectively. The peaks of the imaginary parts of FRFs shown in Figure 3.3, occur close

to a frequency of 5.5 Hz. The peak values of the imaginary parts of FRF are –1.48, -1.45, -1.19, and –0.85 for seat to mass 1, mass 2, mass 3, and mass 4, respectively.

3.3 Driving-Point Mechanical Impedance (DPMI)

According to the definition given by the International Standard ISO/DIS 5982 (2000) [6], the DPMI is calculated from:

$$Z(j\omega) = \frac{F(j\omega)}{v(j\omega)} = \left|Z(j\omega)\right| \cdot e^{j\phi_z(\omega)} \tag{3.6}$$

where $Z(j\omega)$ and $F(j\omega)$ represent the complex driving-point mechanical impedance and the force driving the system at the angular frequency ω; $v(j\omega)$ is the resulting vertical velocity of the system due to the applied force; $\left|Z(j\omega)\right|$ is the magnitude of the complex impedance; and $\phi_z(\omega)$ is the phase angle between the applied force and the resultant velocity.

The DPMI is a complex quantity, that is, it possesses real and imaginary parts, from which may be computed the modulus and phase.

The International Standard ISO 5982 (2000) is based on measurements in which both vertical force and velocity were measured at the same point, this being the point of introduction of vibration to the body, namely the buttocks or seat-body interface.

In the case of non-harmonic vibration, DPMI is determined from the force and velocity frequency spectra.

The DPMI of the 4-DOF linear human driving model is derived from:

$$Z(j\omega) = \frac{(k_4 + j\omega c_4)[X_0(j\omega) - X_4(j\omega)]}{j\omega X_0(j\omega)}$$

$$= \frac{k_4 + j\omega c_4}{j\omega}[1 - H_4(j\omega)]$$

$$= \frac{k_4 + j\omega c_4}{j\omega}\left[1 - 2|H_4(j\omega)|\cos\phi_4 + |H_4(j\omega)|^2\right]^{\frac{1}{2}} \tag{3.7}$$

where $H_4(j\omega)$, and $|H_4(j\omega)|$ are the complex and magnitude transmissibility from seat-to-mass 4.

The magnitude of DPMI, $|Z(j\omega)|$ may be obtained from Equation (3.7), and the phase of DPMI may be computed from:

$$\phi_z(j\omega) = \tan^{-1}\left(\frac{\text{Imag}(Z(j\omega))}{\text{Real}(Z(j\omega))}\right) \tag{3.8}$$

where $\text{Imag}(Z(j\omega))$ and $\text{Real}(Z(j\omega))$ represent the imaginary and real parts, respectively, of the complex DPMI, $Z(j\omega)$.

The DPMI characteristics of the 4-DOF system is illustrated in Figure 3.4, from which the peak mechanical impedance modulus is observed to occur around 5 Hz, that is next to the first natural frequency of 4.7 Hz computed for the model. The peak model response of the DPMI is 2833 Ns/m.

Figure 3.5 illustrates the real part and imaginary part vs. frequency plots of DPMI. The peak values of real and imaginary parts of DPMI occur at the frequency 6.2 Hz and 4.3 Hz, respectively.

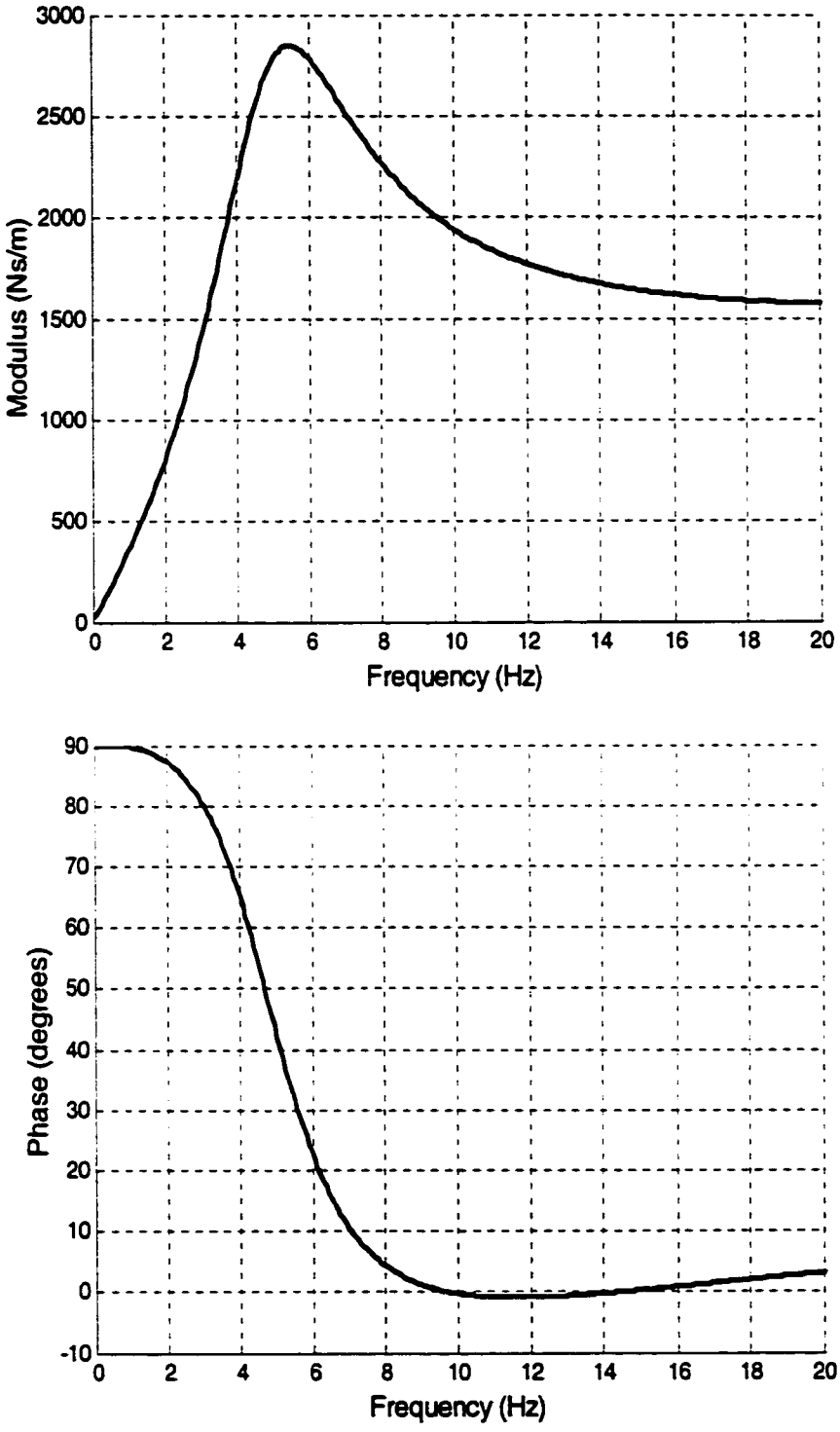

Figure 3.4 Driving-point mechanical impedance characteristics computed from the 4-DOF model

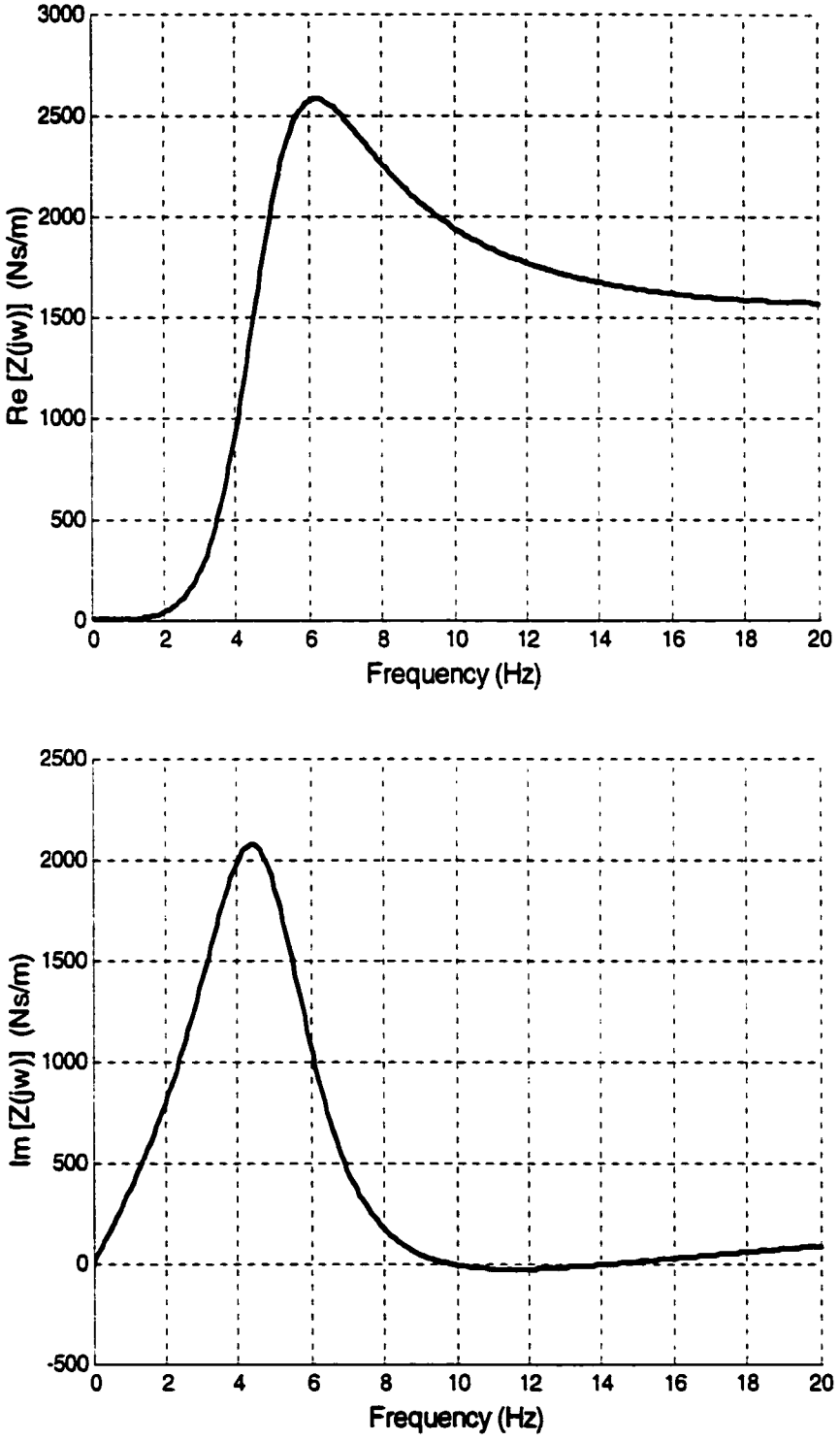

Figure 3.5 Real and imaginary parts of DPMI of the 4-DOF model

3.4 Apparent Mass (APMS)

The apparent mass (APMS) relates the driving force and the resulting acceleration response, and is related to the DPMI by:

$$M(j\omega) = \frac{F(j\omega)}{a(j\omega)} = \frac{Z(j\omega)}{j\omega} \tag{3.9}$$

where $a(j\omega)$ is the driving-point acceleration response.

The magnitude of APMS, $|M(j\omega)|$ may be obtained from Equation (3.9), and the phase of APMS may be calculated from:

$$\phi_M(j\omega) = \tan^{-1}\left(\frac{\text{Imag}\left(M(j\omega)\right)}{\text{Real}\left(M(j\omega)\right)}\right) \tag{3.10}$$

where $\text{Imag}(M(j\omega))$ and $\text{Real}(M(j\omega))$ represent the imaginary and real parts, respectively, of the complex APMS, $M(j\omega)$.

The APMS characteristics of the 4-DOF model is illustrated in Figure 3.6, from which peak apparent mass modulus is observed to occur at 4.6 Hz, that is next to the first natural frequency of 4.7 Hz computed for the model. The peak model response of the APMS is 90.5 kg.

Figure 3.7 illustrates the real and imaginary parts of APMS. The peak values of real and imaginary parts of APMS occur at the frequency of 4.0 Hz and 5.6 Hz, respectively.

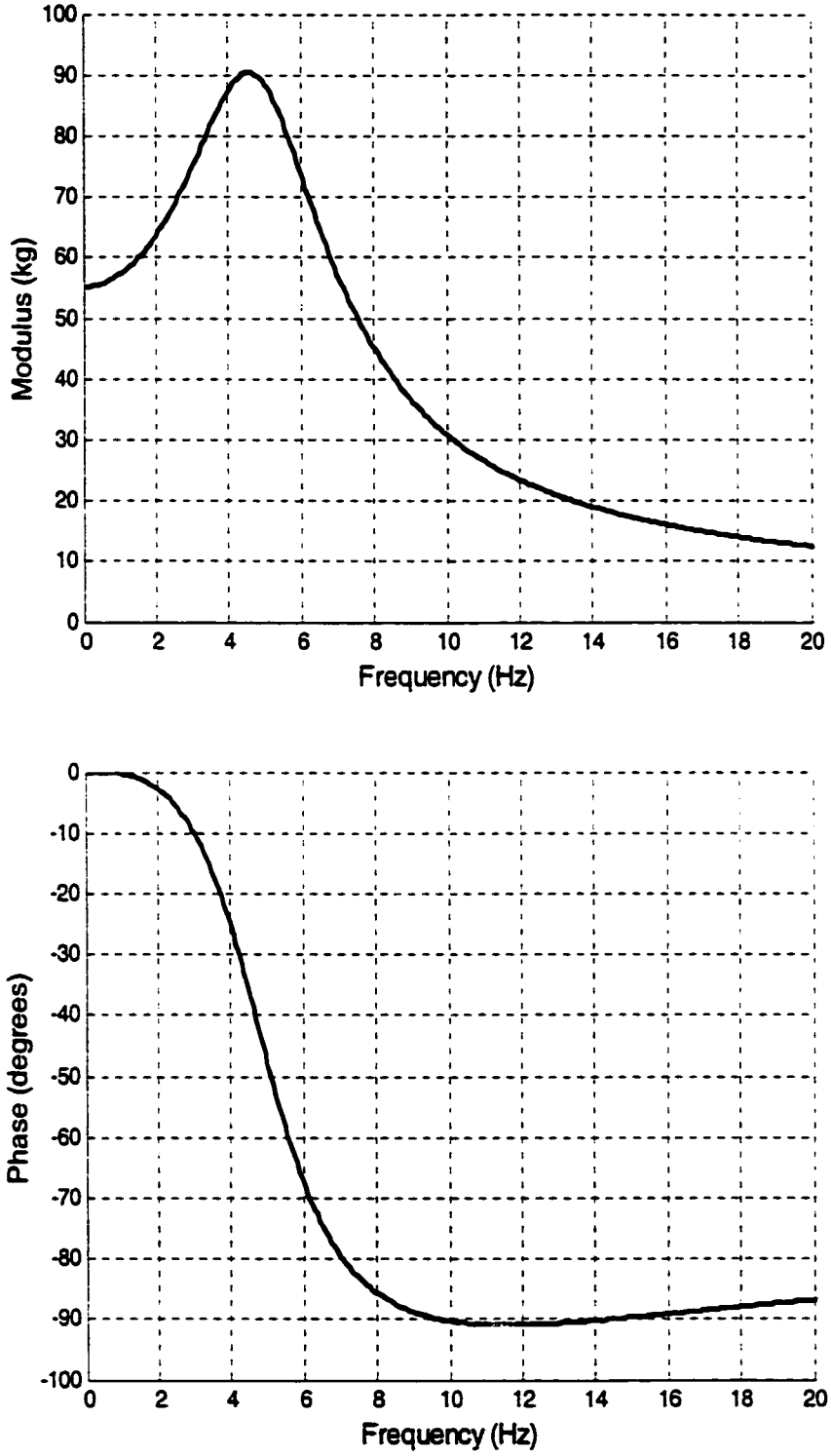

Figure 3.6 Apparent mass characteristics computed from the 4-DOF model

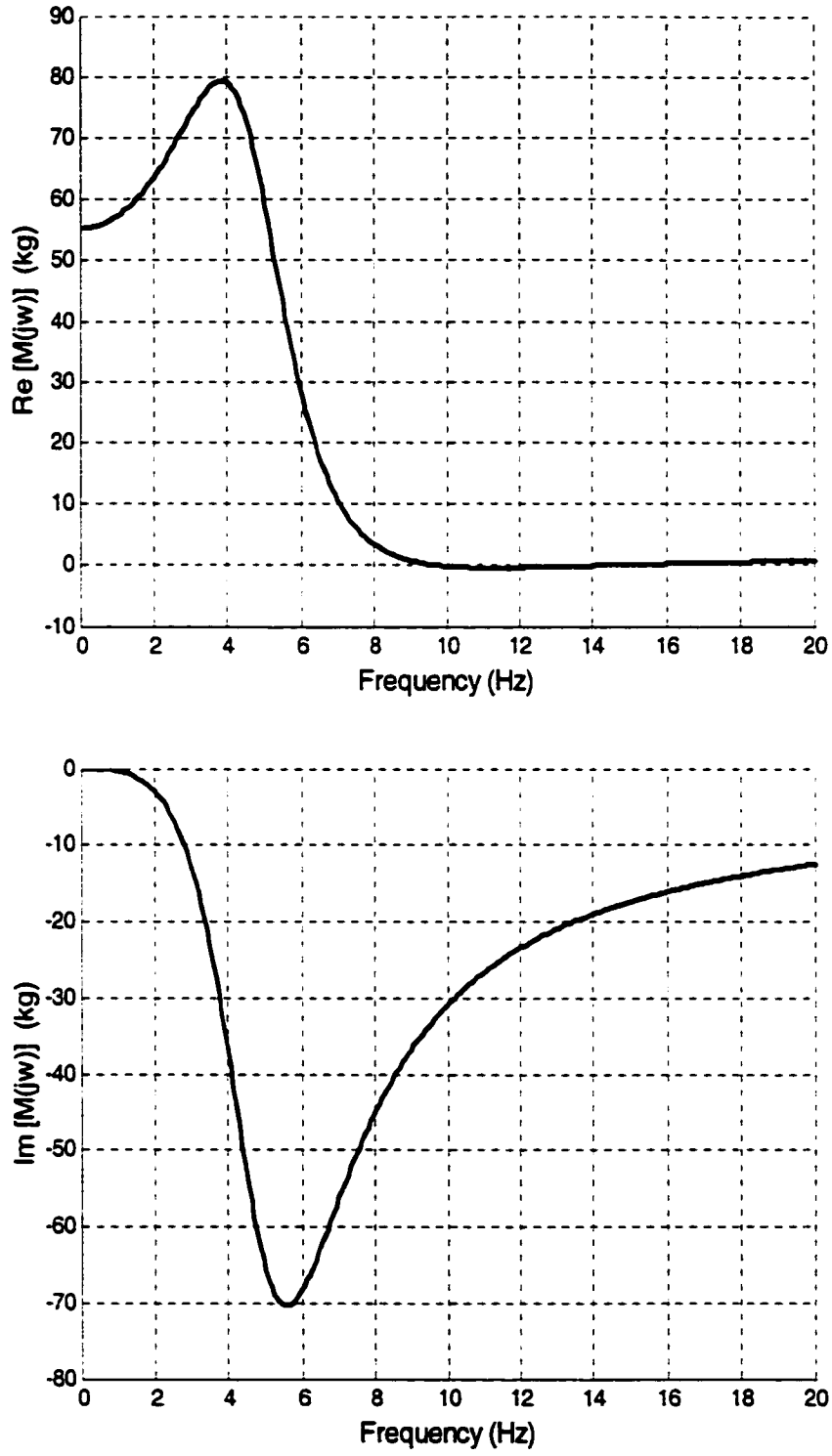

Figure 3.7 Real and imaginary parts of APMS of the 4-DOF model

3.5 Frequency Weighting

According to ISO 2631-1 (1997), the assessment of the hazardous effects of WBV shall be made with respect to the highest directional component of frequency-weighted rms acceleration measured at the point of contact of the body with the vibrating surface. For computing the frequency-weighted acceleration time history, the frequency weighting defined in chapter 1 should be applied. The purpose for applying a frequency weighting procedure is to compensate for the differences in human susceptibility at different frequencies. Frequency weighting functions may differ for different axes of vibration, for different measurement points and whether the influence of vibration is regarded with respect to health, comfort, perception and motion sickness.

For assessing the health effects of vertical vibration measured on the seat, the frequency weighting, W_k defined in International Standard ISO 2631-1 (1997), is used as defined in the frequency range of 0.4 to 100 Hz.

The frequency weighting function is defined from the combination of a band-limiting transfer function, $H_h(p)\cdot H_l(p)$ (*i.e.* high-pass and low-pass filters), and the actual weighting transfer function for a certain application, $H_t(p)\cdot H_s(p)$. The total frequency weighting function is obtained by:

$$W_k(p) = H_h(p)\cdot H_l(p)\cdot H_t(p)\cdot H_s(p) \tag{3.11}$$

where, $H_h(p)$ is high pass of the band-limiting pole filter with Butterworth characteristic, $Q_1 = Q_2 = 1/\sqrt{2}$, and it is mathematically expressed as:

$$|H_h(p)| = \left| \frac{1}{1+\sqrt{2}\omega_1 / p + (\omega_1 / p)^2} \right| = \sqrt{\frac{f^4}{f^4 + f_1^4}} \tag{3.12}$$

in which, f_1 is the corner frequency (intersection of asymptotes), and

$$p = j2\pi f \qquad \omega_1 = j2\pi f_1$$

$H_l(p)$ is low pass of the band-limiting pole filter with Butterworth characteristic, $Q_1 = Q_2 = 1/\sqrt{2}$, and it is mathematically represented as:

$$|H_l(p)| = \left| \frac{1}{1+\sqrt{2}p/\omega_2 + (p/\omega_2)^2} \right| = \sqrt{\frac{f_2^4}{f^4 + f_2^4}} \tag{3.13}$$

in which, f_2 is the corner frequency, and:

$$p = j2\pi f \qquad \omega_2 = j2\pi f_2$$

$H_t(p)$ is the acceleration-velocity transition, and it is mathematically expressed as:

$$|H_t(p)| = \left| \frac{1 + p/\omega_3}{1 + p/(Q_4\omega_4) + (p/\omega_4)^2} \right|$$

$$= \sqrt{\frac{f^2 + f_3^2}{f_3^2}} \cdot \sqrt{\frac{f_4^4 \cdot Q_4^2}{f^4 \cdot Q_4^2 + f^2 \cdot f_4^2 (1 - 2Q_4^2) + f_4^4 \cdot Q_4^2}} \tag{3.14}$$

in which:

$$\omega_3 = j2\pi f_3 \qquad \omega_4 = j2\pi f_4$$

$H_s(p)$ is the upward step (steepness approximately 6 dB per octave, proportionality to jerk), and it is mathematically expressed as:

$$|H_s(p)| = \left| \frac{1 + p/(Q_5\omega_5) + (p/\omega_5)}{1 + p/(Q_6\omega_6) + (p/\omega_6)^2} \cdot \left(\frac{\omega_5}{\omega_6}\right)^2 \right|$$

$$= \frac{Q_6}{Q_5} \cdot \sqrt{\frac{f^4 \cdot Q_5^2 + f^2 \cdot f_5^2 \left(1 - 2Q_5^2\right) + f_5^4 \cdot Q_5^2}{f^4 \cdot Q_6^2 + f^2 \cdot f_6^2 \left(1 - 2Q_6^2\right) + f_6^4 \cdot Q_6^2}} \qquad (3.15)$$

in which,

$$\omega_5 = j2\pi f_5 \qquad \omega_6 = j2\pi f_6$$

The parameters of the transfer functions are given in Table 3.1.

Table 3.1 Parameters of the transfer functions of the principal frequency weighting, W_k.

Band-limiting		Acceleration-velocity transition (a-v transition)			Upward step			
f_1 (Hz)	f_2 (Hz)	f_3 (Hz)	f_4 (Hz)	Q_4	f_5 (Hz)	Q_5	f_6 (Hz)	Q_6
0.4	100	12.5	12.5	0.63	2.37	0.91	3.35	0.91

The frequency-weighting curve for principal weighting, W_k are shown in Figure 1.1, where the weighting factors are expressed in dB.

3.6 Random Responses

3.6.1 Basic concepts and terminology

First, some concepts and terminology required to describe random signals need to be established. A random signal is stationary if its statistical properties (such as its root mean square value) are time-independent. For random signals, it is not possible to focus on the details of the signal, as it with a pure deterministic signal. Thus, random signals are classified and manipulated in terms of their statistical properties.

In the time domain, the average of the random acceleration signal $a(t)$ is defined and denoted by:

$$\bar{a}(t) = \lim_{T \to \infty} \frac{1}{T} \int_0^T a(t)dt \tag{3.16}$$

For a digital signal, the definition of average becomes:

$$\bar{a}(t_i) = \lim_{N \to \infty} \frac{1}{N} \sum_{i=1}^{N} a(t_i) \tag{3.17}$$

where N is the number of samples.

The rms value of acceleration $a(t)$ is just the square root of the variance, *i.e.*:

$$a_{rms} = \left[\frac{1}{T} \int_0^T a^2(t)dt \right]^{1/2} \tag{3.18}$$

or, in digital form:

$$a_{rms} = \left[\lim_{N \to \infty} \frac{1}{N} \sum_{i=1}^{N} a^2(t_i) \right]^{1/2} \tag{3.19}$$

The rms value of frequency-weighted acceleration $a_w(t)$ is computed from:

$$a_{w,rms} = \left[\frac{1}{T} \int_0^T a_w^2(t) dt \right]^{1/2} \tag{3.20}$$

or in digital form,

$$a_{w,rms} = \left[\lim_{N \to \infty} \frac{1}{N} \sum_{i=1}^{N} a_w^2(t_i) \right]^{1/2} \tag{3.21}$$

The autocorrelation function used as a measure of how fast the signal $a(t)$ is changing in the time domain, denoted by $R(t)$, is defined by [32]:

$$R(t) = a^2 = \lim_{T \to \infty} \frac{1}{T} \int_0^T a(\tau) a(\tau + t) d\tau \tag{3.22}$$

Note that $R(0)$ is the mean square value of $a(t)$. The autocorrelation function is also useful for detecting the presence of periodic signals contained in, or buried in, random signals. If $a(t)$ is periodic or has a periodic component, then $R(t)$ will be periodic instead of approaching zero as $T \to \infty$, as required for a purely random $a(t)$.

The digital form of the autocorrelation function is:

$$R(r,\Delta t)=\frac{1}{N-r}\sum_{i=0}^{N-r}a_i a_{i+r} \tag{3.23}$$

Here, N is the number of samples, Δt the sampling interval, and r is an adjustable parameter, called a lag value, that controls the number of points used to calculate the autocorrelation function.

In the frequency domain, the power spectral density (PSD) is used to measure the speed with which the random variable $a(t)$ changes. The power spectral density of acceleration, denoted by $S(\omega)$, is defined to be the Fourier transform of $R(t)$, *i.e.*:

$$S(\omega)=\frac{1}{2\pi}\int_{-\infty}^{+\infty}R(\tau)e^{-j\omega\tau}d\tau \tag{3.24}$$

In frequency domain, the rms value of acceleration is defined as:

$$a_{rms}=\left[\int_{\omega_1}^{\omega_2}S(\omega)d\omega\right]^{1/2} \tag{3.25}$$

The frequency-weighted rms acceleration is defined as:

$$a_{w,rms}=\left[\int_{\omega_1}^{\omega_2}|W(j\omega)|^2 S(\omega)d\omega\right]^{1/2}=\left[\int_{\omega_1}^{\omega_2}S_w(\omega)d\omega\right]^{1/2} \tag{3.26}$$

where $W(j\omega)$ represents the frequency weighting function given by Equation (3.11), and $S_w(\omega)$ is the frequency-weighted acceleration PSD.

3.6.2 Acceleration PSD for input spectral class IT 1

A random excitation input is considered having characteristics as defined in a proposed European Standard prEN 13490 (1999) [33] to represent the vertical vibration acting at the seat base for a particular category of forklift trucks. The input spectral class identified as IT 1 (*i.e.* industrial truck, category 1) is represented by the power spectral density $S_0(jf)$ of input vibration expressed as:

$$S_0(jf) = 1.66(HP24)^2(LP12)^2 \tag{3.27}$$

where HP24 designates high-pass filters of the butter-worth type with attenuation of 24 dB per octave, while LP12 indicates a corresponding low-pass filter with 12 dB attenuation per octave.

These filter transfer functions are given by:

$$(HP24) = \frac{s_0^4}{1+2.613s_0+3.414s_0^2+2.613s_0^3+s_0^4} \tag{3.28}$$

$$(LP12) = \frac{1}{1+1.414s_0+s_0^2} \tag{3.29}$$

in which, $s_0 = j\frac{f}{f_c}$; f = frequency in Hz; f_c = filter cut-off frequency in Hz. For *HP*24 and *LP*12, f_c is set equal to 4.5 and 5.0 Hz, respectively.

Figure 3.8 shows the acceleration power spectral density (PSD) of forklift excitation class IT 1 defined by Equations (3.27) to (3.29). The peak PSD acceleration, 0.58 $(ms^{-2})^2$/Hz is seen to occur at a frequency of 5.12 Hz, which is close to the first natural frequency 4.7 Hz of the whole body as given by the biodynamic model.

3.6.3 PSD of acceleration response for each mass

When a system is subjected to a random excitation, the corresponding system responses will also be random.

For a SDOF system, the PSD of unweighted acceleration response is given by:

$$S(j\omega) = H^*(j\omega)H(j\omega)S_0(j\omega) \tag{3.30}$$

in which $H^*(j\omega)$ is the complex conjugate of FRF, $H(j\omega)$; $S_0(j\omega)$ and $S(j\omega)$ are PSD of acceleration for input and PSD of acceleration response, respectively.

Alternatively, if $|H(j\omega)|$ denotes the magnitude of the complex quantity:

$$S(j\omega) = |H(j\omega)|^2 S_0(j\omega) \tag{3.31}$$

For a MDOF system, the PSD of unweighted and weighted acceleration responses may be calculated from following expressions:

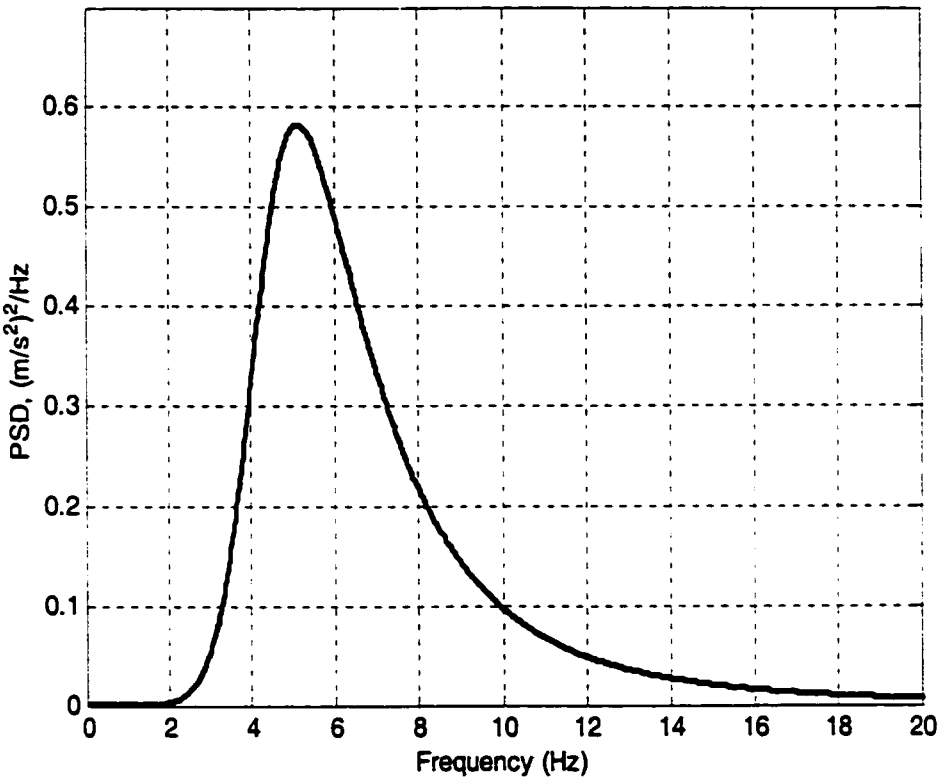

Figure 3.8 Acceleration PSD of IT 1 excitation in the vertical direction as defined in European Standard prEN 13490 (1999) [33]

$$\{S(j\omega)\} = \{|H(j\omega)|^2\}\{S_0(j\omega)\} \tag{3.32}$$

$$\{S_w(j\omega)\} = W_k^2(j\omega)\{|H(j\omega)|^2\}\{S_0(j\omega)\} \tag{3.33}$$

These are rewritten as:

$$S_i(j\omega) = |H_i(j\omega)|^2 S_0(j\omega) \quad (i = 1, 2, \ldots, n) \tag{3.34}$$

$$S_{wi}(j\omega) = W_k^2(j\omega)|H_i(j\omega)|^2 S_0(j\omega) \quad (i = 1, 2, \ldots, n) \tag{3.35}$$

where $S_i(j\omega)$, $S_{wi}(j\omega)$ denote the unweighted and weighted acceleration PSD responses of mass i due to excitation of acceleration PSD, $S_0(j\omega)$; $|H_i(j\omega)|$ represents the acceleration transmissibility magnitude between mass i and base; and $W_k(j\omega)$ represents the frequency weighting function given by Equation (3.11).

Figures 3.9 and 3.10 illustrate PSD of unweighted and weighted acceleration responses computed for mass 1, 2, 3, and 4, respectively under IT1 excitation using Equations (3.35) and (3.36). Each of the maximum values of unweighted and weighted PSD acceleration responses of different body segments occurs around the first natural frequency of 4.7 Hz. Figures 3.9 and 3.10 also illustrate that the largest PSD acceleration response occurs in mass 1 (head), while the smallest PSD acceleration occurs in mass 4 (thighs and pelvis) in contact with the seat.

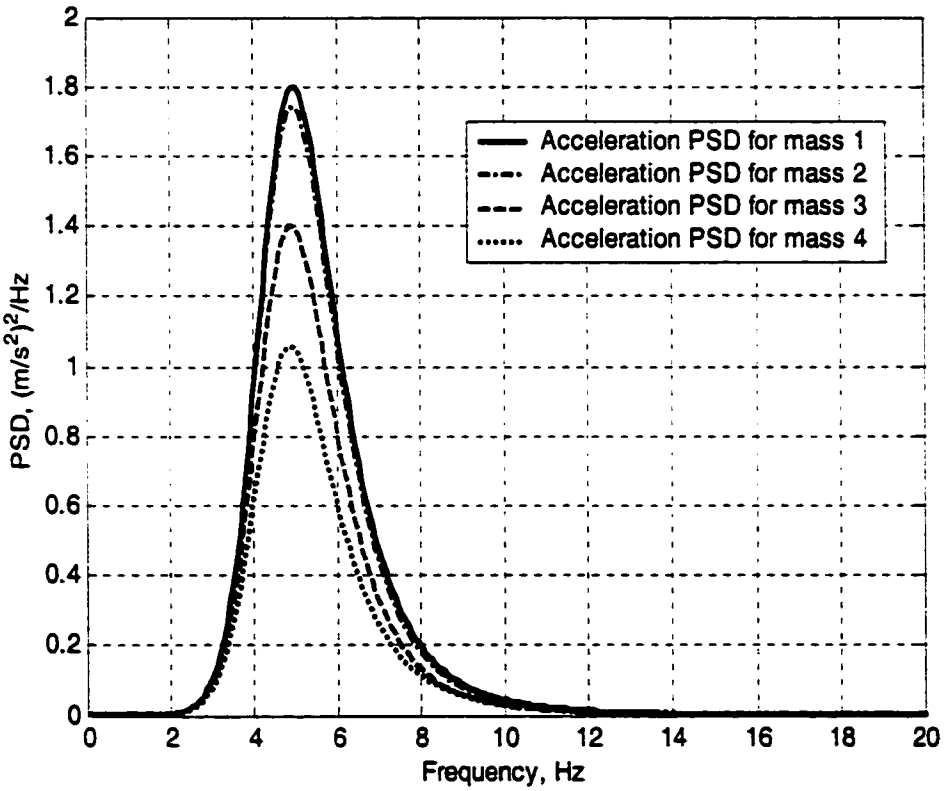

Figure 3.9 Unweighted acceleration PSD responses for different body segments under the random excitation IT 1

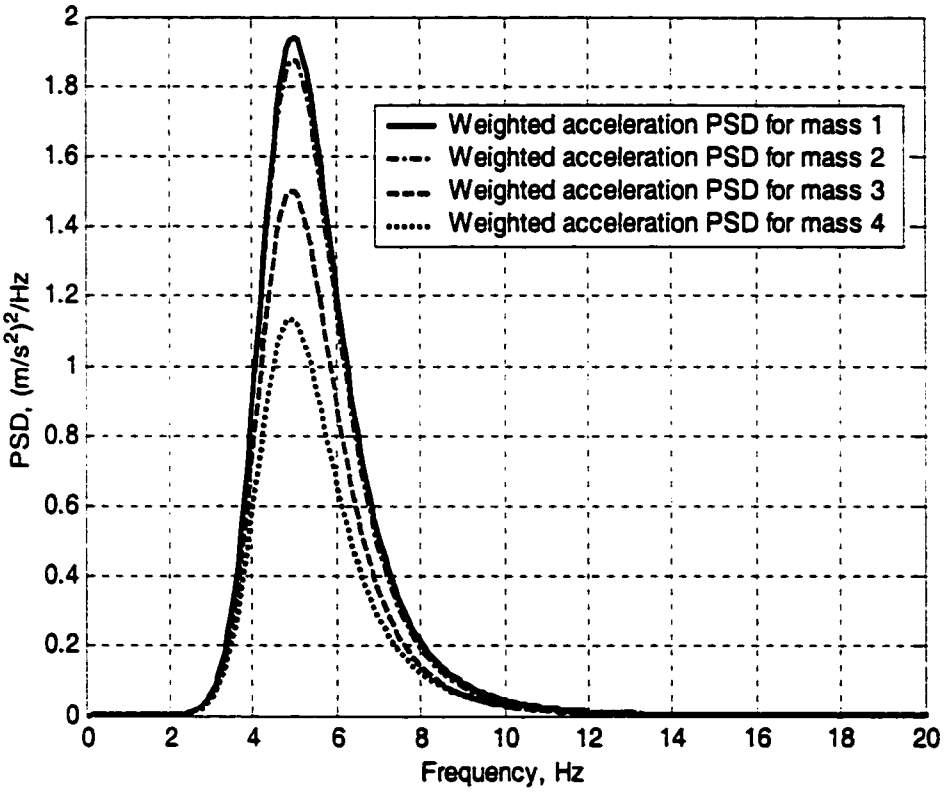

Figure 3.10 Weighted acceleration PSD responses for body segments under the random excitation IT 1

3.7 Summary

The transmissibility characteristics from seat to different body segments are determined. The peak transmissibility magnitude values for seat to mass 1, 2, 3, and 4 are 1.77, 1.74, 1.59, and 1.40, respectively. The transmissibilities from seat to different body segments resemble each other since all of masses (segments) are parts of the same vibrating system. Peaks occur near the first natural frequency, 4.7 Hz, for each of the above transmissibilities.

The curves of transmissibilities from seat to mass 1 and 4 have two peaks: one occurring at the first natural frequency of 4.7 Hz and the other at the second natural frequency of 40.4 Hz. The curves of transmissibilities from seat to masses 2 and 3 have only one peak at the first natural frequency of 4.7 Hz. These results are in agreement with the computations of natural frequencies and damping ratios reported in the previous chapter.

The calculations and plots of DPMI and APMS of the model show that the maximum values of the both DPMI and APMS occur near the first natural frequency, 4.7 Hz, of the 4-DOF model. The results are in agreement with those of transmissibility characteristics.

CHAPTER 4

ABSORBED POWER, HEALTH RISK

4.1 Introduction

In this chapter, the 4-DOF biodynamic model is analyzed to compute the absorbed power within the different body segments and for the total body. On the basis of the model and of the guidance provided in ISO 2631-1 (1997) to relate vibration exposure with health risks, computations are performed to define a health guidance caution zone based on absorbed power.

4.2 Absorbed Power Under Harmonic Excitation

4.2.1 Basic derivation of absorbed power

By definition, the instantaneous power transmitted to the body may be represented by:

$$P_{tr}(t) = F(t).v(t) = P_{abs}(t) + P_{el}(t) \tag{4.1}$$

where $F(t)$ and $v(t)$ represent the instantaneous force acting on the body and the input velocity, respectively; $P_{abs}(t)$ is the absorbed power; and $P_{el}(t)$ is the elastic power. For a system such as that shown in Figure 2.1, absorbed power is the power dissipated in the dampers while the elastic power is the power stored and released in the spring.

Averaged over a complete number of cycles, the fluctuating component is given by:

$$< P_{tr} >=< F(t).v(t) >=< P_{abs}(t) > + < P_{el}(t) > \tag{4.2}$$

where, the average elastic power per cycle is computed from:

$$< P_{el} >= \frac{E_{el}}{T} = \frac{1}{T}\int_0^T kx(x)dt \tag{4.3}$$

When the system is subjected to a sinusoidal excitation, $x_0 = X_0 \sin(\omega t + \phi_0)$, the absorbed power in each damper and the total absorbed power, averaged over a complete number of cycles, are derived as follows:

For each damper i shown in Figure 2.1, the unweighted absorbed powers in different segments of the body, averaged over a complete number of cycles, are given by:

$$< P_{abs} >_i = \frac{1}{T}\int_0^T c_i(\dot{x}_i - \dot{x}_{i+1})^2 dt$$

$$= \frac{\omega}{2\pi}\int_0^{2\pi/\omega} c_i\omega^2[X_i\cos(\omega t + \phi_i) - X_{i+1}\cos(\omega t + \phi_{i+1})]^2 dt \tag{4.4}$$

Solving for the integral, the absorbed power in the ith segment of the body becomes:

$$< P_{abs} >_i = \frac{1}{2}c_i\omega^2\left[X_i^{\,2} - 2X_iX_{i+1}\cos(\phi_i - \varphi_{i+1}) + X_{i+1}^{\,2}\right] \tag{4.5}$$

Letting $H_i(j\omega) = X_i / X_0$, then Equation (4.5) becomes:

$$< P_{abs} >_i = \frac{1}{2} c_i \omega^2 X_0^2 \left[|H_i(j\omega)|^2 - 2|H_i(j\omega)| \cdot |H_{i+1}(j\omega)| \cos(\phi_i - \phi_{i+1}) + |H_{i+1}(j\omega)|^2 \right]$$

$$= \frac{1}{2} c_i \omega^2 X_0^2 |H_i(j\omega) - H_{i+1}(j\omega)|^2 \qquad (4.6)$$

where i =1 to 4, $c_5 = c_0$, $\phi_5 = \phi_0$, $H_5(j\omega) = H_0(j\omega) = 1$, and $H_i(j\omega)$, $|H_i(j\omega)|$ are the complex and modulus of the transmissibility function of seat-to-mass i, respectively; ϕ_i is the corresponding phase. All of these functions may be obtained from Equations (3.3) to (3.5).

Introducing the frequency weighting, $W_k(j\omega)$, into Equation (4.6), the local weighted absorbed powers in different segments of the body are calculated from:

$$< P_{w.abs} >_i = \frac{1}{2} c_i W_k^2(j\omega) \omega^2 X_0^2 |H_i(j\omega) - H_{i+1}(j\omega)|^2 \qquad (4.7)$$

For each spring i shown in Figure 2.1, averaged over a complete number of cycles the elastic power is given by:

$$< P_{el} >_i = \frac{1}{T} \int_0^T k_i (x_i - x_{i+1})(\dot{x}_i - \dot{x}_{i+1}) dt$$

$$= \frac{1}{T} \int_0^T k_i \left[X_i \sin(\omega t + \phi_i) - X_{i+1} \sin(\omega t + \phi_{i+1}) \right] d\left[X_i \sin(\omega t + \phi_i) - X_{i+1} \sin(\omega t + \phi_{i+1}) \right]$$

$$= \frac{\omega}{2\pi} k_i \frac{1}{2} [X_i \sin(\omega t + \phi_i) - X_{i+1} \sin(\omega t + \phi_{i+1})]^2 \Big|_0^{2\pi/\omega} = 0 \tag{4.8}$$

That is:

$$< P_{el} >_i = 0 \tag{4.9}$$

Thus, the total elastic energy per cycle for the whole body is zero:

$$< P_{el} >_{Tot} = \sum_{i=1}^{4} < P_{el} >_i = 0 \tag{4.10}$$

In consequence, averaged over a complete number of cycles for the whole body, the fluctuating component of the power transmitted to the body is expressed as:

$$< P_{tr} >_{Tot} = < P_{abs} >_{Tot} \tag{4.11}$$

4.2.2 Two methods to calculate total absorbed power

The total absorbed power can be computed in two ways. The first method is through the summation of the local absorbed powers in each body segment, and the second method is by obtaining the power input at the driving point.

Method 1: Computation from the summation of local absorbed powers

The total absorbed power per cycle for the whole body may be obtained from the summation of the absorbed powers in different segments (dampers) of the body:

$$< P_{abs} >_{Tot} = \sum_{i=1}^{4} < P_{abs} >_i \tag{4.12}$$

Hence, the unweighted total absorbed power are computed as follows:

$$< P_{abs} >_{Tot} = \frac{1}{2}\omega^2 \sum_{i=1}^{4} c_i \left[X_i^{\,2} - 2X_i X_{i+1} \cos(\phi_i - \phi_{i+1}) + X_{i+1}^{\,2} \right]$$

$$= \frac{1}{2}\omega^2 X_0^{\,2} \sum_{i=1}^{4} c_i \left[|H_i(j\omega)|^2 - 2|H_i(j\omega)| \cdot |H_{i+1}(j\omega)| \cos(\phi_i - \phi_{i+1}) + |H_{i+1}(j\omega)|^2 \right]$$

$$= \frac{1}{2}\omega^2 X_0^{\,2} \sum_{i=1}^{4} c_i |H_i(j\omega) - H_{i+1}(j\omega)|^2 \tag{4.13}$$

Similarly, the weighted total absorbed power is given by:

$$< P_{w,abs} >_{Tot} = \frac{1}{2} W_k^2(j\omega)\omega^2 \sum_{i=1}^{4} c_i \left[X_i^{\,2} - 2X_i X_{i+1} \cos(\phi_i - \phi_{i+1}) + X_{i+1}^{\,2} \right]$$

$$= \frac{1}{2} W_k^2(j\omega)\omega^2 X_0^{\,2} \sum_{i=1}^{4} c_i |H_i(j\omega) - H_{i+1}(j\omega)|^2 \tag{4.14}$$

Method 2: Computation at the driving-point

Since the unweighted total absorbed power per cycle for the whole body is transferred from the vibrating source, it can also be calculated from the product of force and velocity at the point excitation to the model:

$$< P_{abs} >_{Tot} = < P_{Tr} >_{input} = < F(t) >_{input} . < v(t) >_{input} \tag{4.15}$$

Namely:

$$< P_{abs} >_{Tot} = \frac{1}{T}\int_0^T [c_4(\dot{x}_0 - \dot{x}_4) + k_4(x_0 - x_4)]\dot{x}_0 dt \tag{4.16}$$

For $x_0 = X_0 \sin(\omega t + \phi_0)$, this gives:

$$\begin{aligned} < P_{abs} >_{Tot} &= \frac{\omega}{2\pi}\int_0^{2\pi/\omega} c_4(\dot{x}_0 - \dot{x}_4)\dot{x}_0 dt + \frac{\omega}{2\pi}\int_0^T k_4(x_0 - x_4)\dot{x}_0 dt \\ &= \frac{\omega}{2\pi}\int_0^{2\pi/\omega} c_4\omega^2[X_0\cos(\omega t + \phi_0) - X_4\cos(\omega t + \phi_4)]X_0\cos(\omega t + \phi_0)dt \\ &+ \frac{\omega}{2\pi}\int_0^{2\pi/\omega} k_4\omega[X_0\sin(\omega t + \phi_0) - X_4\sin(\omega t + \phi_4)]X_0\cos(\omega t + \phi_0)dt \end{aligned} \tag{4.17}$$

Solving the integrals, the unweighted total absorbed power is derived as:

$$\begin{aligned} < P_{abs} >_{Tot} &= \frac{1}{2}\omega X_0[c_4\omega X_0\cos\phi_0 - c_4\omega X_4\cos\phi_4 - k_4 X_4\sin(\phi_4 - \phi_0)] \\ &= \frac{1}{2}\omega^2 X_0^2\left[c_4\cos\phi_0 - c_4 H_4(j\omega)\cos\phi_4 - \frac{k_4}{\omega}H_4(j\omega)\sin(\phi_4 - \phi_0)\right] \end{aligned} \tag{4.18}$$

where

$$H_4(j\omega) = X_4(j\omega)/X_0(j\omega)$$

Introducing the frequency weighting, $W_k(j\omega)$, into Equation (4.18), the weighted total absorbed power is calculated from:

$$< P_{w,abs} >_{Tot} = \frac{1}{2} W_k^2(j\omega)\omega X_0 [c_4 \omega X_0 \cos\phi_0 - c_4 \omega X_4 \cos\phi_4 - k_4 X_4 \sin(\phi_4 - \phi_0)]$$

$$= \frac{1}{2} W_k^2(j\omega)\omega^2 X_0^2 \left[c_4 \cos\phi_0 - c_4 H_4(j\omega)\cos\phi_4 - \frac{k_4}{\omega} H_4(j\omega)\sin(\phi_4 - \phi_0) \right] \quad (4.19)$$

Consequently, the unweighted total absorbed power per cycle for whole body can be calculated from either Equation (4.13) or Equation (4.18), while the weighted total absorbed power per cycle can be calculated from either Equation (4.14) or Equation (4.19). The results should be identical, and the right sides of both equations should be equal to each other, namely:

$$\frac{1}{2}\omega^2 \sum_{i=1}^{4} c_i \left[X_{i+1}^{\ 2} - 2X_i X_{i+1} \cos(\phi_{i+1} - \phi_i) + X_i^{\ 2} \right]$$

$$= \frac{1}{2}\omega X_0 [c_4 \omega X_0 \cos\phi_0 - c_4 \omega X_4 \cos\phi_4 - k_4 X_4 \sin(\phi_4 - \phi_0)] \quad (4.20)$$

If $\phi_0 = 0$, the above expression yields:

$$\omega \sum_{i=1}^{4} c_i \left[X_i^{\ 2} - 2X_i X_{i+1} \cos(\phi_i - \phi_{i+1}) + X_{i+1}^{\ 2} \right]$$

$$= X_0 [c_4 \omega X_0 - c_4 \omega X_4 \cos\phi_4 - k_4 X_4 \sin\phi_4] \quad (4.21)$$

or

$$\omega \sum_{i=1}^{4} c_i \left[|H_i(j\omega)|^2 - 2|H_i(j\omega)| \cdot |H_{i+1}(j\omega)| \cdot \cos(\phi_i - \phi_{i+1}) + |H_{i+1}(j\omega)|^2 \right]$$

$$= c_4\omega - c_4\omega|H_4(j\omega)|\cos\phi_4 - k_4|H_4(j\omega)|\sin\phi_4 \qquad (4.22)$$

4.2.3 Equivalent damping coefficient

If the 4-DOF model can be replaced by a simple SDOF model subjected to a sinusoidal displacement excitation at the base, its equivalent damping coefficient can be obtained by equating the energy dissipation in the two models.

For a SDOF system, the dissipated power per cycle is determined by:

$$< P_{abs} >= \frac{1}{T}\int_0^T c_{eq}(\dot{x} - \dot{x}_0)^2 dt \qquad (4.23)$$

Substituting $x = X\sin(\omega t + \phi)$, $x_0 = X_0\sin(\omega t)$, and $T = 2\pi/\omega$, and integrating Equation (4.23), yields

$$< P_{abs} >= \frac{1}{2}c_{eq}\omega^2(X^2 - 2XX_0\cos\phi + X_0^2) \qquad (4.24)$$

That is

$$< P_{abs} >= \frac{1}{2}c_{eq}\omega^2 X_0{}^2\left[|H(j\omega)|^2 - 2|H(j\omega)|\cos\phi + 1\right]$$

$$= \frac{1}{2}c_{eq}\omega^2 X_0{}^2|H(j\omega) - 1|^2 \qquad (4.25)$$

where $H(j\omega)$ and $|H(j\omega)|$ are the complex and magnitude transmissibility function of the equivalent SDOF model.

According to the "equivalent energy dissipation", the right-hand sides of Equations (4.13) and (4.25) should be equal to each other. Thus, the equivalent damping coefficient is derived as:

$$c_{eq} = \sum_{i=1}^{4} c_i \left[\left| H_i(j\omega) - H_{i+1}(j\omega) \right| / \left| H(j\omega) - 1 \right| \right]^2 \qquad (4.26)$$

4.2.4 Plots of absorbed power under harmonic displacement excitation

Assume the system is excited by a harmonic excitation $x_0 = X_0 \sin \omega t$, where $X_0 = 0.02$ m. Figure 4.1 illustrates the unweighted absorbed power in damper 1 computed from Equation (4.5). The peak value occurs near the second natural frequency of the biodynamic model. Figure 4.2 shows unweighted absorbed powers in damper 2 and 3. Total unweighted absorbed power in the body and unweighted absorbed power in damper 4 are illustrated in Figure 4.3. Weighted absorbed power in damper 1 is plotted in Figure 4.4. The maximum value of weighted absorbed power is 36.5 W at the second natural frequency 40.4 Hz of the model. Weighted absorbed powers in damper 2, 3, and 4 are illustrated in Figure 4.5, from which it can be seen that the maximum values of weighted absorbed powers in damper 2 and 3 occurs close to the first natural frequency 4.7 Hz, while that of weighted absorbed power in damper 4 occurs close to the second natural frequency 40.4 Hz. Figure 4.6 illustrates weighted total absorbed power in the body. The local absorbed powers show that the second natural frequency 40.4 Hz of the biodynamic model is only for mass 1 (head) and mass 4 (thighs and pelvis). This is in agreement with Figures 3.1 and 3.2, in which only the transmissiblities from seat to

mass 1 and seat to mass 4 have the peaks near the second natural frequency 40.4 Hz. These results clearly illustrate that very little energy is absorbed in damper 1 associated with the head, and most of the absorbed power occurs in damper 4, which is closest to the source of excitation, which is associated with the thighs and pelvis in contact with the seat. A significant portion of the total body weighted absorbed power is also seen to be absorbed in damper 4.

4.3 Absorbed Power Under Constant Acceleration Excitation

In section 4.2, the absorbed powers for different segments of the body and the total absorbed power under a constant sinusoidal displacement were discussed. However, it is not fully meaningful to study the local absorbed power and total power absorption in the body in the frequency range of 0.4 Hz to 100 Hz, since it is not realistic to have constant displacement excitation at higher frequencies. For instance, when the amplitude of displacement excitation is 0.02 m, and frequency of the excitation is 50 Hz, the magnitude of acceleration is $0.02\times(100\pi)^2 = 1972\ m/\sec^2$. This value is unrealistically high and it would not be possible to subject human body to such an excitation.

In this section the local absorbed powers in different segments of the body and total body absorbed power under a constant acceleration excitation are discussed.

4.3.1 Analysis

Substituting the amplitude of acceleration, $A_0 = \omega^2 X_0$ into Equation (4.6), the local unweighted absorbed powers in different segments of the body are computed from:

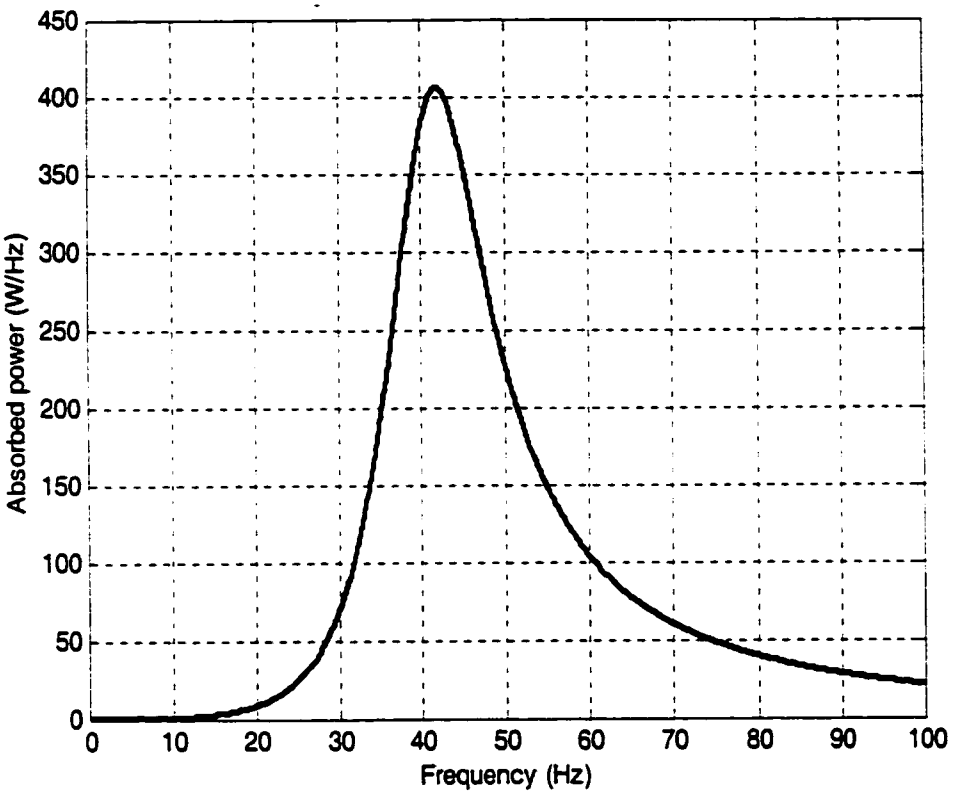

Figure 4.1 Unweighted absorbed power in damper 1 under a sinusoidal excitation of a displacement amplitude of 0.02 m

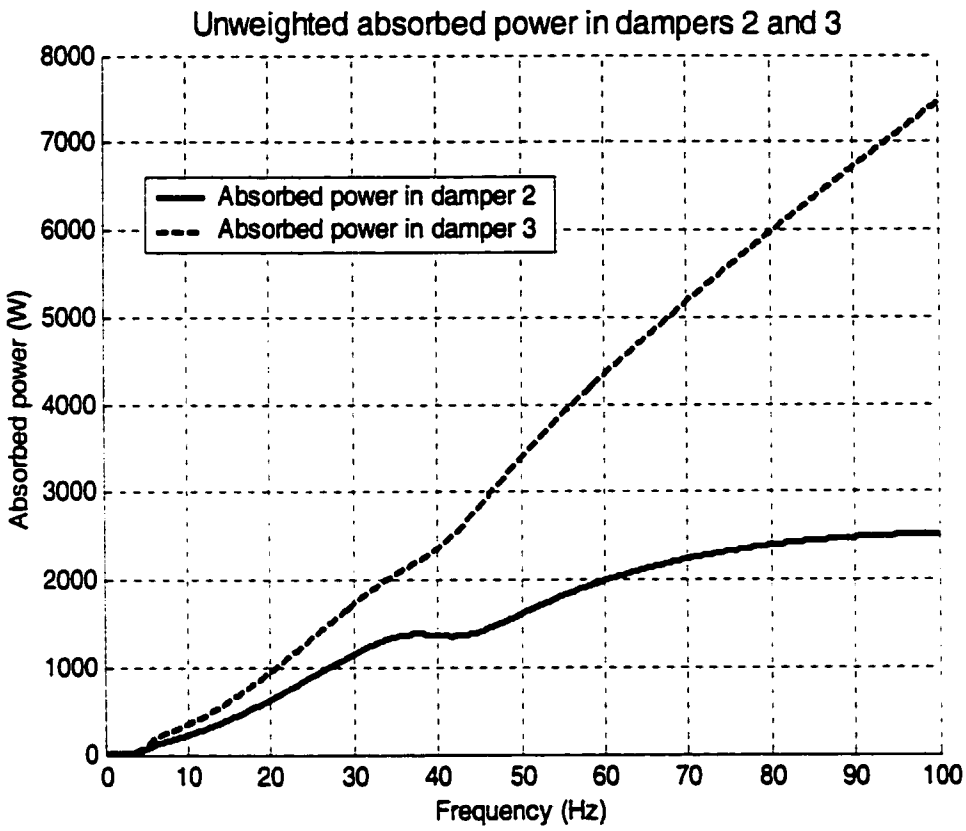

Figure 4.2 Unweighted absorbed powers in dampers 2 and 3 under a sinusoidal excitation of a displacement amplitude of 0.02 m

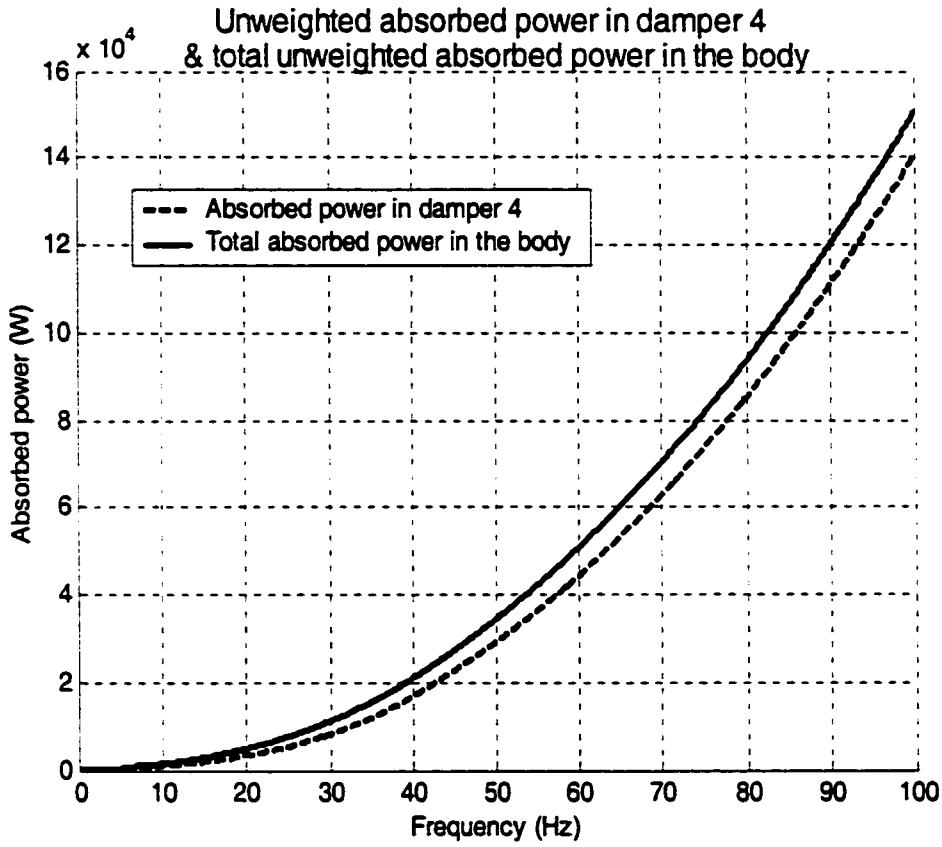

Figure 4.3 Total unweighted absorbed power in the body and unweighted absorbed power in damper 4 under a sinusoidal excitation of a displacement amplitude of 0.02 m

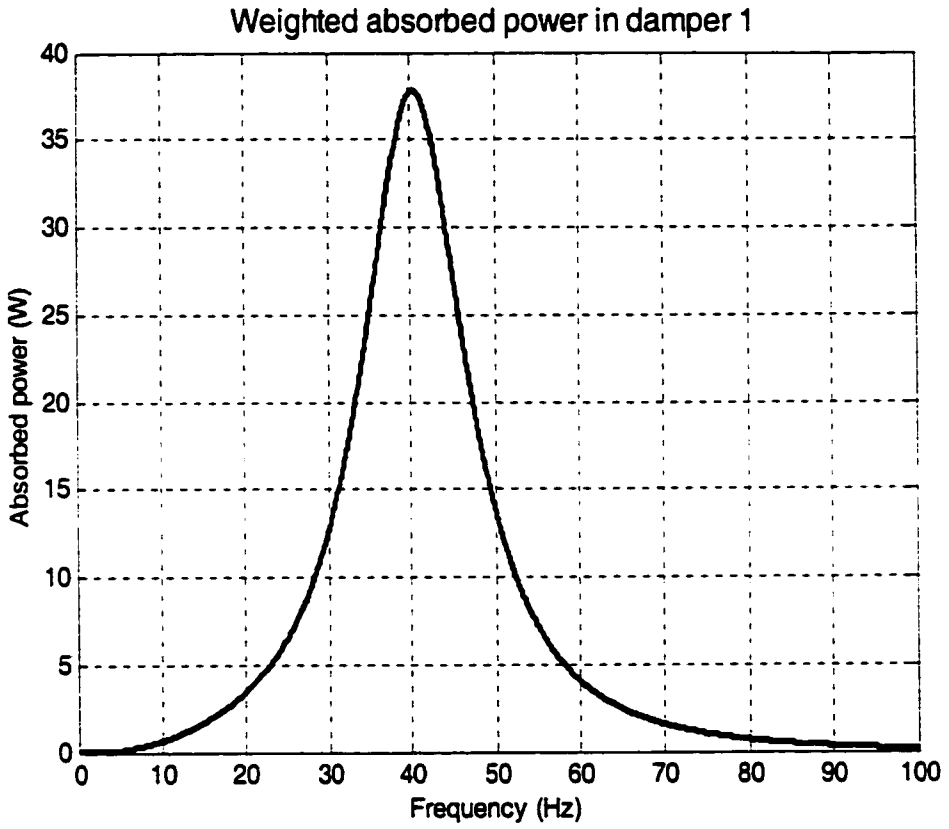

Figure 4.4 Weighted absorbed power in damper 1 under a sinusoidal excitation of a displacement amplitude of 0.02 m

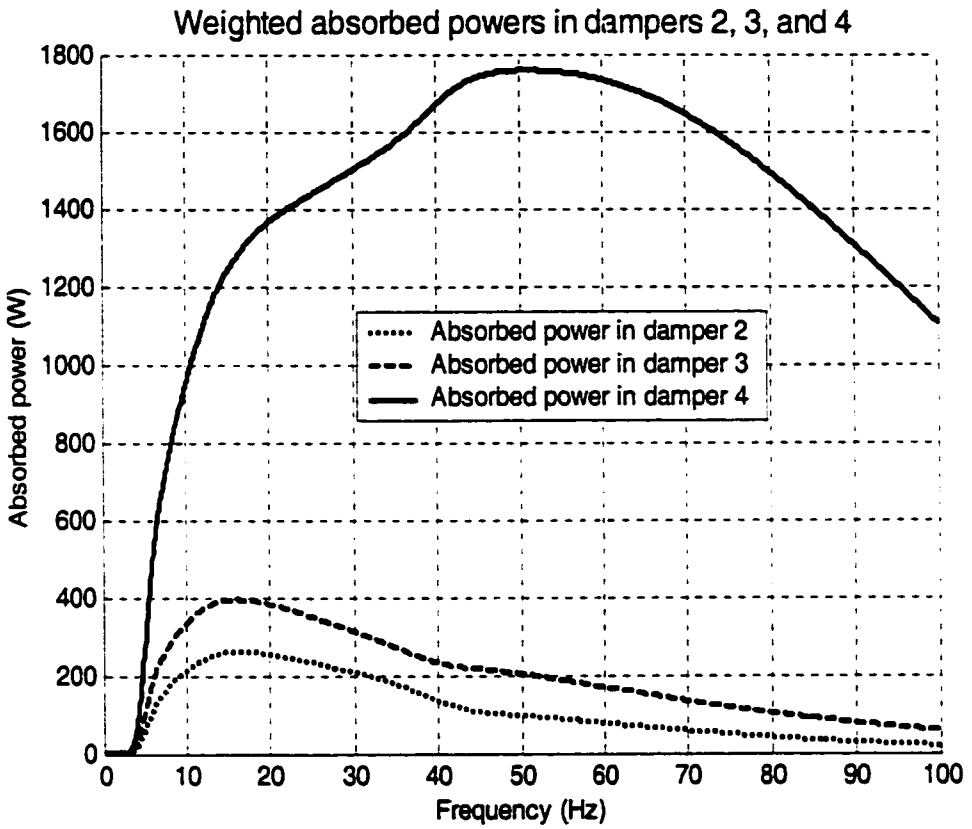

Figure 4.5 Weighted absorbed powers in dampers 2, 3, and 4 under a sinusoidal excitation of a displacement amplitude of 0.02 m

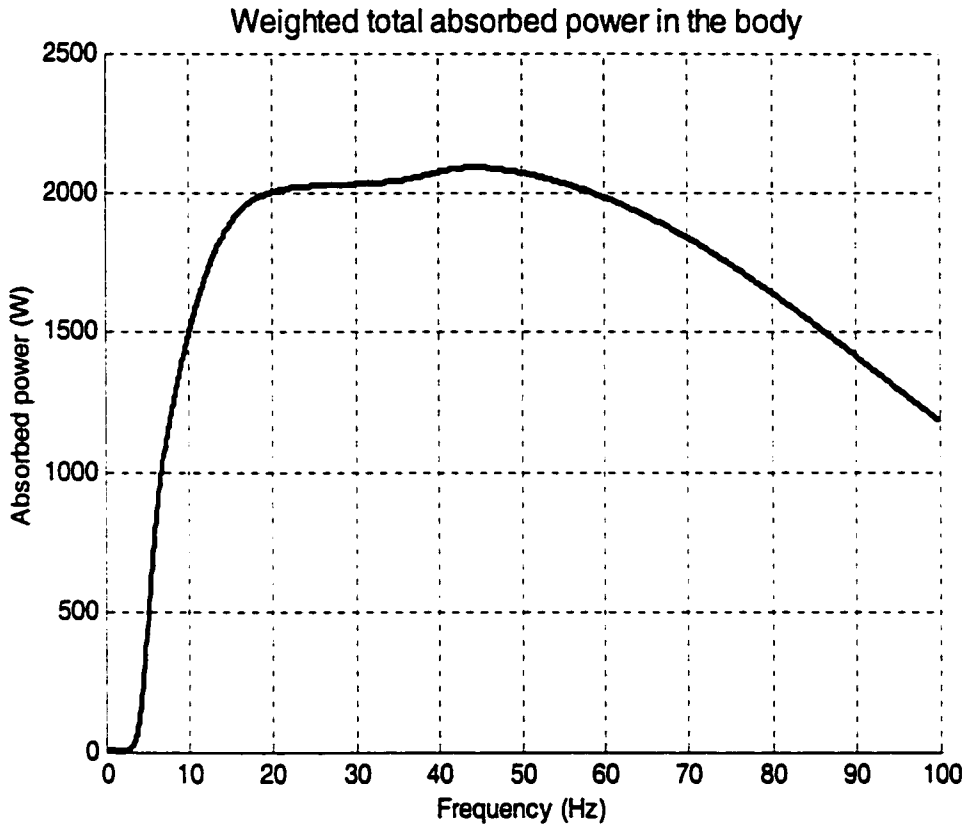

Figure 4.6 Weighted total absorbed power in the body under a sinusoidal excitation of a displacement amplitude of 0.02 m

$$< P_{abs} >_i = \frac{1}{2} c_i \left(\frac{A_0}{\omega} \right)^2 \left[|H_i(j\omega)|^2 - 2|H_i(j\omega)| \cdot |H_{i+1}(j\omega)| \cos(\phi_i - \phi_{i+1}) + |H_{i+1}(j\omega)|^2 \right]$$

$$= \frac{1}{2} c_i \left(\frac{A_0}{\omega} \right)^2 |H_i(j\omega) - H_{i+1}(j\omega)|^2 \qquad (4.27)$$

Introducing the frequency weighting, $W_k(j\omega)$, into Equation (4.27), the local weighted absorbed powers in different segments of the body are calculated from:

$$< P_{abs} >_{wi} = \frac{1}{2} c_i \left(\frac{W_k(j\omega) A_0}{\omega} \right)^2 \left[|H_i(j\omega)|^2 - 2|H_i(j\omega)||H_{i+1}(j\omega)| \cos(\phi_i - \phi_{i+1}) + |H_{i+1}(j\omega)|^2 \right]$$

$$= \frac{1}{2} c_i \left(\frac{W_k(j\omega) A_0}{\omega} \right)^2 |H_i(j\omega) - H_{i+1}(j\omega)|^2 \qquad (4.28)$$

Similarly, substituting $A_0 = \omega^2 X_0$ into Equation (4.13), the total absorbed power in the body may be obtained as:

$$< P_{abs} >_{Tot} = \frac{1}{2} \left(\frac{A_0}{\omega} \right)^2 \sum_{i=1}^{4} c_i \left[|H_i(j\omega)|^2 - 2|H_i(j\omega)| \cdot |H_{i+1}(j\omega)| \cos(\phi_i - \phi_{i+1}) + |H_{i+1}(j\omega)|^2 \right]$$

$$= \frac{1}{2} \left(\frac{A_0}{\omega} \right)^2 \sum_{i=1}^{4} c_i |H_i(j\omega) - H_{i+1}(j\omega)|^2 \qquad (4.29)$$

Introducing the frequency weighting, $W_k(j\omega)$, into Equation (4.29), the total weighted absorbed power in the body may be obtained as:

$$< P_{abs} >_{w,Tot} = \frac{1}{2}\left(\frac{W_k(j\omega)A_0}{\omega}\right)^2 \sum_{i=1}^{4} c_i \left[|H_i(j\omega)|^2 - 2|H_i(j\omega)||H_{i+1}(j\omega)|\cos(\phi_i - \phi_{i+1}) + |H_{i+1}(j\omega)|^2\right]$$

$$= \frac{1}{2}\left(\frac{W_k(j\omega)A_0}{\omega}\right)^2 \sum_{i=1}^{4} c_i |H_i(j\omega) - H_{i+1}(j\omega)|^2 \qquad (4.30)$$

4.3.2 Plots of absorbed powers under constant acceleration excitation

Figures 4.7 and 4.8 present the unweighted and frequency-weighted absorbed power of damper 1 (head) during vibration exposure to an acceleration level of 1 ms^{-2} (10%g), respectively. The curves of both unweighted and weighted absorbed power in damper 1 have two peaks near the first frequency 4.7 Hz, and the second frequency 40.4 Hz, respectively. For the unweighted absorbed power in damper 1, the peak at the second natural frequency 40.4 Hz is higher than that at the first natural frequency 4.7 Hz. In contrast, for the weighted absorbed power in damper 1 the peak at the first natural frequency is higher than that at the second natural frequency because of heavier weight or low frequency components. Consequently, the figure of weighted absorbed power resembles the transmissibility characteristics of seat to mass 1 (head), shown in Figure 3.2, in which the peak of transmissibility at the first natural frequency is higher than that at the second one. Figures 4.9 and 4.10 illustrate the unweighted and weighted absorbed powers of dampers 2, 3, and 4, respectively. Similar to the transmissibilities from seat to mass 2, 3, and 4, each of the curves of both unweighted and weighted absorbed powers in damper 2, 3, and 4 has only one peak near the first natural frequency 4.7 Hz. The total unweighted and weighted absorbed powers of the whole body are shown in Figures 5.11 and 5.12, respectively. The peaks occur at the first natural frequency of the model.

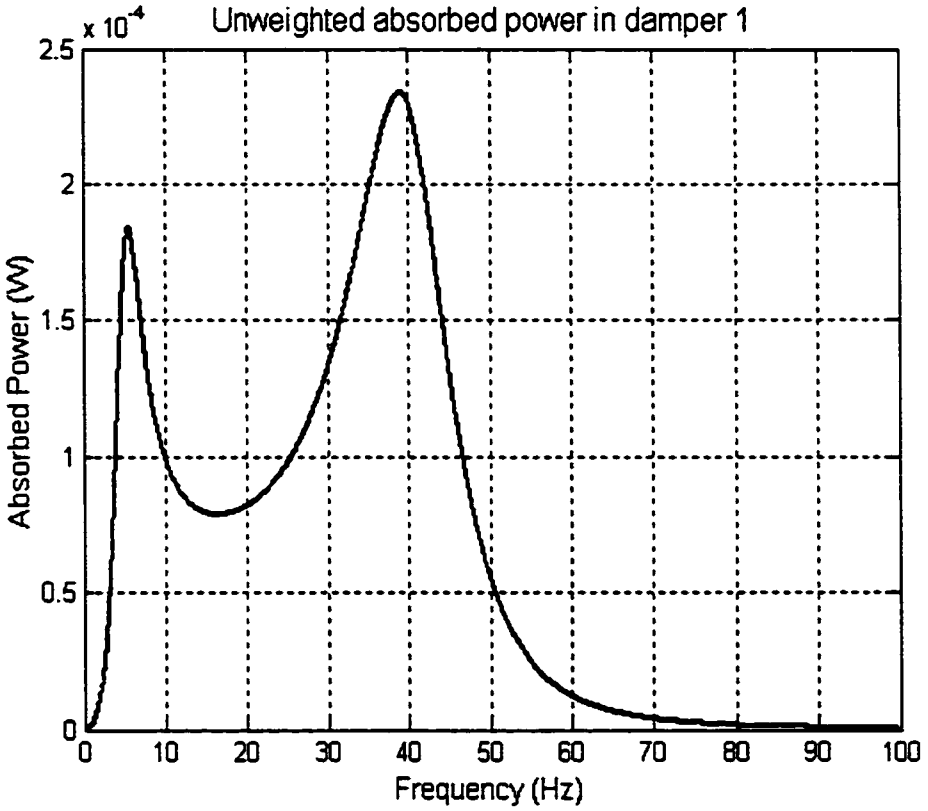

Figure 4.7 Unweighted absorbed power in damper 1 during excitation of an acceleration level of 10%g

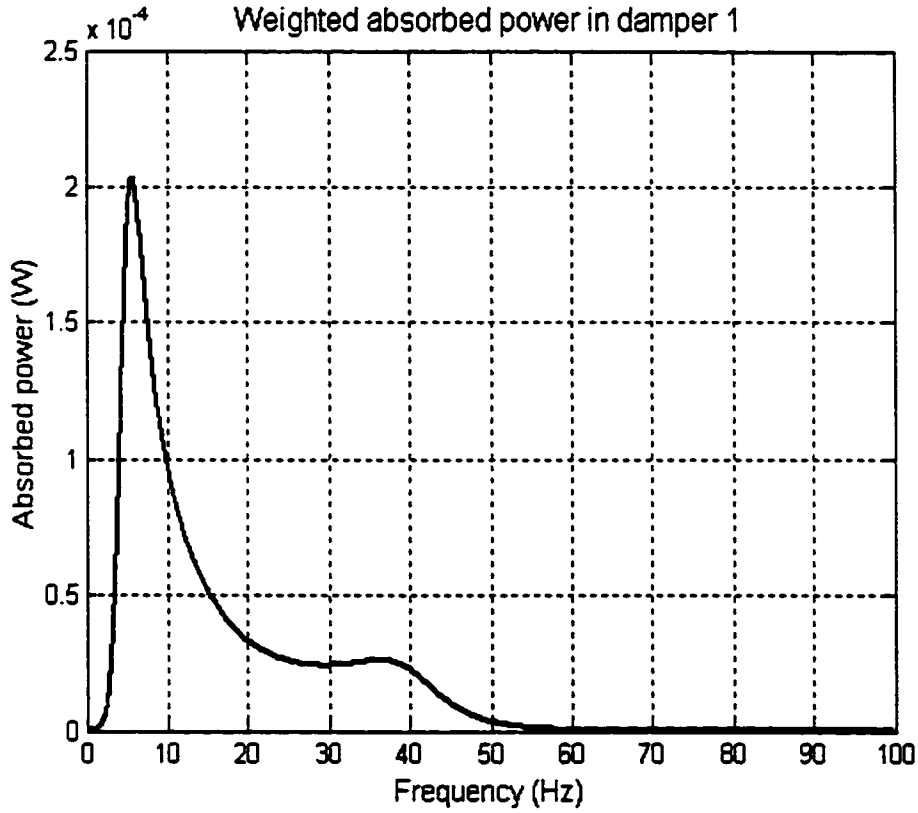

Figure 4.8 Weighted absorbed power in damper 1 during excitation of an acceleration level of 10%g

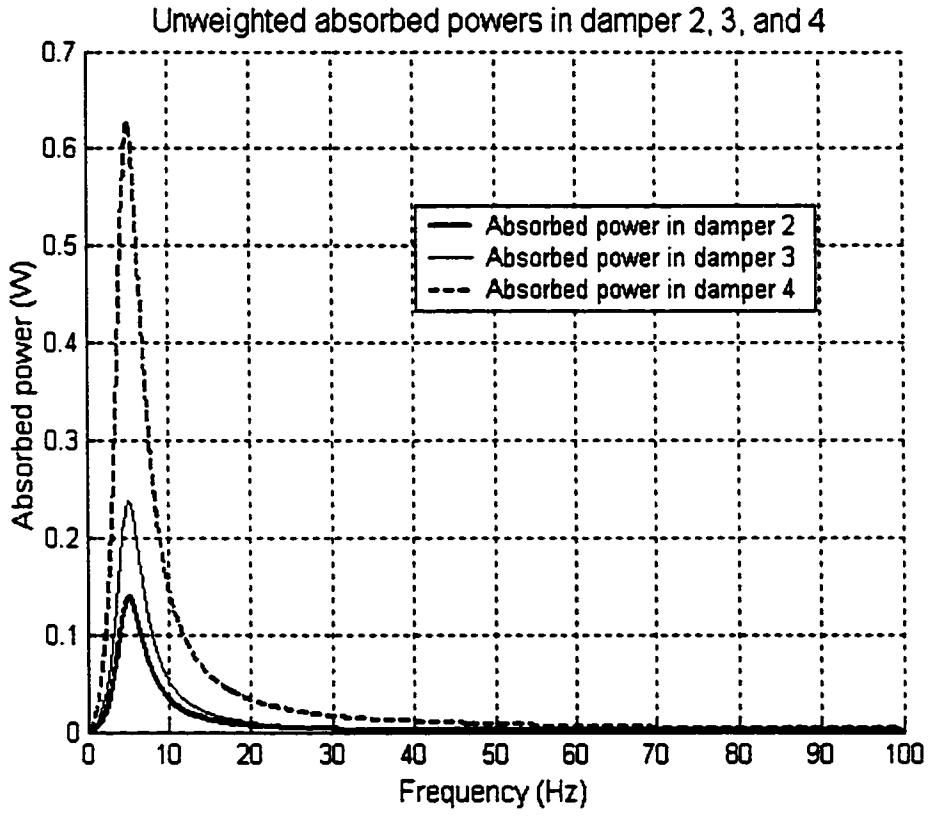

Figure 4.9 Unweighted absorbed powers in dampers 2, 3, and 4 under excitation of an acceleration level of 10%g

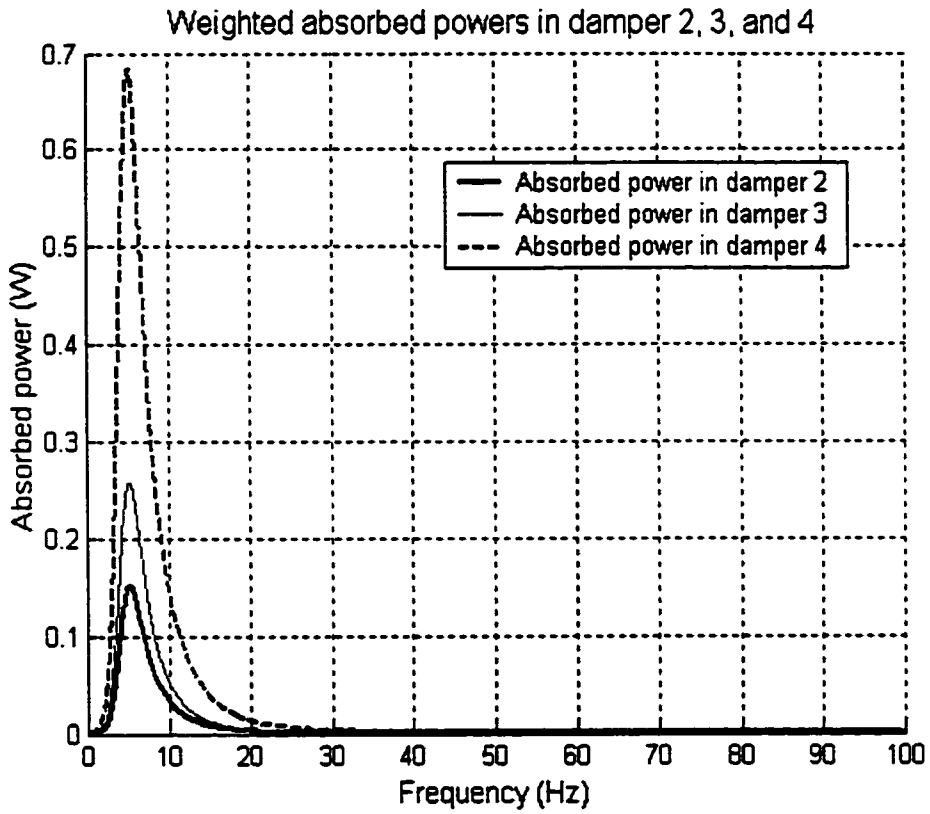

Figure 4.10 Weighted absorbed powers in dampers 2, 3, and 4 under excitation of an acceleration level of 10%g

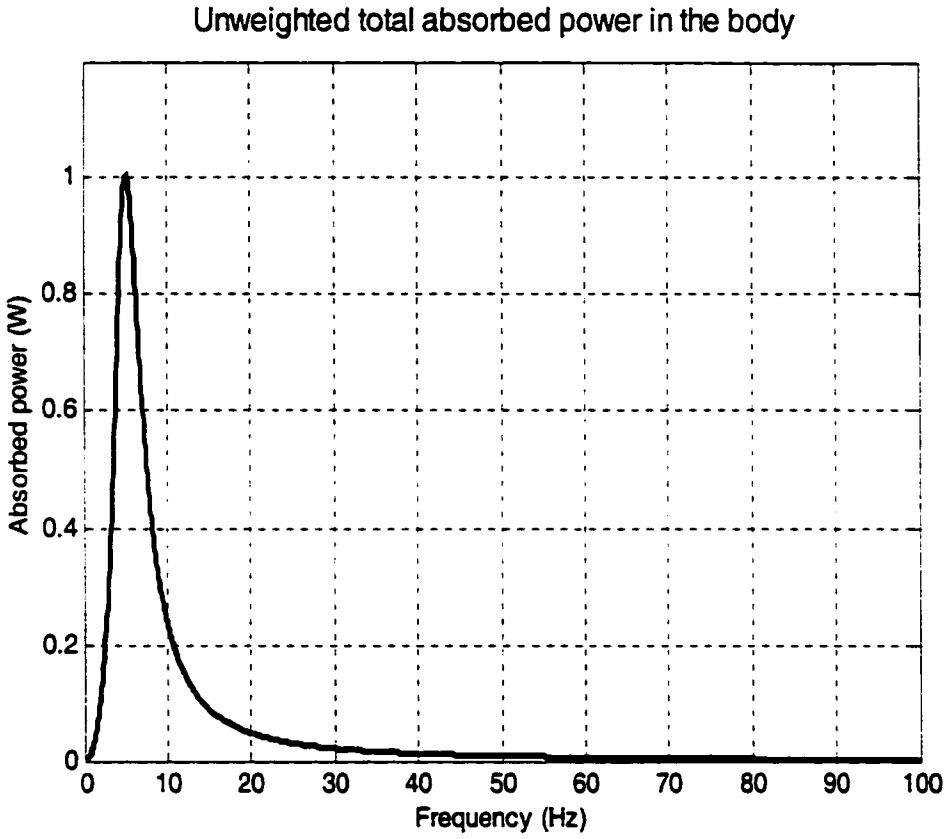

Figure 4.11 Unweighted total absorbed power in the body under excitation of an acceleration level of 10%g

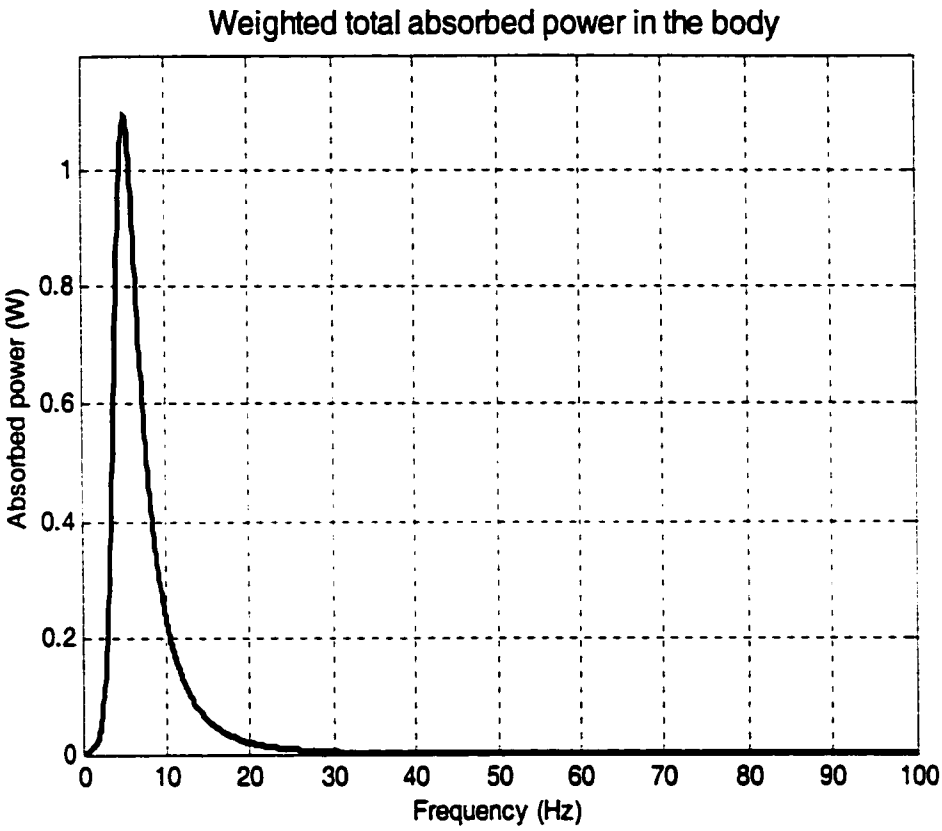

Figure 4.12 Weighted total absorbed power in the body under excitation of an acceleration level of 10%g

These results clearly illustrate that very little energy is absorbed in damper 1 associated with the head, and most of the power absorption occurs in damper 4 which is close to the source of excitation, and is associated with the thighs and pelvis in contact with the seat.

4.4 Absorbed Power Under Random Excitation IT 1

The random excitation IT 1 having characteristics as defined in a proposed European Standard prEN 13490 (1999) to represent the vertical vibration acting at the seat base for a particular category of forklift trucks was specially described in section 3.6. The peak excitation is seen to occur at a frequency of 5.12 Hz, which is close to the first natural frequency 4.7 Hz of the 4-DOF biodynamic model. In this section, the random excitation IT 1 is chosen as the input to the model to compute absorbed power.

4.4.1 Basic derivation

With the excitation IT 1 used as input to the model shown in Figure 2.1, the unweighted absorbed power per unit frequency (absorbed power density) for i-th damper may be given by:

$$p_{abs,i}(j\omega) = c_i S_{\dot{x}_i - \dot{x}_{i+1}}(j\omega) \tag{4.31}$$

where $S_{\dot{x}_i - \dot{x}_{i+1}}(j\omega)$ is the power spectral density of the difference of velocity, $\dot{x}_i - \dot{x}_{i+1}$, and is computed from:

$$S_{\dot{x}_i-\dot{x}_{i+1}}(j\omega)=\left|H_{\dot{x}_i-\dot{x}_{i+1}}(j\omega)\right|^2 S_0(j\omega) \tag{4.32}$$

where $S_0(j\omega)$ is the PSD acceleration input to the seat. $\left|H_{\dot{x}_i-\dot{x}_{i+1}}(j\omega)\right|$ represents the magnitude of transfer function from the acceleration input on the seat $\ddot{X}_0$ to the difference of velocity, $\dot{X}_i-\dot{X}_{i+1}$. It can be calculated from:

$$\left|H_{\dot{x}_i-\dot{x}_{i+1}}(j\omega)\right|=\left|\dot{X}_i-\dot{X}_{i+1}\right|/\left|\ddot{X}_0\right|=\frac{1}{\omega}\left|H_i(j\omega)-H_{i+1}(j\omega)\right| \tag{4.33}$$

Thus, the unweighted absorbed power per unit frequency (W/Hz) for the *i*-th damper may be expressed as:

$$\begin{aligned} p_{abs,i}(j\omega) &= c_i\left|H_{\dot{x}_i-\dot{x}_{i+1}}(j\omega)\right|^2 S_0(j\omega) \\ &= \frac{c_i}{\omega^2}\left|H_i(j\omega)-H_{i+1}(j\omega)\right|^2 S_0(j\omega) \end{aligned} \tag{4.34}$$

where $c_5=c_0$, $H_5(j\omega)=H_0(j\omega)=1$, $\phi_5=\phi_0=0$, $H_i(j\omega)$ is the complex seat-to-mass *i* transmissibility function.

Correspondingly, the total unweighted absorbed power density in the whole body is thus obtained through the summation of all the local unweighted absorbed power densities:

$$p_{abs,Tot}(j\omega) = \sum_{i=1}^{4} p_{abs,i}(j\omega) \tag{4.35}$$

Hence:

$$p_{abs,Tot}(j\omega) = \sum_{i=1}^{4} \frac{c_i}{\omega^2} \left| H_i(j\omega) - H_{i+1}(j\omega) \right|^2 \cdot S_0(j\omega) \tag{4.36}$$

Similarly, introducing the frequency-weighting factor into Equation (4.34), the weighted absorbed power density (W/Hz) for *i*-th damper may be obtained as:

$$p_{w,abs,i}(j\omega) = c_i W_k^2(j\omega) \left| H_{\dot{x}_i - \dot{x}_{i+1}}(j\omega) \right|^2 S_0(j\omega) \tag{4.37}$$

That is

$$p_{w,abs,i}(j\omega) = c_i \left(\frac{W_k(j\omega)}{\omega} \right)^2 \left| H_i(j\omega) - H_{i+1}(j\omega) \right|^2 S_0(j\omega) \tag{4.38}$$

Correspondingly, the total weighted absorbed power density in the whole body is thus obtained through the summation of all the local weighted absorbed power densities:

$$p_{w,abs,Tot}(j\omega) = \sum_{i=1}^{4} p_{w,abs,i}(j\omega) \tag{4.39}$$

Hence the total absorbed power density is given as:

$$p_{w,abs,Tot}(j\omega) = \sum_{i=1}^{4} c_i \left(\frac{W_k(j\omega)}{\omega} \right)^2 \left| H_i(j\omega) - H_{i+1}(j\omega) \right|^2 S_0(j\omega) \tag{4.40}$$

4.4.2 Plots of absorbed powers under IT1 random excitation

The unweighted absorbed power density in damper 1 under the random excitation IT 1 is illustrated in Figure 4.13. The peak value is 2.2×10^{-4} W/Hz at the resonance frequency 5.5 Hz (close to the first natural frequency 4.7 Hz of the biodynamic model). Figure 4.14 shows unweighted absorbed power densities in dampers 2, 3, and 4 under the random excitation IT 1. The peak absorbed power density values in dampers 2, 3, and 4 are 0.17 W/Hz at the frequency 5.3 Hz, 0.28 W/Hz at the frequency 5.2 Hz and 0.76 W/Hz at the frequency 5.1 Hz, respectively. Peaks of each of the local absorbed power densities in the body exhibit around the first natural frequency 4.7 Hz. Total unweighted absorbed power density in the body under the random excitation IT 1 is presented in Figure 4.15, from which it can be seen that the maximum value of unweighted total absorbed power density is 1.21 W/Hz at the frequency 5.2 Hz. The weighted absorbed power density in damper 1 under the random excitation IT 1 is illustrated in Figure 4.16. The maximum value is 2.37×10^{-4} W/Hz at the frequency 5.5 Hz. Figure 4.17 shows weighted absorbed power densities in dampers 2, 3, and 4 under the random excitation IT 1. The peak values of absorbed power densities in dampers 2, 3, and 4 are 0.18 W/Hz at the frequency 5.3 Hz, 0.30 W/Hz at the frequency 5.2 Hz and 0.82 W/Hz at the frequency 5.1 Hz. Peaks of each of the local absorbed power densities in the body exhibit around the first natural frequency 4.7 Hz. Total weighted absorbed power densities in the body under the random excitation IT 1 is presented in Figure 4.18, from which it can be seen that the maximum value of weighted total absorbed power density is 1.31 W/Hz at the frequency 5.2 Hz.

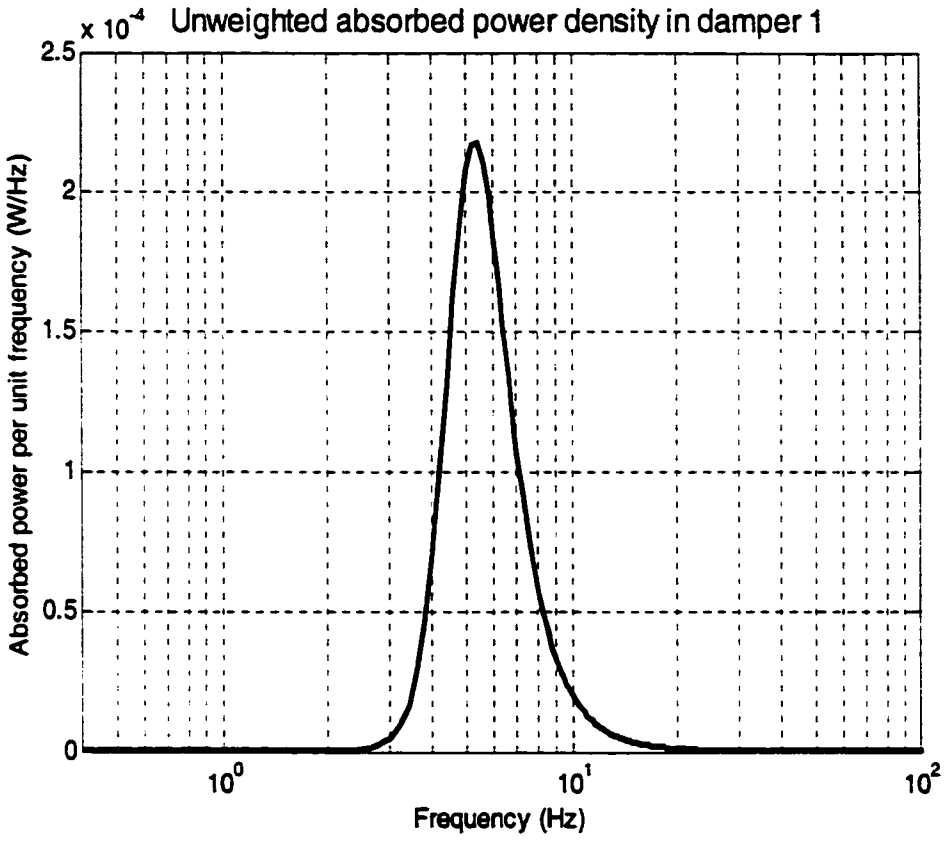

Figure 4.13 Unweighted absorbed power density in damper 1 under the random excitation IT 1 defined in European Standard prEN 13490 (1999)

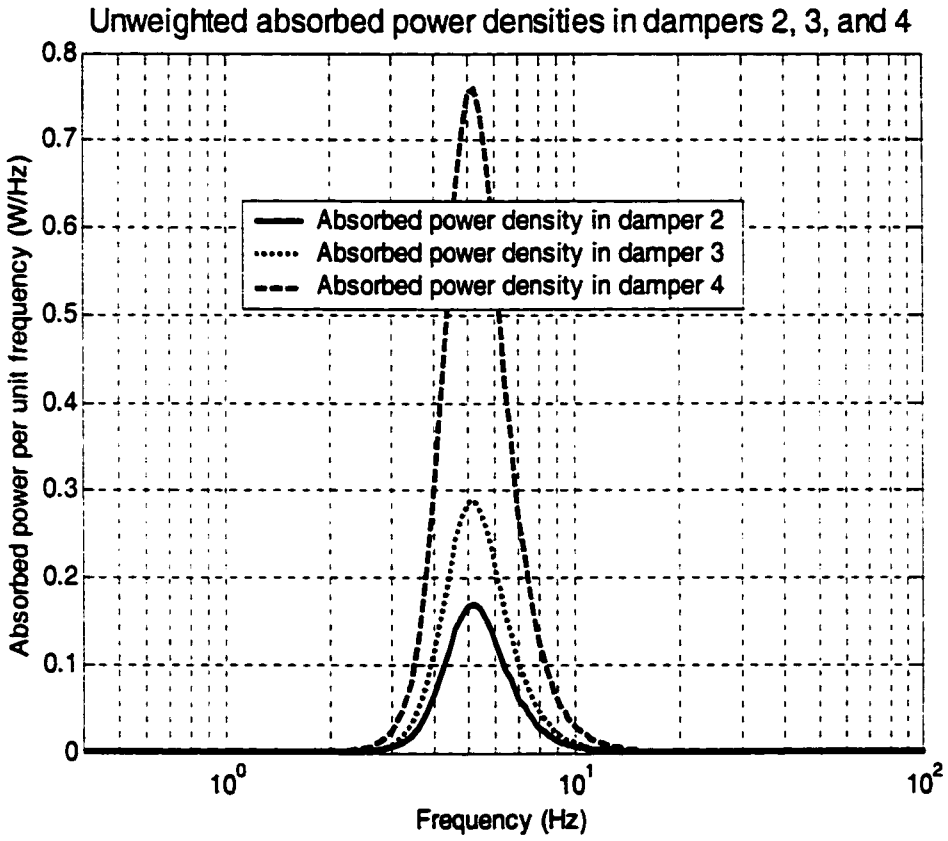

Figure 4.14 Unweighted absorbed power densities in dampers 2, 3, and 4 under the random excitation IT 1 defined in European Standard prEN 13490 (1999)

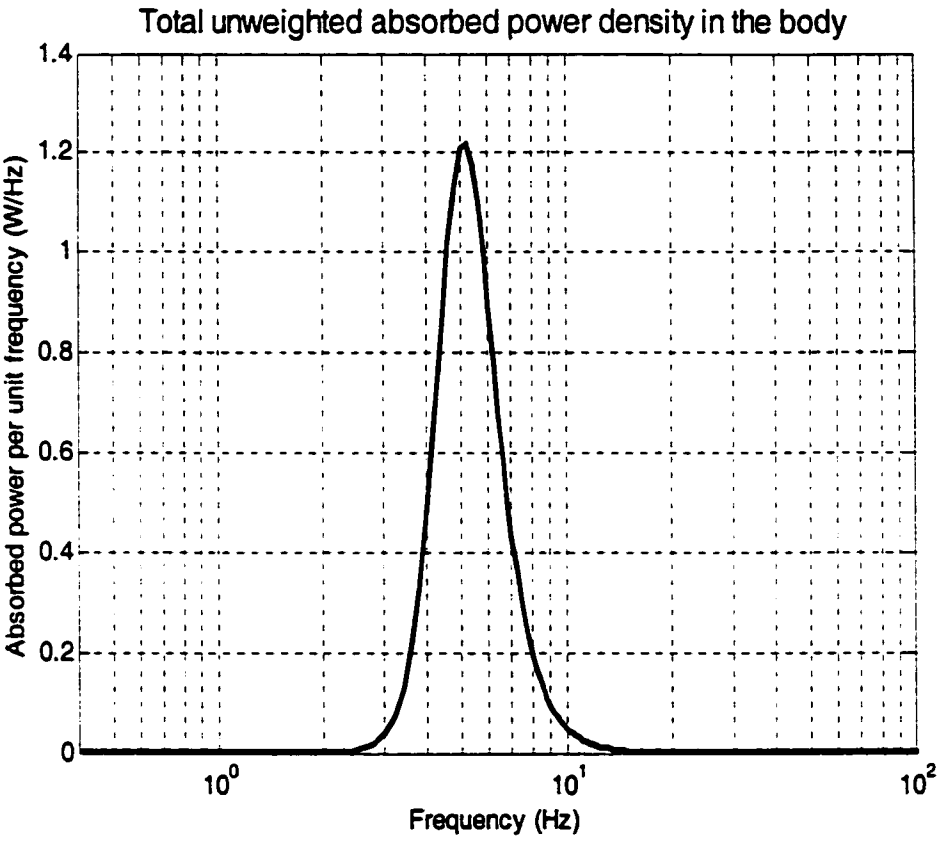

Figure 4.15 Total unweighted absorbed power density in the body under the random excitation IT 1 defined in European Standard prEN 13490 (1999)

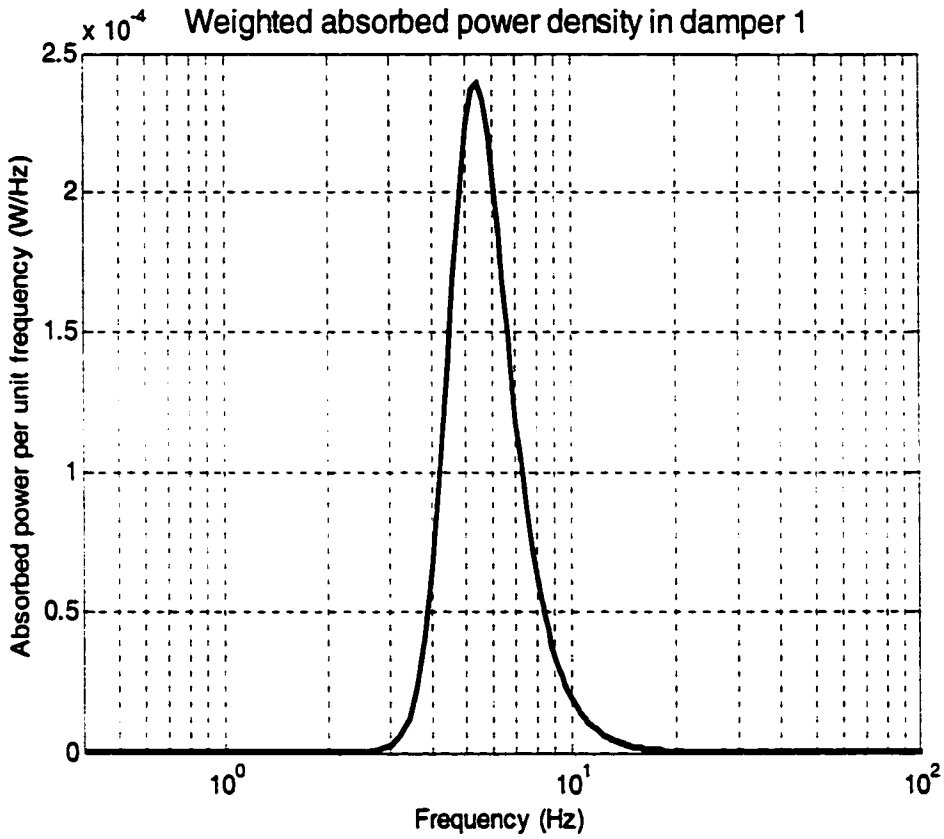

Figure 4.16 Weighted absorbed power density in damper 1 under the random excitation IT 1 defined in European Standard prEN 13490 (1999)

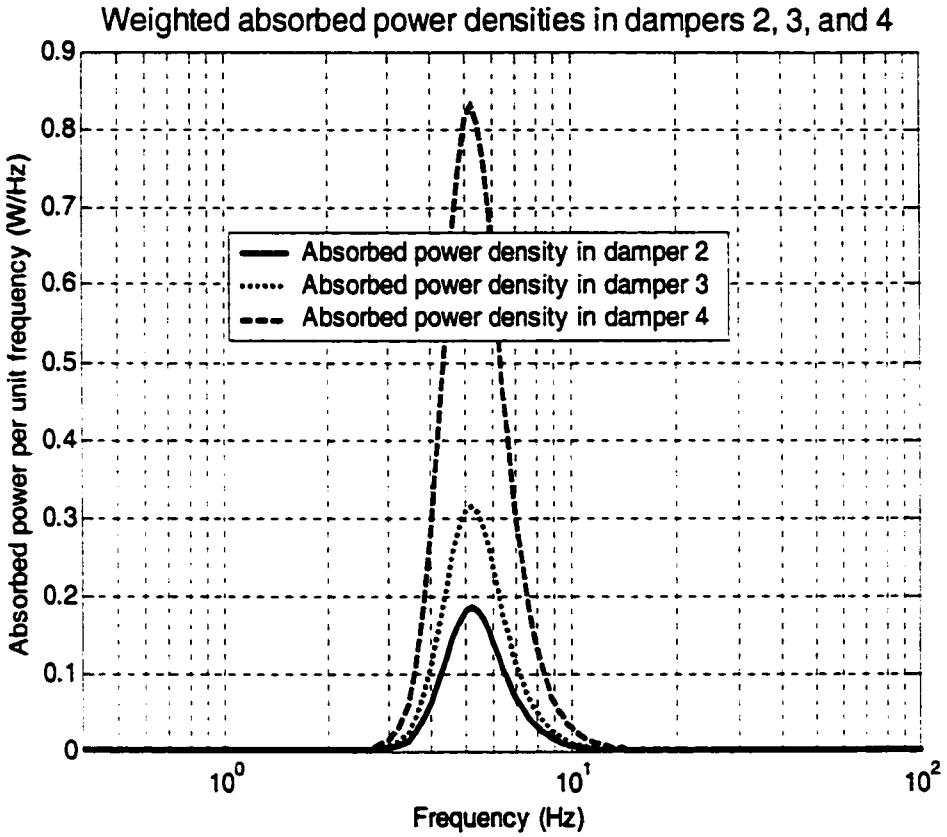

Figure 4.17 Weighted absorbed power densities in dampers 2, 3, and 4 under the random excitation IT 1 defined in European Standard prEN 13490 (1999)

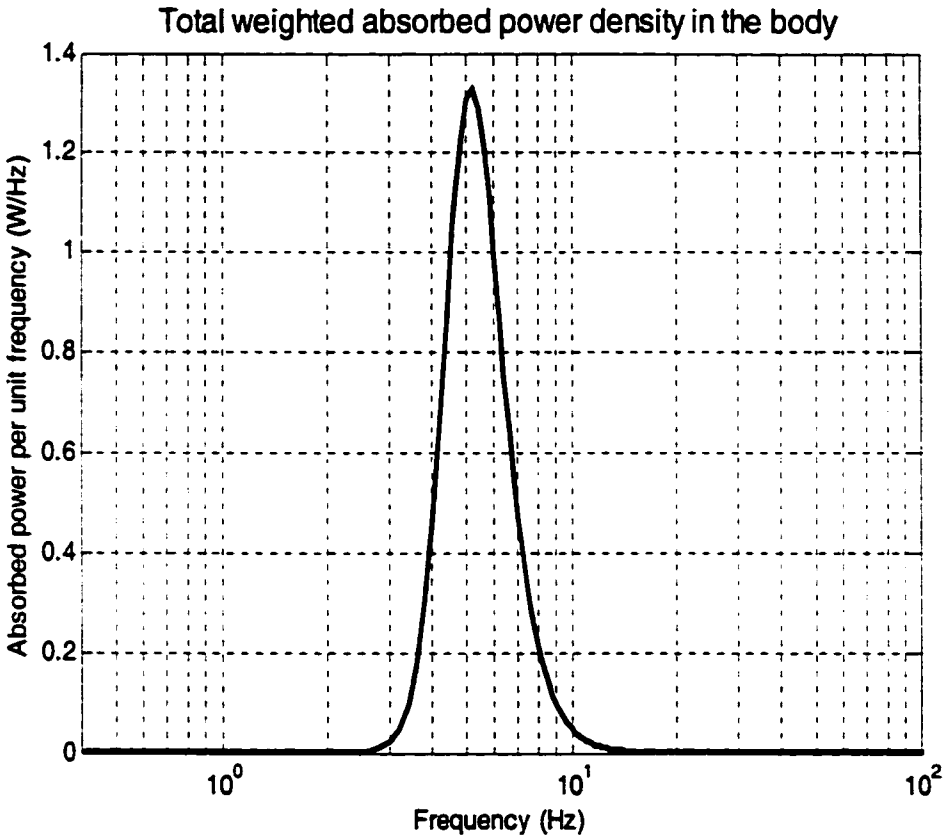

Figure 4.18 Total weighted absorbed power density in the body under the random excitation IT 1 defined in European Standard prEN 13490 (1999)

Similar to the sinusoidal excitations, the results of absorbed power density under the random excitation IT 1 clearly illustrate that very little energy is absorbed in damper 1 associated with the head, while most of the absorbed power occurs in damper 4 which is close to the source of excitation, and is associated with the thighs and pelvis in contact with the seat. A significant portion of the total absorbed power per unit frequency is also seen to be in damper 4.

4.5 Definition of A Health Guidance Caution Zone Based on Absorbed Power

4.5.1 Relationship between absorbed power and rms acceleration

In ISO 2631-1 (1997), the concept of equal energy is used to relate two different vibration exposures characterized by different frequency-weighted rms accelerations a_{wi} and different exposure durations T_i. For broad-band random vibration with minor shock content, the relationship is based on a "square power" law given by:

$$a_{w1}^{\ 2} \cdot T_1 = a_{w2}^{\ 2} \cdot T_2 \tag{4.41}$$

This relationship is used to define a "health guidance caution zone" relating permissible vibration levels a_{wi} as a function of daily exposure duration T_i. In ISO 2631-1 (1997), the health guidance caution zone is defined specifically for daily exposure duration varying between 4 and 8 hours, although extension to other daily exposure durations is possible through application of Equation (4.40).

Applying the concept of equal energy to "absorbed power", it may be inferred that two exposures for which the total body weighted absorbed power are P_{w1} and P_{w2} would be judged equivalent whenever:

$$P_{w1} \cdot T_1 = P_{w2} \cdot T_2 \tag{4.42}$$

In Figure 4.19 total weighted absorbed power density and the PSD of frequency weighted rms acceleration (*i.e.* $a_{w,0}^2$) are shown in order to ascertain whether these two are correlated. As seen, the curve of PSD of weighted acceleration of the excitation appears to resemble the total body weighted absorbed power. Further, it may also be inferred from Equation (4.40) that the total body weighted absorbed power density is proportional to the PSD of weighted acceleration as:

$$p_{w,abs,Tot}(j\omega) \propto S_{0,w}(j\omega) = |W_k(j\omega)|^2 S_0(j\omega) \tag{4.43}$$

This relation is extended to relate the frequency weighted rms acceleration $a_{w,0}$ to the total body weighted absorbed power such that:

$$P_{w,TOT} \approx C \cdot a_{w,0}^2 \tag{4.44}$$

where, C is a constant coefficient of correlation in $W/(m/s^2)^2$,

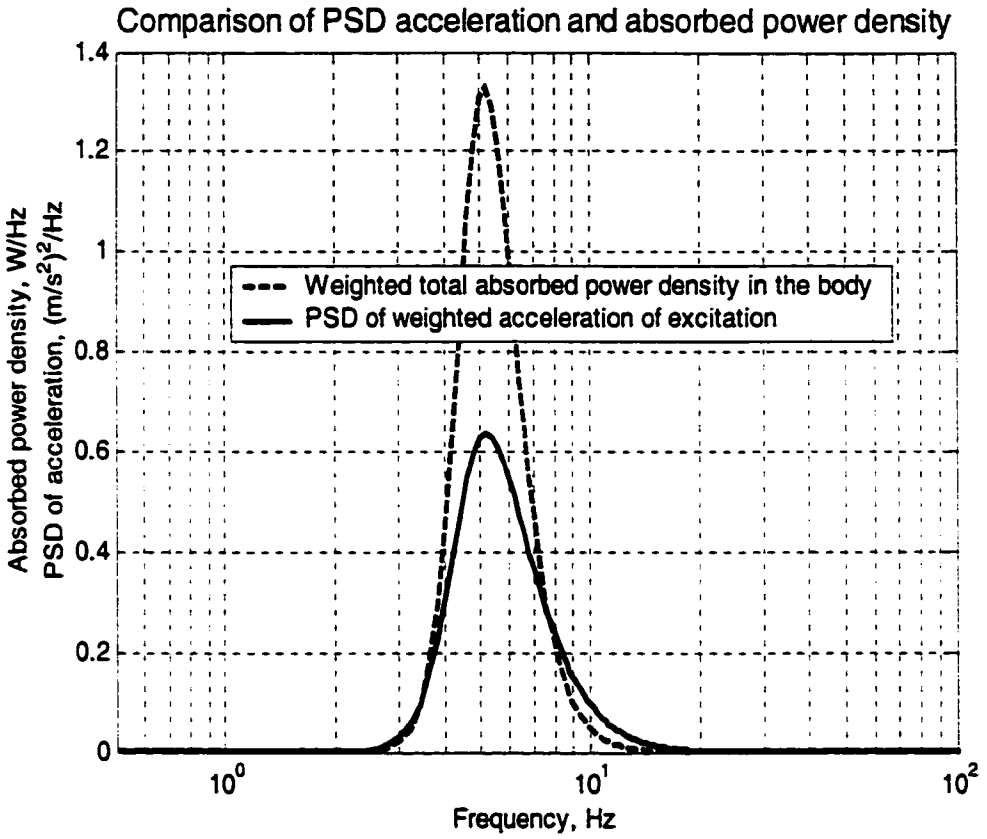

Figure 4.19 The comparisons of total weighted absorbed power density in the body with PSD of weighted acceleration to the seat

The rms weighted acceleration of the excitation, $a_{w,0}$, in the frequency range ω_1 to ω_2 is obtained by:

$$a_{w,0} = \left[\int_{\omega_1}^{\omega_2} |W_k(p)|^2 S_0(j\omega) d\omega \right]^{\frac{1}{2}} \tag{4.45}$$

The weighted absorbed power in the whole body, $P_{w.TOT}$, is given by:

$$P_{w.TOT} = \int_{\omega_1}^{\omega_2} p_{w.abs.Tot}(j\omega) d\omega \tag{4.46}$$

where the total body weighted absorbed power density $p_{w.abs.Tot}(j\omega)$ is given in Equation (4.40).

The computed results of frequency-weighted rms acceleration of excitation IT 1, and weighted absorbed power of the whole body in the frequency range 0.4 to100 Hz, as well as the correlation coefficient C, are presented in Table 4.1:

Table 4.1 Weighted absorbed power of the whole body, weighted rms acceleration of the excitation IT 1 and correlation coefficient.

Weighted absorbed power of the whole body ($P_{w.TOT}$)	Weighted rms acceleration of excitation IT 1 ($a_{w,0}$)	Correlation coefficient ($C = P_{w.TOT} / a_{w,0}^2$)
3.65 W	1.60 m/s^2	1.43 $W/(m/s^2)^2$

4.5.2 Health guidance based on absorbed power

The health guidance caution zone proposed in ISO 2631-1 (1997), according to the "equivalent energy dissipation" $a_{w1}T_1^{1/2} = a_{w2}T_2^{1/2}$, is illustrated in Figure 4.20. The equivalent health guidance caution zone based on absorbed power computed from Equations (4.44) and (4.46) is plotted in Figure 4.21. Similar to the guideline represented in ISO 2631-1 (1997), the health guidance based on absorbed power also shows the exposure range of 4 to 8 hours as indicated by the shaded area.

4.6 Summary

Based on the analysis on a 4 DOF biodynamic model representing a seated human body, it has been possible to derive expressions relating the local and total body absorbed powers in the body, and the vibration transmissibility characteristics to the vibration excitation. The variation of total body weighted absorbed power with frequency was seen to follow closely the shape of the PSD spectrum of the weighted acceleration of the random excitation, which occurs in a particular category of forklift trucks with dominant excitation frequency close to that of the body. The frequency weighting defined to apply to the acceleration response in ISO 2631-1 was also assumed to apply to the calculated values of absorbed power. Whether frequency weighting is needed for the assessment of absorbed power is not yet known.

The equations derived in this study have shown that the weighted absorbed power per unit frequency in each damper is not only proportional to the damping coefficient c_i, but also to the square modulus of the relative transfer functions given by

$|H_i(j\omega) - H_{i+1}(j\omega)|^2$. This implies that the relative transfer functions associated with the relative motion and phase within each body segment is likely to have a most significant influence on the nature of absorbed power within that body segment. Consequently, individual body mass vibration transmissibility cannot be considered to provide good indications of the amount of absorbed power within the body segment. However, there appears to exist a good correspondence in the frequency response behavior between body mass transmissibility and absorbed power. The peaks in body mass transmissibility modulus translate well to peaks in absorbed power. The quantity of absorbed power was found to be most important within the body segment, which is the closest to the source of the vibration excitation, while constituting the most significant contribution to the total body absorbed power. This result thus suggests that it should be possible to get an approximation to the total body absorbed power based on the assessment of the local absorbed power of the body segment closest to the vibration source.

Finally, the analysis of the 4-DOF biodynamic model has shown that total body absorbed power can be related to the frequency-weighted root mean square acceleration used to quantify the vibration exposure level in the current ISO 2631-1:1997. On that basis, a health guidance caution zone equivalent to that defined in ISO 2631-1 was developed based on total body frequency weighted absorbed power by retaining the concept of equal energy. The applicability of such guidance to cases involving other types of excitations would need to be investigated further.

The next chapter will deal with the response of the human body to transient excitation input.

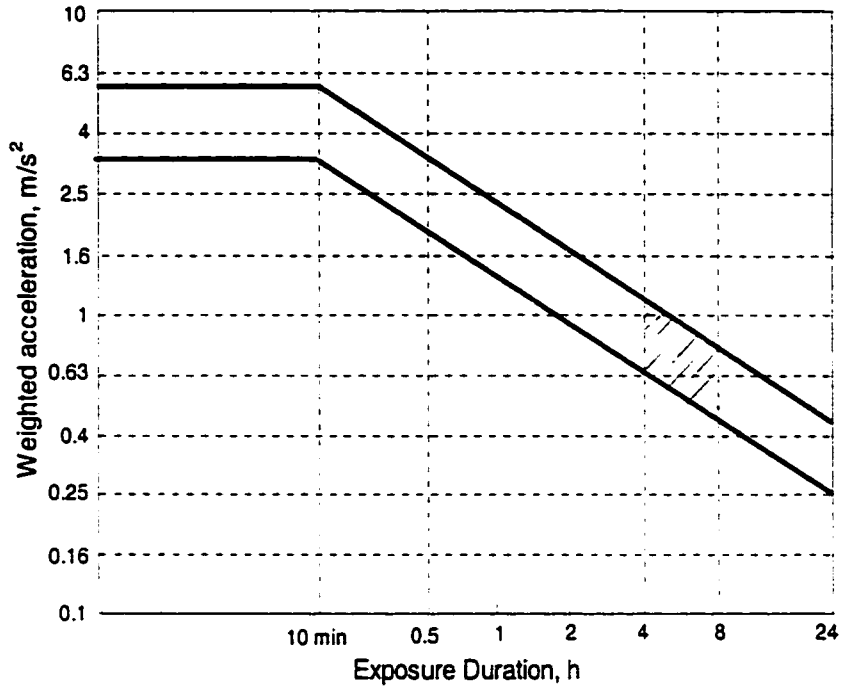

Figure 4.20 Health guidance caution zone proposed in ISO 2631-1 (1997)

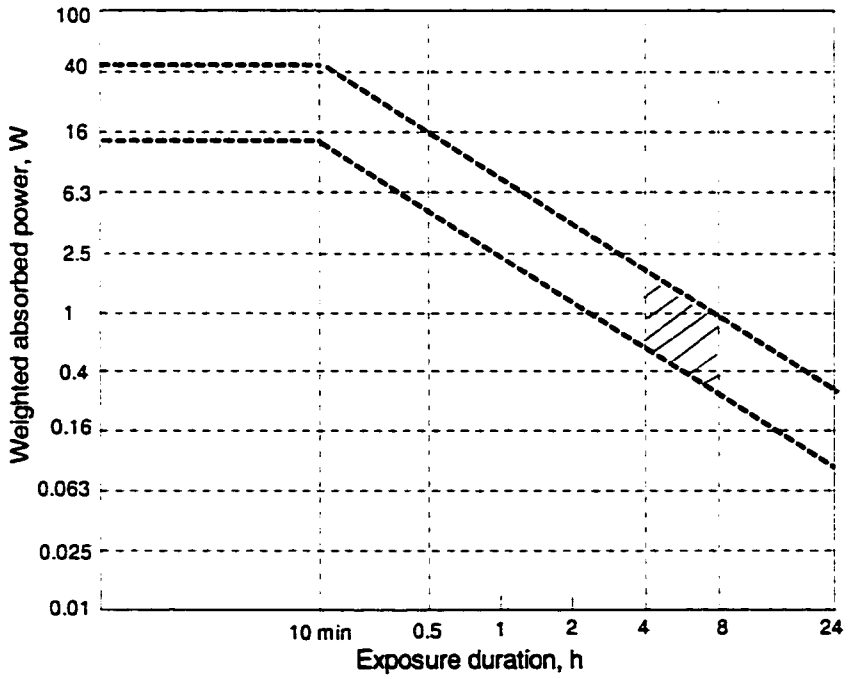

Figure 4.21 Health guidance caution zone based on absorbed power

CHAPTER 5

RESPONSE TO TRANSIENT EXCITATION

5.1 Introduction

In the previous chapters, the response of the human body to steady-state and to random excitations were studied. In this chapter, the response to a transient input is considered.

When a dynamic system is subjected to a suddenly applied excitation for a short duration, the resulting response is called transient response, since steady-state oscillations are generally not produced. Such oscillations take place at the natural frequencies of the system with the amplitude varying in a manner dependent on the type of excitation.

Under steady state oscillations, the body absorbs power continuously and hence an estimation of the total absorbed power will be an indicator of the whole body exposure to vibrations. However, when the body is subjected to transient input, the input may decay fart and hence a fourth power of the signal would be able to emphasize the intensity of the input better. This leads to the notion of a vibration dosage value (VDV) as defined in ISO 2631-1 (1997), and VDV is calculated using Equation (1.6). The estimated vibration dose value (eVDV) is also used in ISO 2631-1 and is defined as:

$$\text{eVDV} = 1.4 a_w T^{1/4} \tag{5.1}$$

where a_w is the frequency-weighted rms acceleration; T is the exposure duration.

In this chapter, the transient responses under different types of excitations will be obtained using the software SIMULINK, which can simulate and analyze numerically any given dynamic systems.

5.2 Equations of Motion

The equations of motion of the 4-DOF biodynamic system given by Equation (2.1) are rewritten as:

$$\begin{cases} \ddot{x}_1 = \dfrac{c_1}{m_1}(\dot{x}_2 - \dot{x}_1) + \dfrac{k_1}{m_1}(x_2 - x_1) \\ \ddot{x}_2 = -\dfrac{c_1}{m_2}(\dot{x}_2 - \dot{x}_1) + \dfrac{c_2}{m_2}(\dot{x}_3 - \dot{x}_2) - \dfrac{k_1}{m_2}(x_2 - x_1) + \dfrac{k_2}{m_2}(x_3 - x_2) \\ \ddot{x}_3 = -\dfrac{c_2}{m_3}(\dot{x}_3 - \dot{x}_2) + \dfrac{c_3}{m_3}(\dot{x}_4 - \dot{x}_3) - \dfrac{k_2}{m_3}(x_3 - x_2) + \dfrac{k_3}{m_3}(x_4 - x_3) \\ \ddot{x}_4 = -\dfrac{c_3}{m_4}(\dot{x}_4 - \dot{x}_3) + \dfrac{c_4}{m_4}(\dot{x}_0 - \dot{x}_4) - \dfrac{k_3}{m_4}(x_4 - x_3) + \dfrac{k_4}{m_4}(x_0 - x_4) \end{cases} \tag{5.2}$$

These equations can be conveniently solved numerically using SIMULINK, which uses symbolic processors such as integrators, differentiators, multipliers, and adders to represent the equations in the form of an analog model.

Simulating a dynamic system is a two-step process with SIMULINK. First, SIMULINK 's model editor is used to create a model of the system to be simulated. The model graphically depicts the time-dependent mathematical relationships among the system's inputs, states, and outputs. Then, SIMULINK is used to simulate the behavior of

the system for a specified time span. SIMULINK uses information entered into the model to perform the simulation.

5.3 The Data of Transient Acceleration Input

Often, the support of a dynamical system is subjected to a sudden movement specified by its displacement, velocity, or acceleration. In this chapter the input is considered in terms of acceleration. The transient acceleration input is obtained from a displacement input which originates from a vehicle (urban bus) traveling over an obstacle and shows a predominant frequency near 1.4 Hz. Since the first natural frequency of the biodynamic model under study is 4.7 Hz, the predominant frequency in the excitation may be made to occur near 5 Hz by modifying the time rate accordingly (Modified Time = 0.28*Time).

Figure 5.1 illustrates the transient acceleration input. The time trace of transient acceleration input has 7 peaks within the time span 0.8 to 1.5 seconds. The values of the two highest peaks of transient acceleration are -4.90 m/sec^2 at time 1.11 sec and 4.12 m/sec^2 at 1.0 sec, respectively.

5.4 Digital Signal Processing

The frequency-domain information can be obtained from time-domain data by using Fourier transformation, and the time-domain information can be derived from frequency-domain data in terms of inverse Fourier transform techniques.

The direct Fourier transform is used to convert a function of time, $x(t)$, into a continuous function of frequency, $X(\omega)$, as:

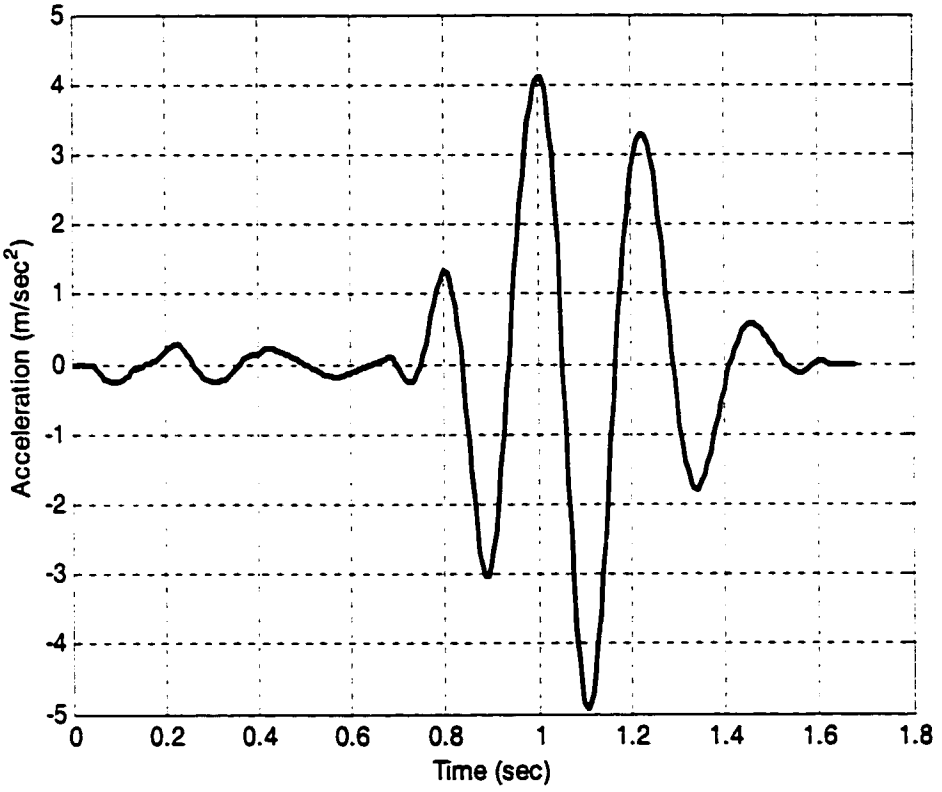

Figure 5.1 Transient acceleration input to the model

$$X(\omega) = \int_{-\infty}^{+\infty} x(t) e^{-j\omega t} dt \tag{5.3}$$

The inverse Fourier transform may be used to convert a continuous function of frequency, $X(\omega)$, into its corresponding function of time:

$$x(t) = \frac{1}{2\pi} \int_{-\infty}^{+\infty} X(\omega) e^{j\omega t} d\omega \tag{5.4}$$

The Fast Fourier Transform (FFT) (or FFT for short) is a computer algorithm for calculating Digital Fourier Transforms (DFT's) of a time series. Instead of estimating spectra by first determining correlation functions and then calculating their Fourier transforms, it is now faster and more accurate to calculate spectral estimates directly from the original time series.

The finite discrete Fourier transform relates an N-element sequence of sampled digital data $\{x_n\} = [x_0, x_1, \cdots, x_{N-1}]$ in the discrete time domain to an N-element sequence $\{X_m\} = [X_0, X_1, \cdots, X_{N-1}]$ in the discrete frequency domain. The forward transform (computed by FFT) is:

$$X_m = \Delta T \sum_{n=0}^{N-1} x_n e^{-j\frac{2\pi mn}{N}} \tag{5.5}$$

in which ΔT is the sample time step, and $m = 0, 1, \cdots, N-1$.

The inverse discrete Fourier transform (computed by IFFT) is given by:

$$x_n = \frac{1}{N \cdot \Delta T} \sum_{m=0}^{N-1} X_m e^{j2\pi mn/N} \tag{5.6}$$

in which $N \cdot \Delta T = T$ is the record length of the sampled signal.

Application of the frequency weighting defined in ISO 2631 (1997) can be performed by transforming the time-domain data to frequency-domain data, using FFT techniques, and subsequently multiplying the frequency components by the weighting factors $W_k(j\omega)$ given by Equation (3.11). Alternatively, the weighted acceleration can be obtained in the time-domain by using Inverse Fast Fourier Transform (IFFT) algorithm.

5.5 The Responses to Transient Acceleration Input

The instantaneous acceleration, rms acceleration, VDV, and absorbed power responses of different body parts under the transient acceleration input are derived in this section.

5.5.1 The acceleration responses

To obtain the acceleration responses of different body segments under the transient acceleration excitation, the SIMULINK model developed for the 4-DOF system is shown in Figure 5.2. In this model, the acceleration responses in different body parts may be observed from scopes (a1, a2, a3, and a4). In order to have a comparison with each other, they also can be observed in a chart form by the open block scope "a1, a2, a3,

a4". The simulation time is also selected as 1.8 seconds since the default time duration is 1.67 seconds. The unweighted acceleration responses are obtained by importing transient acceleration signal into "Accel" in the block "From Workspace", while the weighted acceleration responses are obtained by importing the weighted acceleration signal.

Figures 5.3 and 5.4 illustrate the unweighted and frequency-weighted acceleration responses in different body segments, respectively, under the transient acceleration input. Similar to transient input signal, each of the local unweighted and frequency-weighted acceleration responses of the body has seven peaks within the default time 0.8 to 1.5 seconds. The maximum amplitudes of unweighted acceleration responses for mass 1, 2, 3, and 4 are 8.20 m/sec^2 at default time 1.13 seconds, 8.10 m/sec^2 at 1.13 seconds, 7.26 m/sec^2 at 1.13 seconds, and 6.50 m/sec^2 at 1.12 seconds, respectively. The largest magnitudes of frequency-weighted acceleration responses for mass 1, 2, 3, and 4 are 7.20 m/sec^2 at default time 1.13 seconds, 7.10 m/sec^2 at 1.13 seconds, 6.38 m/sec^2 at 1.13 seconds, and 5.61 m/sec^2 at 1.12 seconds.

5.5.2 Rms acceleration and VDV computation for the different body segments

In this section, the basic evaluation of vibration exposure, root-mean-square (rms) acceleration and the additional evaluation of vibration, fourth power vibration dose value (VDV), under unweighted and weighted acceleration are determined, respectively, using SIMULINK models.

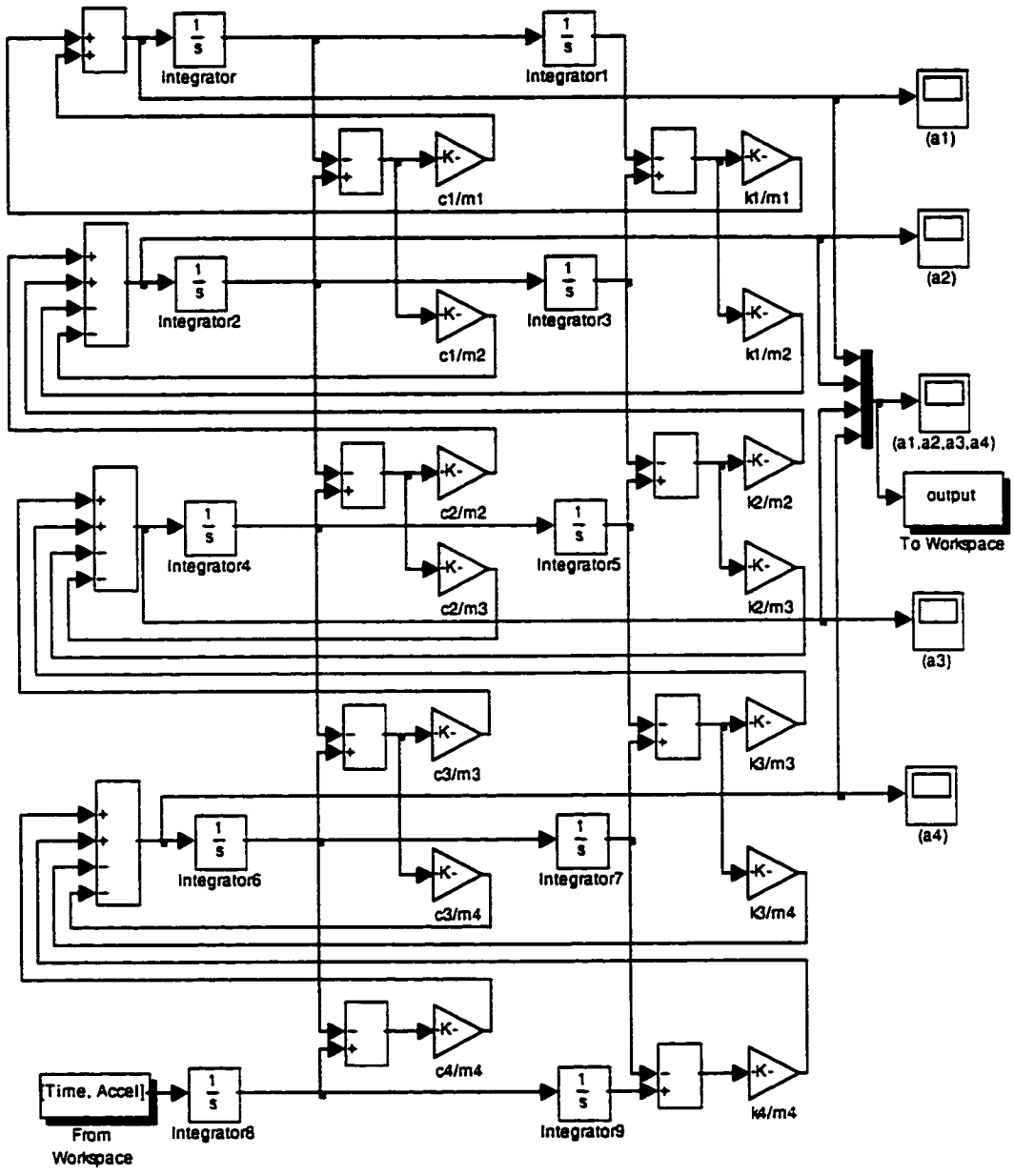

Figure 5.2 A SIMULINK model of the 4-DOF system subjected to an acceleration excitation to get the local acceleration responses

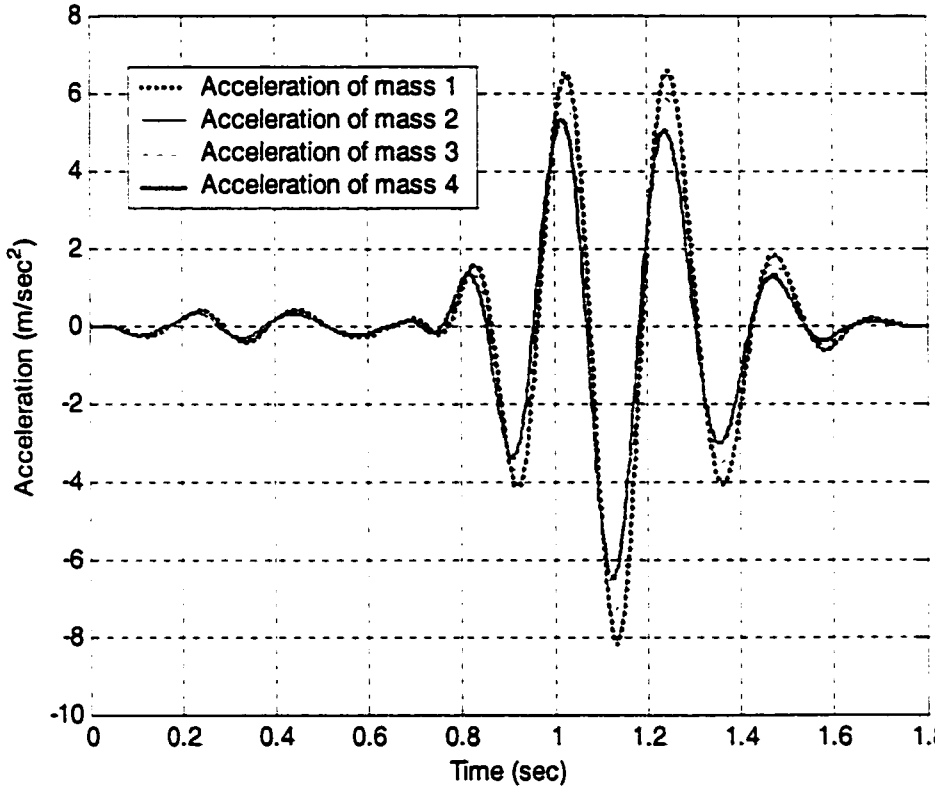

Figure 5.3 Unweighted acceleration responses of different body segments under the transient acceleration input

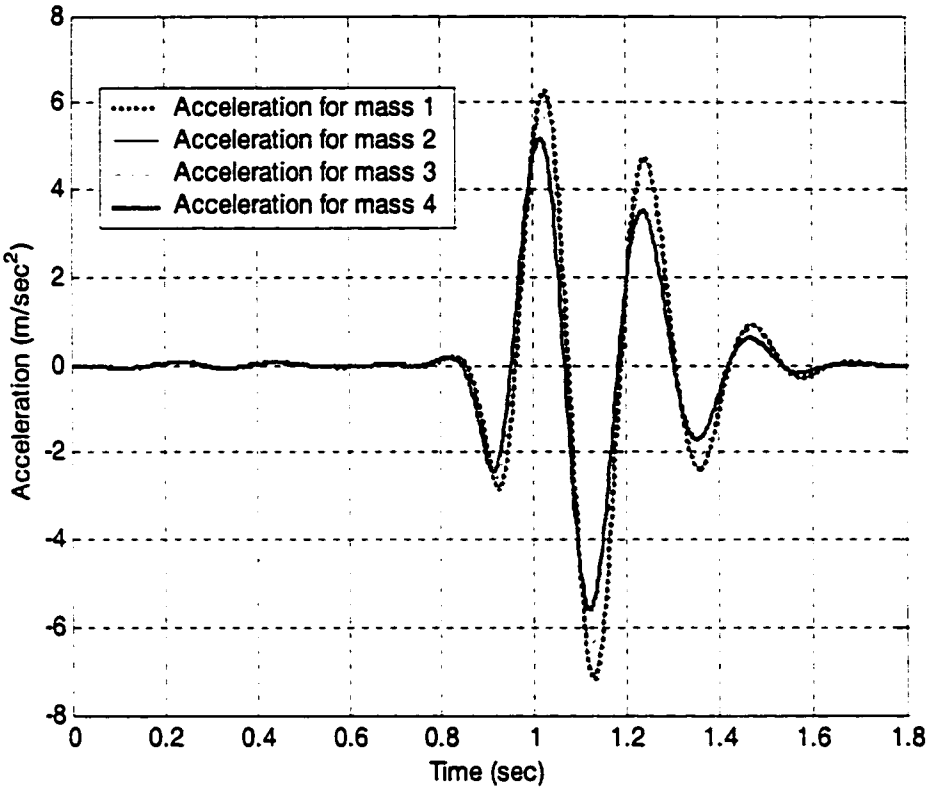

Figure 5.4 Frequency-weighted acceleration responses of different body segments under the transient acceleration input

The unweighted rms acceleration (a_{rms}) and weighted rms acceleration ($a_{w,rms}$) are expressed in the time domain as:

$$a_{rms} = \left[\frac{1}{T}\int_0^T a^2(t)dt\right]^{1/2} \tag{5.7}$$

$$a_{w,rms} = \left[\frac{1}{T}\int_0^T a_w^2(t)dt\right]^{1/2} \tag{5.8}$$

where $a(t)$ and $a_w(t)$ are the instantaneous unweighted and frequency-weighted acceleration as functions of time; and T is the duration of the measurement.

For a digital signal, the unweighted rms acceleration (a_{rms}) and weighted rms acceleration ($a_{w,rms}$) are computed from:

$$a_{rms} = \left[\lim_{N\to\infty}\frac{1}{N}\sum_{i=1}^{N} a^2(t_i)\right]^{1/2} \tag{5.9}$$

$$a_{w,rms} = \left[\lim_{N\to\infty}\frac{1}{N}\sum_{i=1}^{N} a_w^2(t_i)\right]^{1/2} \tag{5.10}$$

where N is the number of samples.

VDV is more sensitive to peaks than the basic evaluation method since it uses the fourth power instead of the second power of the acceleration time history as the basis for averaging. The unweighted vibration dose value (VDV_u) and weighted vibration dose value (VDV_w) are defined as:

$$VDV_u = \left[\int_0^T a^4(t)dt\right]^{1/4} \tag{511}$$

$$VDV_w = \left[\int_0^T a_w^4(t)dt\right]^{1/4} \tag{5.12}$$

For a digital signal, the unweighted vibration dose value (VDV_u) and weighted vibration dose value (VDV_w) are defined as:

$$VDV_u = \left[\lim_{N\to\infty}\frac{T}{N}\sum_{i=1}^{N} a^4(t_i)\right]^{1/4} \tag{5.13}$$

$$VDV_w = \left[\lim_{N\to\infty}\frac{T}{N}\sum_{i=1}^{N} a_w^4(t_i)\right]^{1/4} \tag{5.14}$$

The SIMULINK model for computing rms accelerations and VDV of the input signal formulated according to the definitions expressed by Equations (5.7), (5.8), (5.11) and (12), is shown in Figure 5.5. The rms acceleration and VDV_u of the input are determined as the vector "Accel" in the block "From Workspace" is imported the transient input signal.

The model for determining rms acceleration and VDV of the body segment responses is illustrated in Figure 5.6. A block "subsystem", whose contents are illustrated in Figure 5.7 is introduced to simplify the model. As the vector "Accel" in the block "From Workspace" shown in Figure 5.7 is imported the input signal, the unweighted acceleration responses of different body segments are obtained, while the weighted

acceleration responses are determined as the vector "Accel" is imported the frequency-weighted acceleration signal.

The rms acceleration and VDV also can be determined in terms of computer (programming) based on Equations (5.9), (5.10), (5.13) and (5.14).

Table 5.1 tabulates the results of unweighted rms acceleration (a_{rms}) and vibration dose values (VDV_u) responses of different body segments under the transient acceleration input.

Table 5.1 The results of unweighted rms acceleration and VDV responses of different body parts under the transient input

Identification	Transient input	Unweighted responses of body segments			
		Mass 1	Mass 2	Mass 3	Mass 4
a_{rms} (m/s^2)	1.51	2.54	2.51	2.28	2.02
VDV_u $(m/s^{1.75})$	2.62	4.38	4.32	3.94	3.48

According to the definitions, the relation between frequency-weighted rms ($a_{w.rms}$) acceleration and weighted vibration dose value (VDV_w) can be established as:

$$VDV_w \approx C_1 \cdot a_{w.rms} T^{1/4} \tag{5.15}$$

where C_1 is a constant coefficient, ant it should be close to 1.4 based on Equation (5.1).

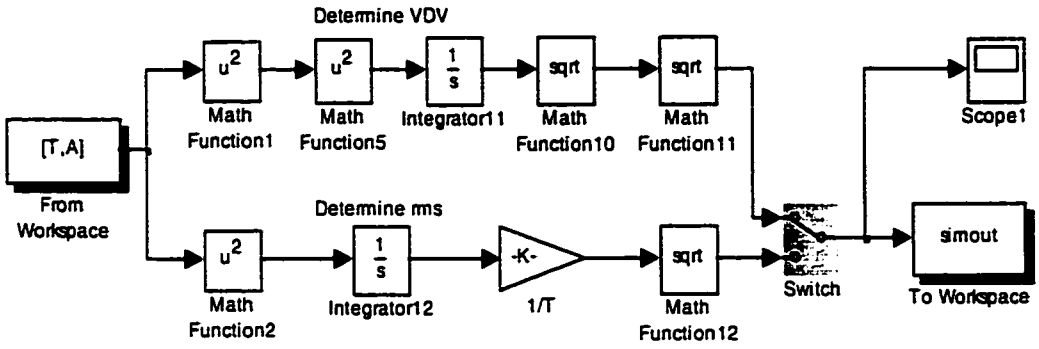

Figure 5.5 A SIMULINK model to determine VDV and rms acceleration of the input transient acceleration signal

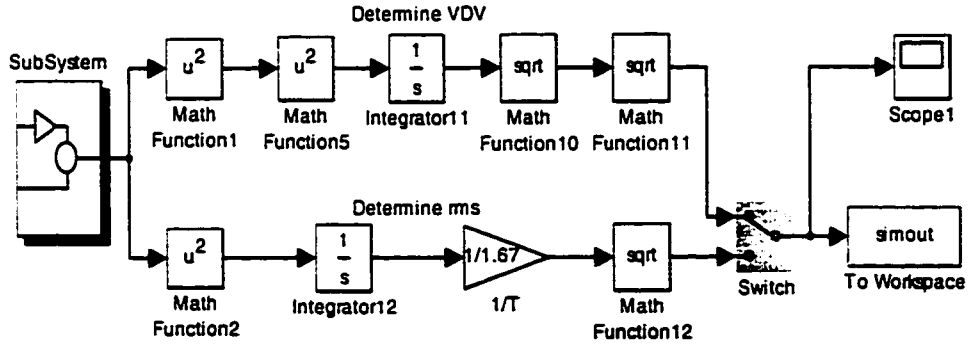

Figure 5.6 A SIMULINK model to determine VDVs and rms accelerations of body segments under the transient acceleration input

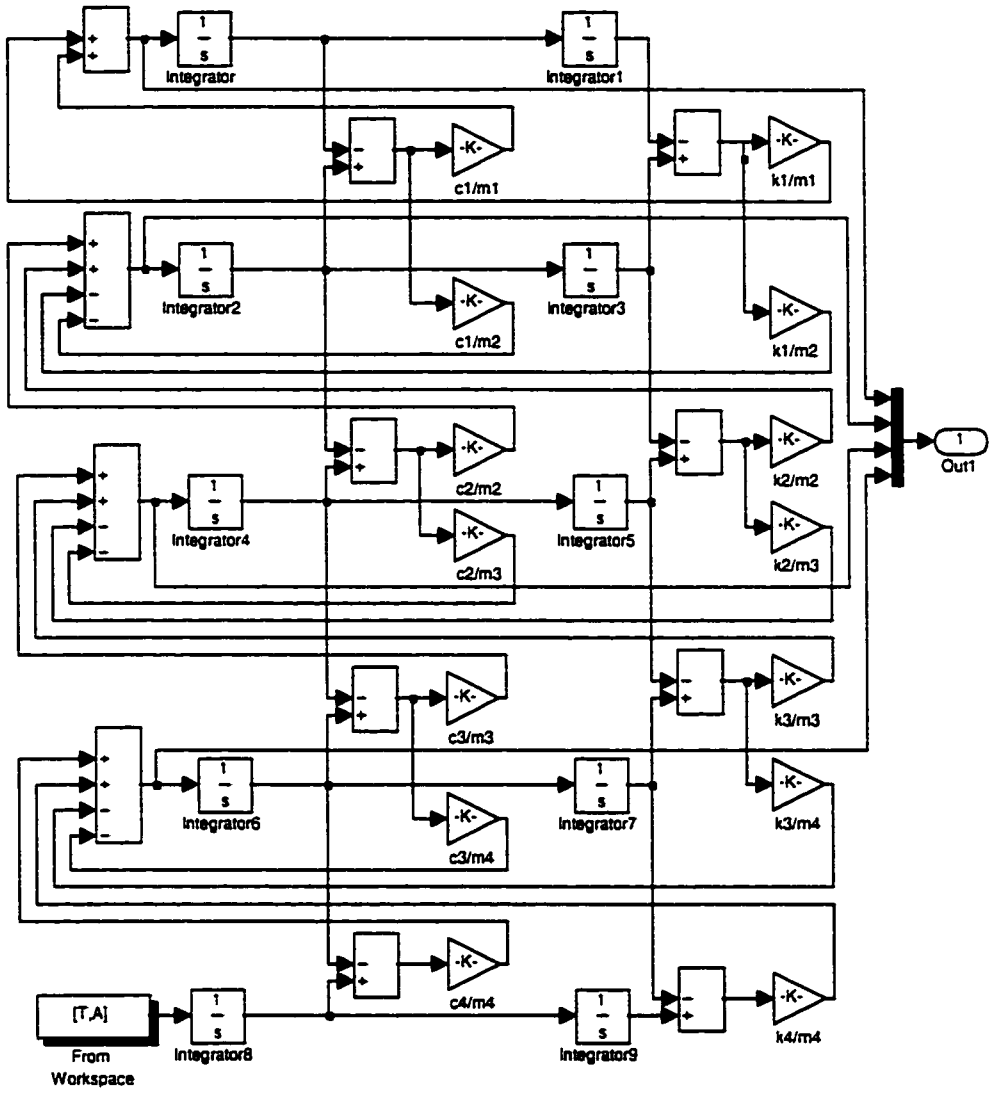

Figure 5.7 The subsystem shown in Figure 5.6

Table 5.2 tabulates the results of weighted rms accelerations ($a_{w,rms}$) and weighted vibration dose values (VDV_w) of the transient acceleration input and responses of different body segments, and the coefficient C_1.

Table 5.2 The results of frequency-weighted rms acceleration and VDV responses of different body parts under the transient input

Identification	Transient Input	Frequency-weighted responses of body segments			
		Mass 1	Mass 2	Mass 3	Mass 4
$a_{w,rms}$ (m/s^2)	1.25	2.06	2.03	1.85	1.64
VDV_w $(m/s^{1.75})$	2.32	3.76	3.71	3.38	3.00
C_1	1.62	1.60	1.60	1.60	1.60

5.5.3 Absorbed power computation

For the studied model, the instantaneous absorbed powers for different body segments are computed from:

$$P_{abs,i}(t) = c_i(\dot{x}_i - \dot{x}_{i+1})^2 \tag{5.16}$$

The total instantaneous absorbed power is given by:

$$P_{Tot}(t) = \sum_{i=1}^{4} c_i (\dot{x}_i - \dot{x}_{i+1})^2 \tag{5.17}$$

To obtain the absorbed powers in different body parts under the transient acceleration excitation, the SIMULINK model for the 4-DOF system can be established as Figure 5.8, based on Equations (5.1), (5.16) and (5.17). In this model, the local absorbed powers may be observed from scopes (Pabs1, Pabs2, Pabs3, and Pabs4), and a bar "Mux" is added in this model to plot the different local absorbed powers in a chart, which can be observed from the scope Pabs1,2,3,4.

The unweighted absorbed power in damper 1 under the transient excitation is illustrated in Figures 5.9, from which it may be observed that the curve has seven peaks within the default time 0.8 to 1.5 seconds, and the maximum amplitude is 5.73×10^{-3} W at the default time 1.09 seconds. The frequency-weighted absorbed power in damper 1 is shown in Figure 5.10, which also has seven peaks within the time 0.8 to 1.5 seconds. The maximum magnitude is 5.10×10^{-3} W at the default time 1.08 seconds.

Figure 5.11 shows the unweighted absorbed powers in damper 2, 3, and 4 under the transient acceleration excitation. Each of the curves has seven peaks within the default time 0.8 to 1.5 Hz. The maximum amplitudes of unweighted absorbed powers in damper 2, 3, and 4 are 5.03 W, 8.64 W, and 22.63 W at default time 1.10 seconds, respectively. The frequency-weighted absorbed powers in dampers 2, 3, and 4 are illustrated in Figure 5.12, in which each of curves also has seven peaks within the default time 0.8 to 1.5 seconds. The maximum amplitudes of frequency-weighted absorbed powers in damper 2, 3, and 4 are 4.35 W, 7.37 W, and 19.42 W at the default time 1.10 seconds.

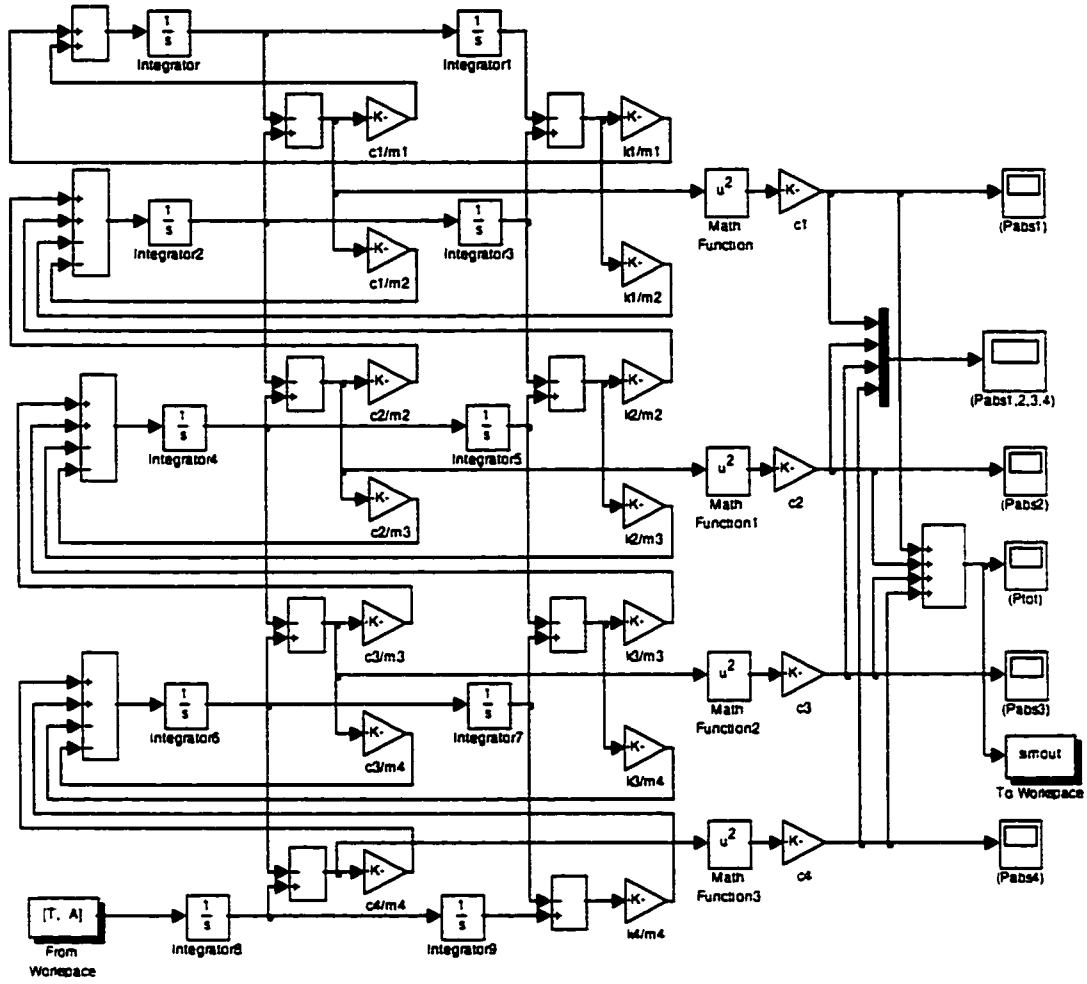

Figure 5.8 A SIMULINK model of the 4-DOF system subjected to an acceleration excitation to get the local absorbed power responses

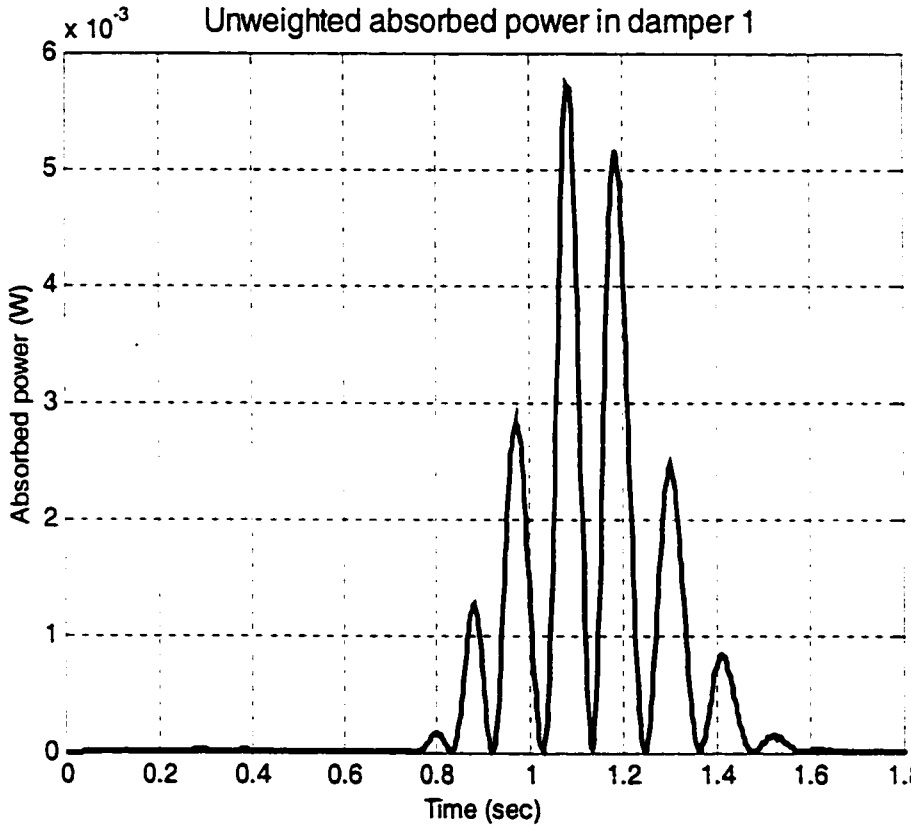

Figure 5.9 Unweighted absorbed power in damper 1 (head) under the transient acceleration input

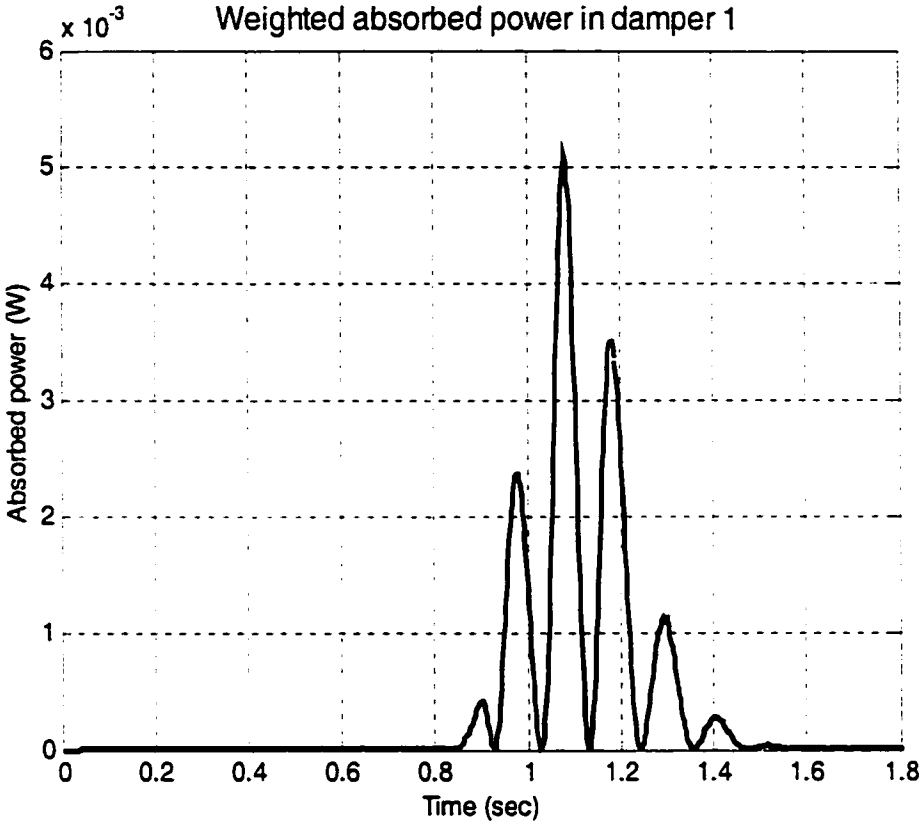

Figure 5.10 Weighted absorbed power in damper 1 (head) under the transient acceleration input

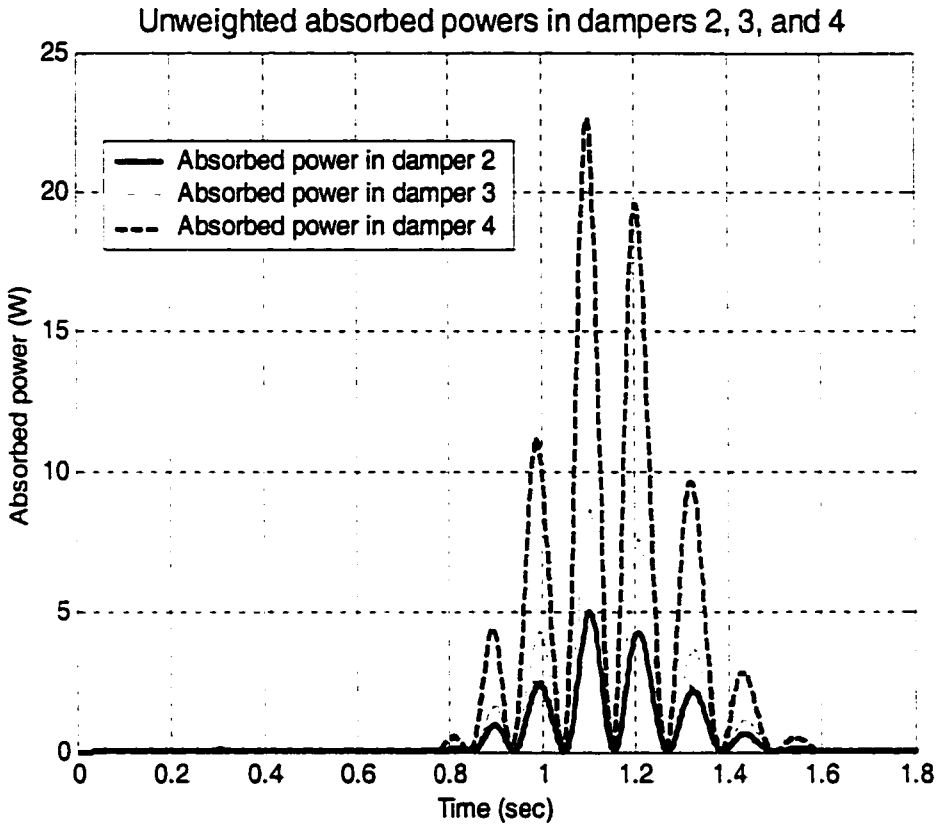

Figure 5.11 Unweighted absorbed powers in dampers 2, 3, and 4 under the transient acceleration input

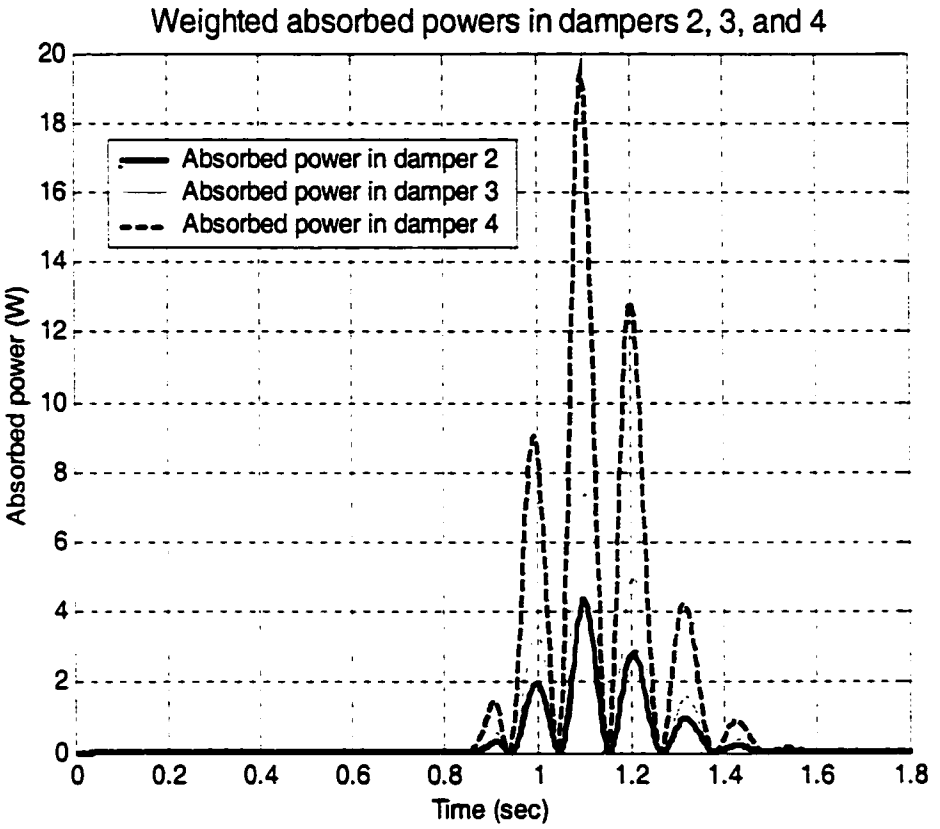

Figure 5.12 Weighted absorbed powers in dampers 2, 3, and 4 under the transient acceleration input

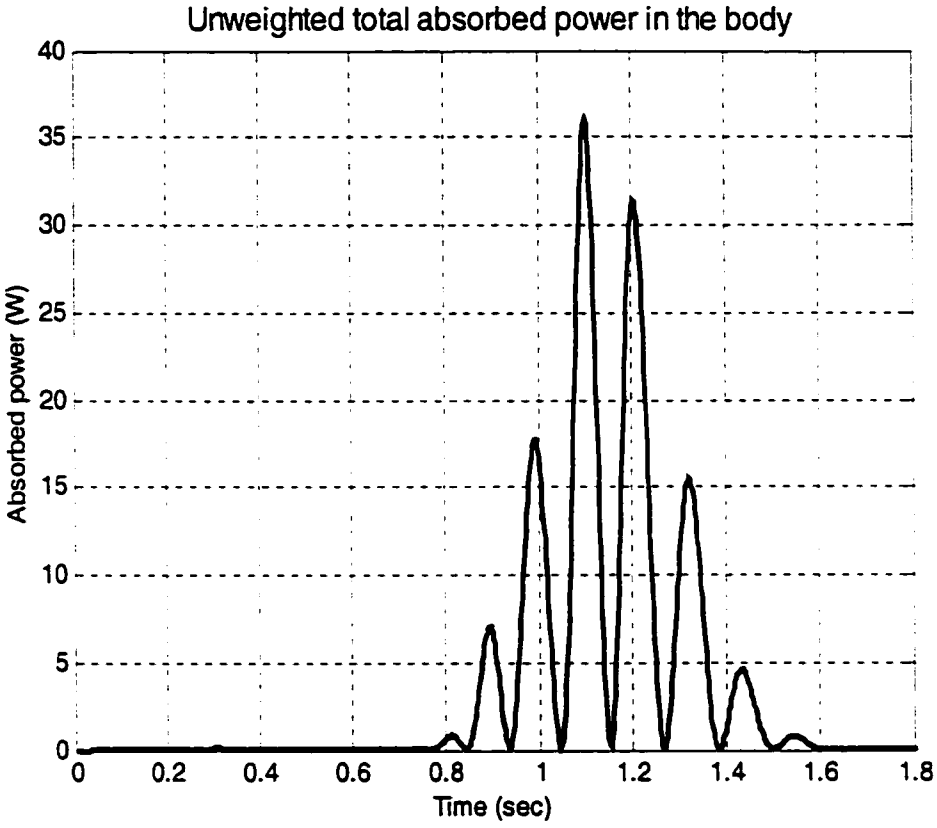

Figure 5.13 Unweighted total absorbed power in the body under the transient acceleration input

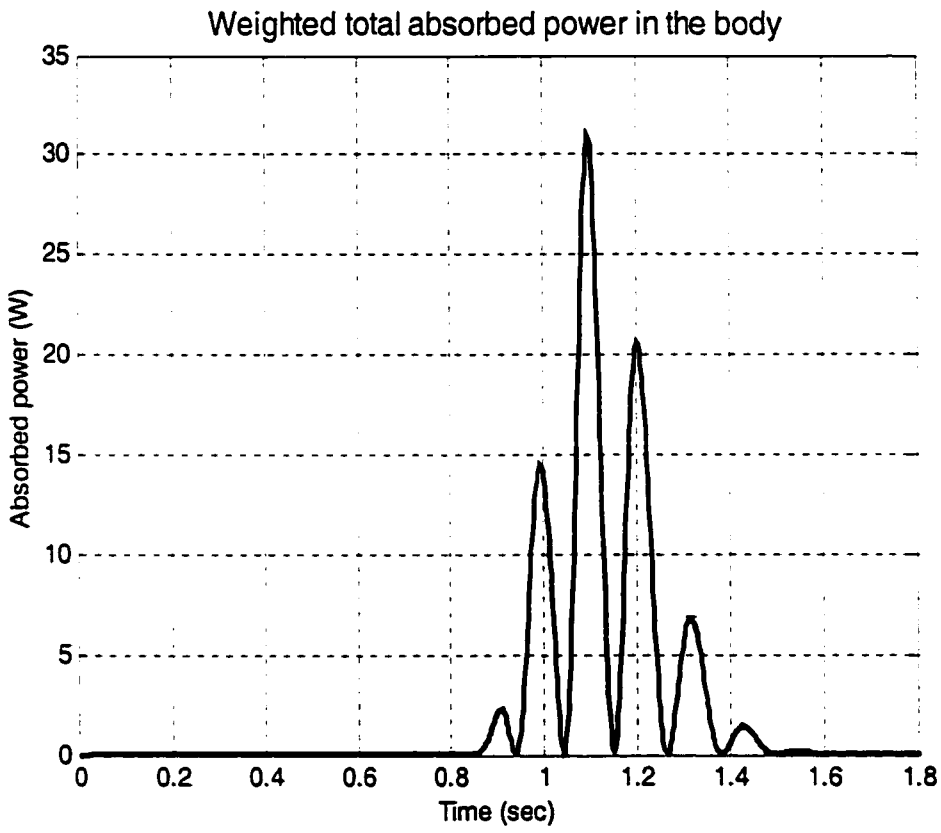

Figure 5.14 Weighted total absorbed power in the body under the transient acceleration input

The unweighted and frequency-weighted total absorbed powers in the body are illustrated in Figures 5.13 and 5.14, respectively. Both curves have seven peaks within the default time 0.8 to 1.5 seconds. The maximum amplitudes of the unweighted and frequency-weighted total absorbed power are 36.05 W and 30.99 W, respectively.

The results show that very little absorbed power response occurs in the damper 1 associated with the head, and most of the absorbed power occurs in damper 4 associated with the thighs and pelvis in contact with the seat. A significant portion of the total absorbed power in the body is also seen to be due to the absorbed power in damper 4.

5.6 Definition of Health Risk Evaluation Based on Absorbed Power

5.6.1 Relationship between absorbed power and rms acceleration

In ISO 2631-1 (1997), the vibration responses are assumed to relate to energy. The equivalent energy is given by:

$$E_{eq} = C \cdot a_{w.rms}^2 \cdot T \tag{5.18}$$

where C is a constant; and $a_{w.rms}$ is the frequency-weighted rms acceleration values for exposure duration T, and it is determined from Equation (5.8) or (5.10).

Absorbed power represents the real energy dissipated per unit exposure time, so that the total absorbed energy in the body for the exposure time T is calculated from:

$$E_{abs} = \int_0^T P_{w.Tot}(t)dt = \overline{P}_{w.TOT} \cdot T \tag{5.19}$$

where $P_{w.Tot}(t)$ is the total instantaneous absorbed power in the body, and is given by Equation (5.17) as the acceleration input is weighted. $\overline{P}_{w.TOT}$ is the mean value of the total weighted absorbed power in the body, and is computed from:

$$\overline{P}_{w.TOT} = \frac{E_{abs}}{T} = \frac{1}{T}\int_0^T P_{w.Tot}(t)dt \tag{5.20}$$

Applying the concept of equivalent energy presented in Equation (5.18) into "absorbed energy" presented in Equation (5.19), it may be inferred that the relationship between the mean value of total frequency-weighted absorbed power and frequency-weighted rms acceleration is:

$$\overline{P}_{w.TOT} \approx C \cdot a_{w.rms}^2 \tag{5.21}$$

where C is a constant correlation coefficient in $W/(m/s^2)^2$.

The computed results of frequency-weighted rms acceleration of the transient input, and the mean value of frequency-weighted absorbed power in the whole body within the exposure duration, as well as the correlation coefficient C, are presented in Table 5.3:

Table 5.3 Mean value of total weighted absorbed power, weighted rms acceleration, and correlation coefficient.

Mean value of total weighted absorbed power in the body ($\overline{P}_{w,TOT}$)	Weighted rms acceleration of the transient input ($a_{w,rms}$)	Correlation coefficient ($C = \frac{\overline{P}_{w,TOT}}{a_{w,rms}^2}$)
2.45 W	1.25 (m/s^2)	1.57 W/(m/s^2)^2

5.6.2 Comparison of the coefficient *C* between transient and random inputs

The correlation coefficient C during the random excitation is 1.43 W/(m/s^2)^2 as shown in Table 4.1. and that during the transient input is 1.57 W/(m/s^2)^2 as shown in Table 5.3. That means the absorbed power in whole body for transient excitation is higher (10%) than for random vibration during the same rms acceleration level excitation. It may be indicate absorbed power is a better measure of health risk than rms acceleration.

5.6.3 Relation between absorbed power and vibration dose value

Equation (5.15), the relations between weighted rms acceleration and vibration dose value may be rewritten as:

$$a_{w,rms} \approx \frac{VDV_w}{C_1 T^{1/4}} \tag{5.22}$$

Introducing Equation (5.22) into Equation (5.21), the relationship between mean value of the total weighted absorbed power in the body and weighted vibration dose value is derived as:

$$\overline{P}_{w.TOT} \approx C \cdot \left(\frac{\mathrm{VDV}_w}{C_1 T^{1/4}} \right)^2 = \frac{C}{C_1^2 T^{1/2}} \left(\mathrm{VDV}_w \right)^2 \tag{5.23}$$

For duration time T fixed, the Equation (5.23) may be written as:

$$\overline{P}_{w.TOT} \approx K \cdot \left(\mathrm{VDV}_w \right)^2 \tag{5.24}$$

where K is a constant correlation coefficient, and computed from:

$$K = \frac{C}{C_1^2 \cdot T^{1/2}} \tag{5.25}$$

Substituting $C = 1.57$ W/(m/s^2)^2 shown in Table 5.3, $C_1 = 1.6$ shown in Table 5.2, and T = 1.67 sec into Equation (5.26), $K = 0.46$ W/(m/s$^{1.75}$)^2.

The relation between the total weighted absorbed power in the body and weighted vibration dose value under the transient acceleration input is given by:

$$\overline{P}_{w.TOT} \approx 0.46 \left(\mathrm{VDV}_w \right)^2 \tag{5.26}$$

In ISO 2631-1 (1997), the estimated vibration dose values corresponding to the lower and upper bounds of the health caution zone given by Equation (1.12) are 8.5 and 17 for exposure time 8 h, respectively. These limits are translated into total absorbed power in the body are 33 W and 133 W for exposure 8 h, respectively.

5.7 Summary

Digital transient acceleration input signal is needed for signal processing, and the acceleration needs to be weighted. FFT and IFFT were applied to make signal processing.

SIMULINK models, which are very efficient to make the dynamic analysis in time-domain, were established to determine the acceleration and absorbed power responses during the acceleration transient excitations and to determine rms acceleration and VDV.

The equations derived in this study have shown that the weighted absorbed power in each damper is not only proportional to the damping coefficient c_i, but also to the square relative weighted acceleration. Thus, it is possible to link the weighted rms absorbed power with the weighted rms acceleration, which is the basic measure for exposure assessment in ISO 2631-1 (1997). In this chapter, the relationship between weighted absorbed power and weighted rms acceleration and VDV were determined, under a transient acceleration input having dominant frequency near 5 Hz. Although the linked relationship was derived from a particular transient acceleration input, the method to link the absorbed power with acceleration evaluation can probably be extended to other transient acceleration inputs.

By comparing the correlation coefficients between absorbed power and frequency-weighted rms acceleration under the random excitation and transient input, it is known that the absorbed power in the body for transient input is larger (10%) than that for random excitation under the same rms acceleration level excitation, i.e. under the same rms acceleration excitation, the transient input will lead to higher health risk on human body than the random excitation. It indicates that the absorbed power is a better measure for health risk than frequency-weighted rms acceleration.

CHAPTER 6

CONCLUSIONS AND RECOMMENDATIONS FOR FUTURE WORK

6.1 General

Whole-body vibration has long been implicated in causing adverse health effects and performance degradation of vehicle operators [34]. A variety of vehicles employed in industry, forestry and transport sectors pose vertical vibration and shock of comprehensive magnitude in the frequency range of 1 to 20 Hz. The most sensitive frequency band for vertical motions of humans is 4 to 6 Hz [35].

The most commonly used standards for assessing exposure from WBV is International Standard ISO 2631-1 (1997), which describes methods for evaluating vibration in relation to human health, interference with activities, discomfort and possibility of motion sickness. Accordingly, measurement of WBV should be conducted on the surface transmitting vibration to the human body. Vibration should be measured within the frequency range of 0.5 to 80 Hz in terms of frequency-weighted rms acceleration. Under transient or shock excitations, this method is complemented with alternate methods such as VDV and MTVV. A disadvantage with this measure is that it only describes the acceleration magnitude on the vibrating surface. Thus, it can be argued that it presents a poor description of the extent of vibration actually being transmitted to the body [14].

The amount of vibration energy, either absorbed or exchanged between the source and body, may therefore be a good indicator of the physical stress on the body since it takes into consideration the interplay between the vibrating structure and the body in

contact with it. Moreover, energy is a scalar quantity that makes it easy to add up contributions from all three directions to a single value. In this study, absorbed power during exposure to vertical WBV was considered as a potential indicator of the physical stress affecting comfort and health.

6.2 Highlights of the Study

The major highlights of this investigation are summarized below:

- ◊ Derivation of damped natural frequencies of the MDOF (4-DOF) model by solving eigenvalue problem of the system. Identification of stability of the system by an examination of obtained eigenvalues.
- ◊ Determination of the damping ratios and damping matrix of the MDOF model. Specification of modal properties (*i.e.* underdamped, overdamped, critically damped).
- ◊ Derivation of frequency response function (FRF) of the 4-DOF model and transmissibilities of seat to different masses (body segments) as well as DPMI of the model.
- ◊ Response analysis to random excitation, establishment of relationship between frequency-weighted rms acceleration and total body absorbed power.
- ◊ Formulation of absorbed powers of different body segments and total body power absorption under the sinusoidal excitation.
- ◊ Derivation of absorbed powers of different body segments and total body power absorption under the random excitation IT 1.

- ◊ Development of the "Health guidance caution zone" under a random excitation based on absorbed power from energy considerations.
- ◊ Formulation of the acceleration responses and absorbed powers of different body segments under transient acceleration excitation using SIMULINK models.
- ◊ Digital signal processing and computation of frequency-weighted accelerations using Fast Fourier Transform (FFT) and Inverse Fast Fourier Transform (IFFT).
- ◊ Calculation of frequency-weighted rms acceleration and vibration dose value of transient acceleration input and acceleration responses and absorbed powers of different body segments using SIMULINK models.
- ◊ Determination of the relationships between the total weighted absorbed power in the body and frequency-weighted rms acceleration and vibration dose value under a transient acceleration input.
- ◊ Linking the absorbed power with ISO 2631-1 (1997) by determining the correlation between weighted total absorbed power in the body and frequency-weighted rms acceleration excitation under both random and transient excitation.

6.3 Conclusions

On the basis of the studies conducted in this thesis, the following major conclusions are drawn:

- ◊ The natural frequencies of the selected model are 4.7 and 40.4 Hz. The model is a mixed damping system in which two modes oscillate and two modes are overdamped. In consequence, the model has only two natural frequencies rather than four.

- ◊ The first mode of the selected model, whose natural frequency is 4.7 Hz, oscillates more strongly than the second one whose natural frequency is 40.4 Hz.
- ◊ The transmissibility magnitude characteristics show that close to the first natural frequency 4.7 Hz, the transmissibility of seat to mass 1 associated with head is the largest, to mass 2 the second largest, to mass 3 the third largest, and to mass 4 is the smallest.
- ◊ Under any excitation (*i.g.* sinusoidal, transient, and random excitation), very little energy is absorbed in damper 1 associated with the head, while most of the absorbed power occurs in damper 4, which is the closest to the source of excitation, and is associated with the thighs and pelvis in contact with the seat. A significant portion of the total absorbed power is also seen to be in damper 4.
- ◊ The total body absorbed power can be related to the frequency-weighted rms acceleration measurement proposed in International Standard ISO 2631-1 (1997) under random. Thus, the evaluation of health risk based on absorbed power can be established.
- ◊ The absorbed power is a scalar quantity that makes it easy to add up contributions from different body segments. Moreover, it is proportional to the squared rms acceleration and is more sensitive than the measure of frequency-weighted rms acceleration. Therefore, the absorbed power in the body will be a potential indicator of fatigue and occupational health hazard.
- ◊ As the absorbed power links with the frequency-weighted rms acceleration, these results are achieved: The correlation coefficient C during the random excitation is 1.43 $W/(m/s^2)^2$ as shown in Table 4.1, and that during the transient input is 1.57

$W/(m/s^2)^2$ as shown in Table 5.3. That means the absorbed power in whole body for transient excitation is higher (10%) than for random vibration during the same rms acceleration level excitation, i.e. under the same rms acceleration excitation, the transient input will lead to higher health risk on human body than the random excitation. It indicates that the absorbed power is a better measure than frequency-weighted rms acceleration.

6.4 Recommendations for Further Investigation

1) The study of absorbed power in other models

The study of absorbed power in the present 4-DOF model may be extended to other linear models, such as the 3-DOF model proposed in ISO/DIS 5982 (2000) illustrated in Figure 1.8, and also can be extended to other non-linear models.

2) The study of local absorbed power

In this study, although the local absorbed powers of different body parts are derived during the sinusoidal, transient, and random excitations, the evaluation of health risk is based on the total absorbed power in the body. However, there are situations where a particular body segment may be experiencing excessive vibrations causing local fatigue and health consequences. Hence, investigations on the local fatigue and health risk should be assessed based on the local absorbed powers.

3) Measurement of absorbed power and model validation

The analysis can be verified using some experimental studies in the laboratory. The experimental part consists of a hydraulically excited seat with a stop switch operated by the subject. The acceleration measurements are carried on a bite bar, and acceleration responses are measured at several points on the body.

Absorbed power during exposure to vehicle WBV in the sitting posture could be measured on a group of subjects (around 20 to 30 people). Different experimental conditions could be applied, such as vibration level, body weight, frequency, and relaxed and erect upper body positions. The experimental results show the relation between absorbed power and the frequency of vibration.

The acceleration response levels are plotted against the frequency of excitation. It is possible to link the vibration levels with the energy dissipated. The experimental results could help in establishing a relation between energy dissipated and fatigue and health hazard.

This study will show that the absorbed power depends on several factors, which vary with frequency and magnitude of vibration. The vibration levels will be linked with the energy dissipated, which will help in establishing a relationship between energy dissipated and fatigue and health hazard.

4) Determination the correlation between absorbed power and rms acceleration

In this thesis the correlation coefficient C between absorbed power and rms acceleration are determined for two excitations. Hence, the results are of some specificity. In order to achieve the general characteristics, more random and transient

excitations should be inputted. Then the general correlation between absorbed power and rms acceleration can be obtained. If the results are similar as that in the thesis, it can be concluded absorbed power is a better indicator than rms acceleration and at least it is so for transient excitation.

REFERENCES

1. M. J. Griffin (1990) "Handbook of human vibration", Academic press, Harcout Brace Jovanovich.

2. L.C. Fothergill and M. J. Griffin (1977) "The subjective magnitude of whole-body vibration", Ergonomics 20: 521-533.

3. D. Simic (1974) "Contribution to the optimization of the oscillatory properties of a vehicle: physiological foundations of comfort during oscillations", Library Translation No. 1707. Royal Aircraft Establishment, Farnborough.

4. A.J. Jones and D.J. Saunders (1972) "Equal comfort contours for whole body vertical, pulsed sinusoidal vibration", Journal of Sound and Vibration 23: 1-14.

5. International Standard ISO 2631-1 (1997) "Mechanical vibration and shock-evaluation of human exposure to whole-body vibration".

6. Draft International Standard ISO/DIS 5982 (2000) "Mechanical vibration and shock-Range of idealized values to characterize seated-body biodynamic response under vertical vibration", International Organization for Standardization, 2000.

7. F. Pradko, R.A. Lee, J.D. Greene (1965a) "Human vibration-response theory". In: Witer Annual Meeting of the Human Factors Division, Chicago. The American Society of Mechanical Engineers.

8. F. Pradko, T.R. Orr, and R.A. Lee (1965b) "Human vibration analysis". Paper 650426. Society of Automotive Engineers, Mid-year Meeting, Chicago.

9. F. Pradko and R.A. Lee (1966) "Vibration comfort criteria". Paper 660139. Society of Automotive Engineers.

10. R.A. Lee and F. Pradko (1968) "Analytical analysis of human vibration". Automotive Engineering Congress, Detroit, Michigan, 8-12 January 1968. Paper 680091. Society of Automotive Engineers.

11. R.N. Janeway (1975a) "Analysis of proposed criteria for human response to vibration". Ride Quality Symposium, national Aeronautics and Space Administration, Williamsburg, Virginia.

12. R.N. Janeway (1975b) "Human vibration tolerance criteria and application to ride evaluation". Society of Automotive Engineers, Engineering Conference, Detroit. SAE Paper 750166.

13. I.-M. Lidstrom (1977) "Vibration injury in rock drillers, chiselers and grinders. Some views on the relationship between the quantity of energy absorbed and the risk of occurrence of vibration injury". In: Proceedings of the International Occupational Hand-Arm Vibration Conference, National Institute for Occupational Safety and Health, Cincinnati, OH, USA. DHEW (NIOSH) Publication No. 77-170, pp. 78-83.

14. R. Lundstrom, P. Holmlund, and L. Lindberg (1998). "Absorption of energy during vertical whole-body vibration exposure". Department of Technical Hygiene, National Institute for Life, Sweden. Journal of Biomechanics 31 (1998) 317-326.

15. N.J. Mansfield, P. Holmlund, and R. Lundstrom (2000). "Comparison of subjective responses to vibration and shock with standard analysis methods and absorbed power". Department of Technical Hygiene, National Institute for Life, Sweden. Journal of Sound and Vibration (2000) 230(3), 477-491.

16. Mansfield, N.J. and Griffin, M.J. (1998) "Effect of magnitude of vertical whole-body vibration on absorbed power for the seated human body", Journal of Sound and Vibration 251, 813-825, 1998.

17. Coermann, R.R. (1962). "The mechanical impedance of the human body in sitting and standing position at low frequencies". Human Factors 4: 227-253.

18. Payne, P.R. (1978) "Method to quantity ride comfort and allowable acceleration". Aviation, Space, and Environmental Medicine, pp.262-269.

19. Fairley, T.E. and Griffin, M.J. (1989) "The Apparent Mass of the Seated Human Body: Vertical Vibration", J. Biodynamics, Vol. 22, No. 2, pp. 81-94.

20. Suggs, C.W., Stikeleather, L.F., et al. (1969) "Application of a dynamic simulator in seat testing", Annual Meeting American Society of Agricultural Engineers, Purdue University, Paper NO. 69-172.

21. Suggs, C.W., Abrams, C.F. and Stikeleather, L.F. (1969) "Application of a damped spring-mass human vibration simulator in vibration testing of vehicle seats", Ergonomics, Vol. 12, 1969, pp. 79-90.

22. Allen, G. (1978) "A critical look at biodynamic modeling in relation to specifications for human tolerance of vibration and shock", Paper A25, AGARD Conference Proceeding NO. 253 "Models and analogues for the evaluation of human biodynamic response, performance and protection", Paris, France. pp. A25-5-A25-15.

23. Demic, M. (1987) "Investigation of human body oscillatory parameters under the action of shock excitations", ISO document TC 108/SC 4/WG 2 N 158, pp15.

24. Payne, P.R. and Band, E.G.U (1971) "A four-degree-of-freedom lumped parameter model of the seated human body", Aerospace Medical Research Laboratories Report AMRL-TR-70-35, Wright-Patterson Air Force Base, Ohio.

25. Boileau, P.E. (1995) "A study of secondary suspensions and human driver response to whole-body vehicular vibration and shock", Ph.D Thesis, Concordia University, Montreal, Quebec, Canada.

26. Inman, D.J.(1980) "Vibration with control, measurement, and stability", Department of Mechanical and Aerospace Engineering State University of New York at Buffalo, Buffalo, New York. Prentice Hall, Englewood Cliffs, New Jersey 07632. pp127.

27. Inman, D.J. and Andry, A.N. (1980) "Some results on the nature of eigenvalues of discrete damped linear system", ASME Journal of Applied Mechanics. 47, no. 4: 927-930.

28. Guignard, J.C. (1959) "The physic response of the seated men to low-frequency vertical vibration". Report 1062. Air Ministry Flying Personnel Research Committee.

29. Rowlands, G.F. (1977) "The transmission of vertical vibration to the head and shoulders of seated men". RAE Technical Report 77068. Royal Aircraft Establishment, Farnborough.

30. Donati, P.M. and Bonthoux, C. (1983) "Biodynamic response of the human body in the sitting position when subjected to vertical vibration". Journal of Sound and Vibration 90: 423-442.

31. Cooper, A.J. (1986) "Effects of head inclination on transmission of vertical vibration to the heads of seated subjects". United Kingdom Group Meeting on Human Response to Vibration, Lougborough University of Technology, 22-23 September 1986.

32. Wirsching, P.H.,Paez, Thomas, L., and Ortiz, H. (1995) "Random vibrations: Theory and practice". John Woley and Sons, New York.

33. European Standard prEN 13490 (1999) "Mechanical vibration-Industrial trucks-Laboratory evaluation of operator seat vibration".

34. Mcleod, R. and Griffin, M. (1989) "A review of the effects of translational whole-body vibration on continuous manual control performance". Journal of Sound and Vibration 133, 55-115.

35. Huston, D.R. and Zhao, X.D. (2000) "Whole-body shock and vibration: Frequency and amplitude dependence of comfort". Journal of Sound and Vibration 230(4), 964-970.